MULTISCALE METHODS FOR FLUID-STRUCTURE INTERACTION WITH APPLICATIONS TO DEFORMABLE POROUS MEDIA

A Dissertation

by

DONALD LEE BROWN

Submitted to the Office of Graduate Studies of
Texas A&M University
in partial fulfillment of the requirements for the degree of

DOCTOR OF PHILOSOPHY

August 2012

Major Subject: Mathematics

MULTISCALE METHODS FOR FLUID-STRUCTURE INTERACTION WITH APPLICATIONS TO DEFORMABLE POROUS MEDIA

A Dissertation

by

DONALD LEE BROWN

Submitted to the Office of Graduate Studies of
Texas A&M University
in partial fulfillment of the requirements for the degree of

DOCTOR OF PHILOSOPHY

Approved by:

Co-Chairs of Committee,	Yalchin Efendiev
	Akhil Datta-Gupta
Committee Members,	Raytcho D. Lazarov
	Jay Walton
Head of Department,	Emil J. Straube

August 2012

Major Subject: Mathematics

ABSTRACT

Multiscale Methods for Fluid-Structure Interaction with Applications to Deformable Porous Media. (August 2012)

Donald Lee Brown, B.A.,University of Cincinnati

Co–Chairs of Advisory Committee: Dr. Yalchin Efendiev
Dr. Akhil Datta-Gupta

In this dissertation we study multiscale methods for slowly varying porous media, fluid and solid coupling, and application to geomechanics. The thesis consists of three closely connected results. We outline them and their relation.

First, we derive a homogenization result for Stokes flow in slowly varying porous media. These results are important for homogenization in deformable porous media. Traditionally, these techniques are applied to periodic media, however, in the case of Fluid-Structure Interaction (FSI) slowly varying domains occur naturally. We then develop a computational methodology to compute effective quantities to construct homogenized equations for such media.

Next, to extend traditional geomechanics models based primarily on the Biot equations, we use formal two-scale asymptotic techniques to homogenize the fully coupled FSI model. Prior models have assumed trivial pore scale deformation. Using the FSI model as a fine-scale model, we are able to incorporate non-trivial pore scale deformation into the macroscopic equations. The primary challenge here being the fluid and solid equations are represented in different coordinate frames. We reformulate the fluid equation in the fixed undeformed frame. This unified domain formulation is known as the Arbitrary Lagrange-Eulerian (ALE).

Finally, we utilize the ALE formulation of the Stokes equations to develop an

efficient multiscale finite element method. We use this method to compute the permeability tensor with much less computational cost. We build a dense hierarchy of macro-grids and a corresponding collection of nested approximation spaces. We solve local cell problems at dense macro-grids with low accuracy and use neighboring high accuracy solves to correct. With this method we obtain the same order of accuracy as we would if we computed all the local problems with highest accuracy.

To my family

ACKNOWLEDGMENTS

First, I would like to thank Dr. Yalchin Efendiev for being my Chair for my doctoral thesis. Without his guidance and instruction this research would not have been possible. I also wish to thank Jay Walton, Dr. Raytcho Lazarov, and Dr. Akhil Datta-Gupta for taking the time and effort to be on my committee.

I would like to thank Dr. Peter Popov for the many useful discussions on Fluid-Structure Interaction and Homogenization. His guidance in the writing of our first paper was invaluable. Thanks needs to be given for taking the time to help me make a fledgling document into a full publication.

I would like to thank Dr. Viet Ha Hoang for his hospitality during my stay in Singapore for those several months. The detailed discussions on hierarchical finite element methods and applications to homogenization are an invaluable part of this thesis. His careful and detailed mathematical analysis of problems helped make me a better mathematician.

Thanks has to also be given to Dr. Juan Galvis for allowing me to adapt his finite element code, and subsequently, teaching me how to use the code. It took great patience to teach detailed algorithms to a fledgling programmer like myself.

I appreciated the time Dr. Jay Walton took in lecturing me about the finer points of continuum mechanics. In addition, for taking the time to explore alternate ways of understanding the Fluid-Structure Interaction process.

I would also like to thank my mentors in my undergraduate career because without there guidance graduate school would not have been possible. I would like to thank Dr. Mike Sokoloff and Dr. Rohana Wijewardhana of the University of Cincinnati, Physics Department for teaching me how to think deeply about physical problems and general advice for graduate school and academic life. Also, Dr. Bingyu

Zhang of the University of Cincinnati, Mathematics Department for being a good mentor and impressing upon me the importance of understanding the fundamentals of mathematical analysis even in the context of applied problems.

I would also like to thank the support of NSF IGERT DGE-0549487 New Mathematical Tools for Next Generation Materials. Also, the NSF EAPSI program for the support during my stay at Nanyang Technological University.

TABLE OF CONTENTS

LIST OF TABLES

LIST OF FIGURES

CHAPTER I

INTRODUCTION

Modeling flow in porous media has wide ranging applications in many areas of science and engineering, such as subsurface simulations in reservoir modeling, industrial applications such as filtration, and modeling biological materials such as bone. Porous media can have a highly heterogeneous pore microstructure with complex geometry, where the pore size is many orders of magnitude smaller than the medium of interest. The small scales involved in modeling porous microstructure limit the accuracy of direct numerical simulation (DNS). More advanced averaging, homogenization schemes, and multiscale techniques must be used. Many of these homogenization procedures exploit the periodic nature of these applications. However, there are natural cases when the medium fails to be periodic and further analysis and methods are needed.

In the case of deformable porous media, pore scale deformation can be relatively very large cf. [21] and references therein. Assuming an initially periodic medium, local Fluid-Structure Interaction (FSI) leads to slowly varying geometry. This breaks the periodicity and it is not clear how standard homogenization techniques can be utilized. This is the main task of Chapter II. Given a slowly varying geometry and assuming Stokes flow in the pore space, we derive a homogenization convergence result. Our work uses asymptotic techniques of [24] where the authors constructed a downscaled velocity which converges to the fine-scale velocity at a rate of $\varepsilon^{1/6}$, where ε is the characteristic length scale. We assume a slowly varying porous medium and study homogenization and corrector estimates for the Stokes equations. Slowly varying media arise, e.g., in Fluid-Structure Interaction (FSI) problems [32], carbonation of

---

The journal model is SIAM Journal of Numerical Analysis.

porous concrete [28, 29], and various other multiphysics processes. To homogenize Stokes flows in such media we restate the cell problems of [24] in a moving RVE framework. Further, to recover the same convergence properties it is necessary to solve an additional cell problem and add one more corrector term to the downscaled velocity. We further extend the framework of [24] to three spatial dimensions in both periodic and variable pore-space cases. The main challenge in this proof is the construction of a proper boundary corrector to properly adjust the correctors to incorporate boundary layer effects.

Next, we also propose an efficient algorithm for computing the correctors by solving a limited number of cell problems at selected spatial locations. We present two computational examples: one for a constructed medium of elliptical perforations, and another for a fractured medium with FSI driven deformation. We obtain numerical estimates that confirm the theory in these two examples. The contents of Chapter II are essentially a decoupled homogenization procedure. We have some *a-prior* computed deformation, or perhaps, some other physical process. Then, we homogenize the fluid equations. This may be accomplished iteratively cf. [32]. Later in Chapter IV, we present a method that offers an improvement on the computational cost of this method at the cost of having to compute a global deformation map.

In Chapter III, we develop a fully coupled fluid and solid mechanics homogenized model. The fully coupled homogenized model is an extension of the traditional geomechanics model first developed by phenomenological considerations in [4]. Later using the method of two-scale asymptotic expansion [8] derived the linear Biot equations. However, such methods assume infinitesimal pore scale deformation. Assuming that the grain size does not change to much, more precisely, the local deformations are non oscillatory [21] developed a nonlinear extension to the Biot equations. This was achieved by using the two-scale expansion in the deformed configuration.

Using the Fluid-Structure Interaction model as our fine scale model we are able to incorporate non-trvial pore scale deformation into the homogenized macroscale equations. The main challenge of applying two-scale homogenization techniques to the FSI model is the difference in coordinate systems. Traditionally, fluid equations are presented in the deformed or Eulerian frame, while the solid equations are presented in the fixed Lagrangian frame. To complicate matters further, the interface traction boundary condition is presented in the Lagrangian frame is nonlinear. We recall in our presentation the derivation of the linear Biot model. If the interface condition is assumed to be linear, the frames do not differ greatly and traditional methods will work and result in the linear Biot equations.

However, when the condition remains nonlinear, we reformulate the equations in the Arbitrary Lagrange-Eulerian configuration cf. [15]. In this setting, we reformulate the Stokes equation in the Lagrange or fixed frame by a change of variable. We arrive at a nonlinearly coupled Stokes equation with deformation gradient tensor coefficients. The equations are more complicated, but we arrive at a unified domain formulation. This allows for formal two-scale asymptotic techniques ([33]) to be used since we assume an initially periodic domain. In this setting, we arrive at auxiliary cell equations that depend nonlinearly on the macroscopic pressure and macroscopic gradient of displacement. Compared to the linear setting, in which the cell equations depend on geometry only. We then homogenize by averaging and arrive at the macroscopic fluid and solid Biot equations. The effective coefficients depend nonlinear on the macroscopic pressure and macroscopic gradient of displacement as they are connected to the auxiliary cell equations. Thus, the equation is highly nonlinear.

In an attempt to make the nonlinear Biot model more amenable to computational techniques, we suggest several useful linearization and simplifications. Indeed, the

primary nonlinearity comes from the Piola transform tensor on the interface of the cell equations. By linearizing this tensor we are able to obtain a significant simplification. We are able to decouple the elasticity cell equations from the macroscopic gradient of displacement. This implies the elasticity cell problems depend on only a one parameter space parametrized by pressure. We then, by a systematic simplification of the displacement obtain a hierarchy of models in decreasing complexity. From here we are able to compute a numerical example with the simplest model. Computational techniques applied to this hierarchy of models is still an area of ongoing research.

Finally, in Chapter IV, we develop an efficient multiscale finite element method (FEM). The method relies heavily on the Arbitrary Lagrange-Eulerian formulation of the Stokes equations first presented in Chapter III. Again, we assume that the deformation of the medium has been precomputed in some way as in Chapter II. With this method we are able to obtain the same order of accuracy in calculation of permeability with much less computational cost. More precisely, if there are $O(N)$ problems and d scales, to solve each local problem with highest accuracy would cost $O(N^d)$. With the hierarchical FEM we obtain a cost of $O(N)$.

The method is essentially as follows. We first build a dense hierarchy of macro-grids over the domain. The first grid being the sparsest and each subsequently more dense. Then, we build a corresponding nested collection of finite element (FE) approximations spaces. We solve at the denser macro-grids using lower accuracy spaces and use nearby higher accuracy solves at sparse grid points to correct. We proceed with this in a systematic way. We show that if the macro-grids have the correct density properties, the corresponding nested approximation spaces' error decreases at a prescribed rate, and the partial differential operator satisfies simple mathematical assumptions, we obtain the same order of accuracy as if we solved the highest accuracy at all points in the domain. We refer to this full accuracy solve at all points as

the full solve.

Assuming a slowly varying geometry, we show that with reasonable mathematical assumptions, that this method can be applied to the Stokes equations in the ALE formulation to compute the permeability tensor. Once this tensor is computed an effective Darcy equation can be constructed. We then apply the method to a "proof of concept" example. Assuming that the initial geometry is periodic. We assume that the precomputed deformation is periodic in the vertical direction. This makes the macro-grid essentially one dimensional. However, the local cell problems are two dimensional perforated domains. All the computation is done in the unified ALE formulation. This is done to ensure the collection of approximation spaces are nested.

CHAPTER II

HOMOGENIZATION OF STOKES EQUATIONS IN SLOWLY VARYING DOMAINS

There are multiphysics multi-scale problems in which, through coupled processes, the media evolves in a manner so that it is no longer periodic. This is the case with Fluid-Structure Interaction (FSI) problems when posed on initially periodic microstructures [31]. Through mechanical deformations of the porous skeleton, due to fluid-solid coupling stresses, the initially undeformed periodic geometry changes in a slowly varying way to a non-periodic one. Another example is modeling carbonation of porous concrete. The concrete evolves via a chemical reaction, creating a slowly varying microstructure [28, 29]. In the context of filtration devices, deposition of contaminants can change the porosity and permeability of the filter [25]. In this chapter, we develop analytical and computational tools to deal with such a medium.

The chapter is organized as follows; first, we cover the background literature, motivate the need for homogenization in slowly varying domains, and clearly state the results of the chapter. We then, give a brief overview of homogenization of Stokes flow in a periodically perforated domain. The formal two-scale expansion is used to recall auxiliary cell problems and homogenized equations in this setting. In the next Section, we then introduce the formal mathematical definition of slowly varying media. We derive auxiliary cell problems, homogenized equations, and auxiliary cell problems for first order correctors for Stokes flow in a slowly varying domain. Then, using the cell problems derived in the previous section, we construct the boundary correctors for the slowly varying domain. We then recall the proof given in [24], and extend it to the slowly varying case. Then, we present our so-called "Moving Averages" numerical algorithm to compute downscaled quantities. This algorithm is

implemented on a constructed domain of elliptic inclusions for various ε's. Finally, a brief introduction to steady state FSI is given, along with our numerical algorithm applied to this geometry.

A. Preliminaries

1. Motivation and Background

Homogenization of the Stokes equation in periodic media is well understood [3, 33, 34] and a number of works have also established convergence results for the downscaled quantities, e.g., first order pressure and velocity correctors [1, 23, 24, 35]. The main goal of the current chapter is to extend asymptotic homogenization methods to slowly changing geometries. The extension of these methods to slowly varying cases must be carefully scrutinized. Furthermore, the application of various advanced iterative upscaling schemes and subgrid resolution methods [11] to non-periodic media rely on theoretical convergence results and estimates for downscaled quantities. In this chapter we establish estimates for downscaled quantities.

In this chapter we consider a creeping flow of an incompressible Newtonian fluid in a complex pore microstructure with slowly varying geometry. These flows are governed by the Stokes equations [3, 33]. The amount of literature pertaining to homogenization methods and techniques for Stokes flow in periodic microstructure is extensive. Two-scale asymptotic homogenization theory was initially used [3, 33, 34] to derive a homogenized Darcy equation [10]. The process also involves auxiliary cell problems in a periodic setting which allow the construction of downscaled quantities. The convergence of this formal homogenization method was proven using the method of oscillatory test functions [35] in 2D. Choosing appropriate oscillatory test functions can be challenging. Using the method of two-scale convergence [1, 26], a convergence

theory framework is developed. In this framework, the oscillatory test functions are chosen as solutions to adjoint auxiliary cell problems. The combination of two-scale convergence theory and Tartar's extensions for the pressure and velocity allows one to prove convergence of periodic Stokes homogenization.

The convergence results in periodic media, although fundamental, are not sufficient when applying the homogenization methods to practical computational problems. When applying these homogenization methods to flows in complex geometries in a computational setting, understanding the error estimates for correctors is essential [11]. Error estimates for correctors in periodic media are also well studied [37]. In the context of an elliptic equation with oscillatory coefficients and Dirichlet data, it is not difficult to obtain $\varepsilon^{1/2}$ convergence order using a simple cut-off method near the boundary, cf. e.g., [22, 27, 37]. The incompressibility condition in Stokes and Navier-Stokes equations complicates the error estimate near the boundary. If one wants to derive estimates with a rate of convergence (in terms of ε), additional boundary correctors are needed. Such a corrector is derived for a simple domain with one impervious wall and an error estimate of order $\varepsilon^{1/6}$ is obtained in [20]. This boundary corrector framework is generalized to an arbitrary domain in $\mathbb{R}^2$ [24], and the authors arrive at the error estimate for correctors of order $\varepsilon^{1/6}$.

In this chapter we extend the estimate in [24] to slowly varying geometry, e.g., in FSI problems. To this end we derive new auxiliary cell problems and generalized homogenized equations. From these equations we extend boundary correctors by adding terms due to the slowly varying geometry. Using a generalization of the construction in [24] we are able to extend the boundary correctors to three spatial dimensions for both periodic and slowly varying geometries. We then present an efficient computational algorithm to compute the correctors for two examples: a constructed medium of elliptical perforations, and a fractured medium with FSI driven

deformation. In contrast to periodic media where we need to solve only one cell, we solve cell problems at a limited number of different spatial locations to construct the correctors.

2. Periodic Stokes Homogenization

In this section a formal asymptotic expansion is used to construct cell problems and downscaled velocity and pressure in a periodic medium. The Stokes equation in a perforated domain is stated first, followed by a brief recall of standard results in periodic media [33]. This will serve as background and present the notation. To extend the estimates of [24] to variable media additional cell problems are needed. Those are stated in the next section together with the main result.

We consider fluid flow in a perforated domain. Denote by Ω the macroscopic medium, a bounded open subset of $\mathbb{R}^d$. It is composed of a solid microstructure occupying the open set $\mathcal{S}_\varepsilon$. The solid surrounds the pore-space $\mathcal{F}_\varepsilon$ in which the fluid resides, that is $\Omega = \mathcal{S}_\varepsilon \cup \mathcal{F}_\varepsilon$ and $\mathcal{S}_\varepsilon \cap \mathcal{F}_\varepsilon = \emptyset$. Those two domains are decomposed into a set of unit cells $\varepsilon \{Y_{\mathcal{S}}^i\}_{i=1}^N$ and $\varepsilon \{Y_{\mathcal{F}}^i\}_{i=1}^N$, respectively and ε is the characteristic size. That is, $Y_{\mathcal{S}}^i$ and $Y_{\mathcal{F}}^i$, $i = 1, \ldots, N$, are unit-sized domains and

$$\mathcal{S}_\varepsilon = \left(\bigcup_{i=1}^N \varepsilon Y_{\mathcal{S}}^i \right) \cap \Omega, \qquad \mathcal{F}_\varepsilon = \left(\bigcup_{i=1}^N \varepsilon Y_{\mathcal{F}}^i \right) \cap \Omega. \tag{2.1}$$

We denote the i-th unit cell by $Y^i = Y_{\mathcal{S}}^i \cup Y_{\mathcal{F}}^i$. Next, denote by $\Gamma_\varepsilon = \bar{\mathcal{S}}_\varepsilon \cap \bar{\mathcal{F}}_\varepsilon$ the fluid-solid interface. The fluid velocity and pressure are denoted by v_ε and p_ε, respectively. The fluid motion is governed by the conservation of linear momentum and mass, which for Newtonian fluids with unit viscosity at creeping velocities reads

$$-\Delta v_\varepsilon + \nabla p_\varepsilon = f, \qquad \text{in } \mathcal{F}_\varepsilon \tag{2.2a}$$

$$\nabla \cdot v_\varepsilon = 0, \qquad \text{in } \mathcal{F}_\varepsilon \tag{2.2b}$$

where v_ε has zero trace on Γ_ε. Additional boundary conditions may be specified at the remainder of the fine-scale boundary, $\Omega \backslash \Gamma_\varepsilon$. Let us also define the average over a unit cell centered at x, that is Y^x, by $\langle \cdot \rangle_{Y^x}$

$$\langle \cdot \rangle_{Y^x} = \frac{1}{|Y^x|} \int_{Y^x} \cdot \, dy. \tag{2.3}$$

We briefly repeat homogenization in periodic media. In periodic media, all unit cells $Y^i_{\mathcal{S}}$ and $Y^i_{\mathcal{F}}$ are identical, so one can drop the superscript i.

Remark In this chapter, we shall use the superscript $^{\#}$ to denote periodic domains and no superscripts for deformed domains. In Chapter III, we will be working primarily in the fixed periodic reference frame. Thus, we will adopt another notation where a periodic media has no superscript and a deformed media has the superscript $\widetilde{\cdot}$.

The homogenization of the Stokes system (2.2) by formal asymptotic expansion was first proposed in [34], where $(v_\varepsilon, p_\varepsilon)$ is expanded as

$$v_\varepsilon = \varepsilon^2 \left(v_0(x,y) + \varepsilon v_1(x,y) + \cdots \right), \tag{2.4a}$$

$$p_\varepsilon = p_0(x) + \varepsilon p_1(x,y) + \cdots, \tag{2.4b}$$

where $y = x/\varepsilon$ is the fast variable. One next substitutes (2.4) into (2.2) and uses the fact that derivatives behave as $\nabla \to \nabla_x + \frac{1}{\varepsilon} \nabla_y$. By collecting powers of ε one obtains

$$v_0(x,y) = \sum_{i=1}^{d} w^i(y) \left(f_i - \frac{\partial p_0}{\partial x_i} \right), \qquad p_1(x,y) = \sum_{i=1}^{d} \pi^i(y) \left(f_i - \frac{\partial p_0}{\partial x_i} \right), \tag{2.5}$$

where $(w^i(y), \pi^i(y))$, $i = 1, \ldots, d$, are the solutions to the d-cell problems

$$-\Delta_y w^i + \nabla_y \pi^i = e_i \qquad \text{in } Y^{\#}_{\mathcal{F}}, \tag{2.6a}$$

$$\operatorname{div}_y \left(w^i \right) = 0 \qquad \text{in } Y^{\#}_{\mathcal{F}}, \tag{2.6b}$$

where w^i and π^i are y-periodic, w^i has zero trace on $Y_\Gamma^\#$, and $\langle \pi^i \rangle_{Y^\#} = 0$. Here e_i is the i-th standard basis unit vector in $\mathbb{R}^d$. Note here that since the pore space $\mathcal{F}_\varepsilon^\#$ is periodic these cell equations only depend on y. Next, inserting (2.4a) into the conservation of mass (2.2b) yields

$$\mathrm{div}_x\left(v_0\right) + \mathrm{div}_y\left(v_1\right) = 0, \tag{2.7}$$

at order ε^0. The classical Darcy equation [10, 33] is finally obtained by averaging (2.7), utilizing (2.5) along with the periodicity of v_1

$$\xi = K\left(f - \nabla_x p_0\right), \qquad \mathrm{div}_x\left(\xi\right) = 0 \qquad \text{in } \Omega^\#, \tag{2.8a}$$

$$\xi \cdot \nu = 0 \qquad \text{on } \partial\Omega^\#, \tag{2.8b}$$

where $K_{ij} = \int_{Y_\mathcal{F}^\#} w_j^i(y)dy$ is the effective permeability tensor and ξ is the averaged (Darcy) velocity. Note that K is constant in $\Omega^\#$. Also, one can take a more general expansion than (2.4) and conclude that the ε^0 and ε^1 terms of the velocity expansion vanish and that ε^0 pressure p_0 is independent of y.

B. Homogenization in Slowly Varying Domains

1. Stokes in Slowly Varying Domains

The derivation of estimates with a rate requires the inclusion of the next term in the velocity expansion (2.4a), namely v_1, along with its associated cell problems and appropriate boundary correctors. This is done in the periodic setting in [24]. In this section we extend the results of [24] to slowly varying media.

First, we define slowly varying media as follows. Let $X_\varepsilon : \Omega^\# \to \Omega$ be a smooth map from a periodic domain $\Omega^\# = \mathcal{S}_\varepsilon^\# \bigcup \mathcal{F}_\varepsilon^\#$ to a non-periodic one Ω. Consequently, $\mathcal{S}_\varepsilon = X_\varepsilon(\mathcal{S}_\varepsilon^\#)$, $\mathcal{F}_\varepsilon = X_\varepsilon(\mathcal{F}_\varepsilon^\#)$ and $\Gamma_\varepsilon = X_\varepsilon(\Gamma_\varepsilon^\#)$. Each unit cell is now different, so

we define a moving RVE. For each $x \in \Omega$, the fluid and solid domains contained in an RVE are denoted by $Y_{\mathcal{S}}^x$ and $Y_{\mathcal{F}}^x$, and the interface by Y_Γ^x. We view these as the translated and mapped periodic unit cell. That is, $Y_{\mathcal{F}}^x = X_\varepsilon(Y_{\mathcal{F}}^\# + k_x)$ and $Y_{\mathcal{S}}^x = X_\varepsilon(Y_{\mathcal{S}}^\# + k_x)$, where $k_x \in \mathbb{Z}^d$ corresponds to the RVE at x. Then, the fluid space is

$$\mathcal{F}_\varepsilon = \bigcup_{x\in\Omega} \varepsilon Y_{\mathcal{F}}^x. \tag{2.9}$$

We say a medium Ω is slowly varying if the map X_ε is sufficiently smooth so that the microstructure geometry varies smoothly for neighboring RVEs. In addition, we assume that the map X_ε is sufficiently smooth so that the expansion (2.4) yields valid cell problems and K, as a function of x (slow variable), is sufficiently smooth.

Remark The concept of slowly varying media has an intuitive mathematical definition. We say a medium Ω is slowly varying if the map X_ε is such that for two close points $x, x' \in \Omega$, that is $\|x - x'\| < O(\varepsilon)$, one has

$$|(Y_{\mathcal{F}}^x \cup Y_{\mathcal{F}}^{x'})\backslash(Y_{\mathcal{F}}^x \cap Y_{\mathcal{F}}^{x'})| < O(\varepsilon). \tag{2.10}$$

The fluid pore space of neighboring RVEs does not differ very much. In this work however, we do not prove that this definition is a sufficient condition for our results.

This mapping X_ε may be any number of physical processes that evolves the microstructure in a slowly varying way. For example, in the context of FSI the mapping is of the form

$$X_\varepsilon(p) = p + u_\varepsilon(p), \tag{2.11}$$

where $p \in \Omega^\#$ are material (Lagrangian) coordinates, X has the meaning of spatial (Eulerian), coordinates and u_ε is the elastic displacement. This will be explained in detail in Chapter III. The solid displacements, fluid velocity, and pressure solve a coupled system of differential equations. A numerical example of homogenization in

FSI generated geometry in a later section.

The cell problems are now stated for a given spatial position. That is, one fixes x and substitutes the expansions (2.4) into the Stokes equations (2.2). As in the periodic case, by gathering ε^0 terms in the conservation of linear momentum, and ε^{-1} terms in the conservation of mass one obtains

$$-\Delta_y v_0(x,y) + \nabla_y p_1(x,y) = f(x) - \nabla_x p_0(x) \qquad \text{in } Y^x_{\mathcal{F}}, \tag{2.12a}$$

$$\operatorname{div}_y (v_0(x,y)) = 0 \qquad \text{in } Y^x_{\mathcal{F}}, \tag{2.12b}$$

where v_0 and p_1 are $y-$periodic, v_0 has zero trace on Y^x_Γ, and $\langle p_1 \rangle_{Y^x} = 0$. Note that we do not have a single set of cell problems, but for each $x \in \Omega$ we have cell problems with different geometries. Note that periodic boundary conditions are still used. As shown by the analysis section, this does not change the order of the downscaled approximation.

Next, due to linearity of (2.12) and the right hand side being a function of the slow variable x only, one has

$$v_0(x,y) = \sum_{i=1}^{d} w^i(x,y) \left(f_i - \frac{\partial p_0}{\partial x_i} \right), \tag{2.13a}$$

$$p_1(x,y) = \sum_{i=1}^{d} \pi^i(x,y) \left(f_i - \frac{\partial p_0}{\partial x_i} \right), \tag{2.13b}$$

where $(w^i(x,y), \pi^i(x,y))$, $i = 1, \ldots, d$, are the solutions to

$$-\Delta_y w^i + \nabla_y \pi^i = e_i \qquad \text{in } Y^x_{\mathcal{F}}, \tag{2.14a}$$

$$\operatorname{div}_y \left(w^i \right) = 0 \qquad \text{in } Y^x_{\mathcal{F}}, \tag{2.14b}$$

with w^i and π^i being $y-$periodic, w^i having zero trace on Y^x_Γ, and $\langle \pi^i \rangle_{Y^X} = 0$. Again, e_i is the i-th standard basis unit vector in $\mathbb{R}^d$. Now, to tie cell problems to the macroscopic equation, one inserts (2.4a) into (2.2b) and, by collecting ε^0 terms,

we obtain

$$\mathrm{div}_x\left(v_0\right)+\mathrm{div}_y\left(v_1\right)=0 \text{ in } \mathcal{F}_\varepsilon. \tag{2.15}$$

Next, fix x and integrate over $Y^x_{\mathcal{F}}$. With the help of the divergence theorem, v_1 having zero trace on Y^x_Γ, and due to $y-$periodicity, one has

$$\mathrm{div}_x\left(\int_{Y^x_{\mathcal{F}}} v_0(x,y)dy\right)+\int_{Y^x_{\mathcal{F}}}\mathrm{div}_y\left(v_1(x,y)\right)dy=\mathrm{div}_x\left(\int_{Y^x_{\mathcal{F}}} v_0(x,y)dy\right).$$

Then, by using (2.13a) for v_0 one obtains

$$\mathrm{div}_x\left(\int_{Y^x_{\mathcal{F}}} v_0(x,y)dy\right)=\sum_{i=1}^{d}\mathrm{div}_x\left(\int_{Y^x_{\mathcal{F}}} w^i(x,y)dy\left(f_i-\frac{\partial p_0}{\partial x_i}\right)\right)=0. \tag{2.16}$$

The above relation is the Darcy Law with the permeability that varies in x. Indeed, the now x-dependent permeability can be written as $K_{ij}(x):=\int_{Y^x_{\mathcal{F}}} w^i_j(x,y)dy$. Then,

$$\xi=K(x)(f-\nabla_x p_0), \qquad \mathrm{div}_x\left(\xi\right)=0 \qquad \text{in } \Omega, \tag{2.17}$$

with $\xi\cdot\nu=0$ on $\partial\Omega$. Here ξ is again the Darcy velocity. The difference from the periodic setting is that the cell solutions (w^i,π^i) depend on x. Therefore, the permeability is now a (slow) variable field; that is $K=K(x)$.

The first order corrector to the velocity is needed to obtain the error estimate of $\varepsilon^{1/6}$. We will use higher order terms to cancel out unwanted lower order terms. To construct the first order velocity corrector one needs two additional cell problems. First, let β be the y-periodic, zero mean unique solution to

$$\mathrm{div}_y\left(\beta^i\right)=-\mathrm{div}_x\left(w^i\right)+|Y^x_{\mathcal{F}}|^{-1}\,\mathrm{div}_x\left(K_i\right) \qquad \text{in } Y^x_{\mathcal{F}}, \tag{2.18a}$$

$$\beta^i=0 \qquad \text{on } Y^x_\Gamma. \tag{2.18b}$$

Observe that the $\langle\beta^i\rangle_{Y^x}=0$ condition is necessary to guarantee uniqueness. Note that the above problem has only Neumann and periodic boundary conditions, which

implies $\langle \mathrm{div}_y\left(\beta^i\right)\rangle_{Y^x} = 0$. Thus, the constant term $\mathrm{div}_x\left(K_i\right)/\left|Y^x_{\mathcal{F}}\right|$ on the right-hand side guarantees a compatible problem. That is, one checks directly that

$$\left\langle -\mathrm{div}_x\left(w^i\right) + \left|Y^x_{\mathcal{F}}\right|^{-1}\mathrm{div}_x\left(K_i\right)\right\rangle_{Y^x} = 0.$$

The second cell problem is for the y-periodic, tensor field γ

$$\mathrm{div}_y\left(\gamma^{ij}\right) = -w^i_j + \left|Y^x_{\mathcal{F}}\right|^{-1}K_{ij} \qquad \text{in } Y^x_{\mathcal{F}}, \tag{2.19a}$$

$$\gamma^{ij} = 0 \qquad \text{on } Y^x_{\Gamma}. \tag{2.19b}$$

Again, $\langle\gamma^{ij}\rangle_{Y^x} = 0$ is needed for uniqueness. Also, the compatibility, $\langle \mathrm{div}_y\left(\gamma^{ij}\right)\rangle_{Y^x} = 0$, is ensured by the $\left|Y^x_{\mathcal{F}}\right|^{-1}K_{ij}$ term on the right-hand side.

The cell solutions β and γ let one write a representation for v_1. To that end, substitute (2.13a) into equation (2.15) and expand $\mathrm{div}_x\left(v_0\right)$. It is seen that v_1 can be written as

$$v_1(x,y) = \sum_{i=1}^{d}\beta^i(x,y)\left(f_i - \frac{\partial p_0}{\partial x_i}\right) + \sum_{i,j=1}^{d}\gamma^{ij}(x,y)\frac{\partial}{\partial x_j}\left(f_i - \frac{\partial p_0}{\partial x_i}\right). \tag{2.20}$$

Indeed, using first (2.18a) and (2.19a), followed by (2.13a) and (2.17) yields

$$\begin{aligned}
\mathrm{div}_y\left(v_1\right) &= \sum_{i=1}^{d} \mathrm{div}_y\left(\beta^i\right)\left(f_i - \frac{\partial p_0}{\partial x_i}\right) + \sum_{i,j=1}^{d} \mathrm{div}_y\left(\gamma^{ij}\right)\frac{\partial}{\partial x_j}\left(f_i - \frac{\partial p_0}{\partial x_i}\right) \\
&= \sum_{i=1}^{d}\left(-\mathrm{div}_x\left(w^i\right) + \left|Y_{\mathcal{F}}^x\right|^{-1}\mathrm{div}_x\left(K_i\right)\right)\left(f_i - \frac{\partial p_0}{\partial x_i}\right) \\
&+ \sum_{i,j=1}^{d}\left(-w_j^i + \left|Y_{\mathcal{F}}^x\right|^{-1}K_{ij}\right)\frac{\partial}{\partial x_j}\left(f_i - \frac{\partial p_0}{\partial x_i}\right) \\
&= \left|Y_{\mathcal{F}}^x\right|^{-1}\sum_{i,j=1}^{d}\frac{\partial K_{ij}}{\partial x_j}\left(f_i - \frac{\partial p_0}{\partial x_i}\right) \\
&+ \left|Y_{\mathcal{F}}^x\right|^{-1}\sum_{i,j=1}^{d} K_{ij}\frac{\partial}{\partial x_j}\left(f_i - \frac{\partial p_0}{\partial x_i}\right) - \mathrm{div}_x\left(v_0\right) \\
&= \left|Y_{\mathcal{F}}^x\right|^{-1}\mathrm{div}_x\left(\xi\right) - \mathrm{div}_x\left(v_0\right) = -\mathrm{div}_x\left(v_0\right).
\end{aligned}$$

Thus, using the representations v_0, v_1 given by (2.13a), (2.20), we satisfy (2.15).

Remark In periodic microstructure one only needs the cell problem (2.19) to construct the first order velocity corrector, cf. [24].

We are now ready to state our main result. It is a generalization of [24] to the case of slowly varying geometry that is important in Fluid-Structure Interaction problems.

Theorem II.1. Let $(v_\varepsilon, p_\varepsilon)$ satisfy (2.2) in the slowly varying geometry $\mathcal{F}_\varepsilon$. Let (v_0, v_1) be as in (2.13a), (2.20) where (w, π) satisfy (2.14) and (β, γ) satisfy (2.18),(2.19). Let p_0 be as in the Darcy velocity (cf. (2.17)). Then, we have the estimate

$$\left\|v_\varepsilon/\varepsilon^2 - \left(v_0 + \varepsilon v_1\right)\right\|_{H(\Omega,\mathrm{div})} \leq C\varepsilon^{1/6}, \tag{2.21a}$$

$$\left\|p_\varepsilon - p_0\right\|_{L_0^2(\Omega)} \leq C\varepsilon^{1/6}. \tag{2.21b}$$

2. Analysis and Proof of Corrector Theorem

In this section we shall proceed with the analysis to prove our main Theorem II.1. To this end, we modify the first order correctors to the velocity and pressure. As noted previously, in [24], unlike in the elliptic case for perforated domains, [22, 27], the divergence equation will lead to a boundary layer near $\partial\Omega$ and destroy any trace estimates. In addition, recall that the current first order corrector to the velocity does not satisfy the global Dirichlet boundary condition $v_\varepsilon = 0$ on $\partial\Omega$. We refer to the resulting modified correctors as the boundary correctors. The boundary correctors shall ameliorate these issues.

To construct the boundary correctors we will need auxiliary functions and related estimates. We state a technical lemma of a construction of a divergence free function, denoted by s^δ, with prescribed trace. The construction of this function in three spatial dimensions allows us to claim that our main result Theorem II.1, is valid in three dimensions for both periodic and slowly varying media. A proof is given in Lemma II.2. We then repeat the proof of [24] and extend their proof to the case of slowly varying media.

a. Boundary Correctors

We will now introduce two technical functions and related estimates needed in our construction of the boundary correctors. First, we construct a divergence free function with Darcy velocity trace ξ and derive related estimates. The summary of the properties of this function may be put into a technical lemma. Throughout the rest of this work we use the notation that $C^k(\bar{\Omega})^d$ is the set of d-valued functions over $\bar{\Omega}$ that are k-times continuously differentiable.

Lemma II.2. Let $\Omega \subset \mathbb{R}^d$, where $d = 2, 3$, be an open bounded, sufficiently smooth

domain. Then, there exists a $\delta_0 > 0$ and a function $s^\delta \in C^3(\bar{\Omega})^d$ such that $s^\delta = \xi$ on $\partial\Omega$, $\mathrm{div}(s^\delta) = 0$ in Ω, and

$$\left\| D^l s^\delta \right\|_{L^q(\Omega)} \leq C\delta^{1/q-l}, \tag{2.22}$$

for $q \in [1, \infty]$ if $d = 2$ and $q = 2$ for $d = 3$, $0 < l \leq 3$ and $0 \leq \delta \leq \delta_0$.

Proof. For $d = 2$ see [24]. For $d = 3$ the construction is essentially an adaptation of the two dimensional case, except we must use a dual-streamfunction construction as the curl of a potential construction is not available. We define $(\nu(x), \tau_1(x), \tau_2(x))$ as a local orthonormal basis for the tangent space at x of Ω. Recall that the, normal component of the Darcy velocity ξ vanishes, but the tangential components may not. Following ideas from [24, 36] we wish to find an s^δ of the form of a cross product of specifically constructed dual-streamfunctions $s^\delta = \nabla\psi \times \nabla\phi$. Clearly from basic vector derivative identities we have $\mathrm{div}\left(s^\delta\right) = 0$ in Ω and $s^\delta \perp \nabla\psi$, $s^\delta \perp \nabla\phi$. We need to construct ψ, ϕ such that

$$\frac{\partial\psi}{\partial\nu} = \xi \cdot \tau_1 \ , \ \frac{\partial\phi}{\partial\nu} = \xi \cdot \tau_2 \text{ on } \partial\Omega,$$

and

$$\psi = 0 \ , \ \phi = 0 \text{ on } \partial\Omega.$$

Using the two dimensional proof as a guide, for some $\eta > 0$ we have a distance function $z(x) = \mathrm{dist}(x, \partial\Omega)$ that is in $C^4(\mathcal{D}_\eta)$. Here, $\mathcal{D}_\eta = \{x \in \bar{\Omega} : \mathrm{dist}(x, \partial\Omega) \leq \eta\}$. We define $(z(x), \chi_1(x), \chi_2(x))$ to be our local orthogonal coordinates in $\mathcal{D}_\eta$. Clearly we have the relations

$$\nu(x) = -\frac{\nabla z(x)}{|\nabla z(x)|} \ , \ \tau_i(x) = -\frac{\nabla\chi_i(x)}{|\nabla\chi_i(x)|},$$

for $i = 1, 2$. We define the function $V(z, \chi_1, \chi_2) = -\xi(x)/|\nabla z(x)|$ for $x = x(z, \chi_1, \chi_2) \in \mathcal{D}_\eta$. For $x \in \partial\Omega$ we have $z(x) = 0$ and $\nabla z(x) \neq 0$, hence the trace of V is well defined and of class $C^4(\partial\Omega)$. We now suppose that our dual-streamfunctions are of the form

$$\psi(x) = z(x)e^{-z(x)/\delta^{1/2}}V(0, \chi_1(x), \chi_2(x)) \cdot \tau_1(x),$$
$$\phi(x) = z(x)e^{-z(x)/\delta^{1/2}}V(0, \chi_1(x), \chi_2(x)) \cdot \tau_2(x).$$

Thus, for $x \in \partial\Omega$ we have $z(x) = 0$, thus $\psi = \phi = 0$ on $\partial\Omega$. Calculating we have, via orthogonality, on $\partial\Omega$

$$\begin{aligned}\frac{\partial\psi}{\partial\nu} &= \left(\nabla z\frac{\partial\psi}{\partial z} + \nabla\chi_1\frac{\partial\psi}{\partial\chi_1} + \nabla\chi_2\frac{\partial\psi}{\partial\chi_2}\right) \cdot \left(-\frac{\nabla z}{|\nabla z|}\right) \\ &= \nabla z\frac{\partial\psi}{\partial z} \cdot \left(-\frac{\nabla z}{|\nabla z|}\right) = -|\nabla z|\left(1 - \frac{z}{\delta^{1/2}}\right)\frac{1}{z}\psi = \xi \cdot \tau_1.\end{aligned}$$

In a similar manner, we obtain the desired identity $\frac{\partial\phi}{\partial\nu} = \xi \cdot \tau_2$ on the boundary. Thus, we have the desired function for s^δ, and now we will derive the desired estimates. We proceed with $q = 2$ as this is the only estimate we will need.

$$\begin{aligned}\|\nabla\psi\|^2_{L^2(\mathcal{D}_\eta)} &= \int_{\mathcal{D}_\eta}\Bigg|\left(\left(1 - \frac{z}{\delta^{1/2}}\right)e^{-z/\delta^{1/2}}V(0, \chi_1, \chi_2)\right)^2 \\ &\quad + \left(ze^{-z/\delta^{1/2}}\frac{\partial V(0, \chi_1, \chi_2)}{\partial\chi_1}\right)^2 + \left(ze^{-z/\delta^{1/2}}\frac{\partial V(0, \chi_1, \chi_2)}{\partial\chi_2}\right)^2\Bigg| \\ &\leq C\int_0^\infty (\frac{z}{\delta^{1/2}})^2 e^{-2z/\delta^{1/2}}dz \leq C\delta^{1/2}.\end{aligned}$$

We clearly have a similar estimate for $\|\nabla\phi\|_{L^2(\mathcal{D}_\eta)}$. Thus, we have

$$\left\|s^\delta\right\|_{L^2(\mathcal{D}_\eta)} \leq C\left\|\nabla\psi\right\|_{L^2(\mathcal{D}_\eta)}\left\|\nabla\phi\right\|_{L^2(\mathcal{D}_\eta)} \leq C\delta^{1/2}.$$

It follows ([24]) that

$$\left\|D^l s^\delta\right\|_{L^2(\mathcal{D}_\eta)} \leq C\delta^{1/2-l}.$$

We then extend the functions ψ, ϕ exponentially small to the whole of Ω by taking $\delta << \eta$ and s^δ will satisfy the estimate (2.22) cf. [24].

Q.E.D.

We will also need the boundary cut-off function, cf. [37], ζ^ε corresponding to $\partial\Omega$. Here, $\zeta^\varepsilon = 1$ on $\partial\Omega$ and $\text{supp}(\zeta^\varepsilon) \subset \{x \in \bar{\Omega} : \text{dist}(x, \partial\Omega) \leq \varepsilon\}$. With regularity conditions $\zeta^\varepsilon \in C^2(\bar{\Omega})$, for $0 \leq l \leq 2$ we have

$$\left\| D^l \zeta^\varepsilon \right\|_{L^\infty(\Omega)} \leq C\varepsilon^{-l}. \tag{2.23}$$

Now, we are ready to introduce the boundary corrector to the velocity

$$\begin{aligned}
\mathcal{V}^{\varepsilon\delta} = & \sum_{i=1}^{d} w^i \left(x, \frac{x}{\varepsilon}\right) \left(f_i - \frac{\partial p_0}{\partial x_i} - (K^{-1}s^\delta)_i\right) \\
& + \varepsilon \sum_{i=1}^{d} \beta^i \left(x, \frac{x}{\varepsilon}\right) (1 - \zeta^\varepsilon) \left(f_i - \frac{\partial p_0}{\partial x_i} - (K^{-1}s^\delta)_i\right) \\
& + \varepsilon \sum_{i,j=1}^{d} \gamma^{ij} \left(x, \frac{x}{\varepsilon}\right) (1 - \zeta^\varepsilon) \frac{\partial}{\partial x_j} \left(f_i - \frac{\partial p_0}{\partial x_i} - (K^{-1}s^\delta)_i\right),
\end{aligned} \tag{2.24}$$

and the boundary corrector to the pressure

$$\mathcal{P}^{\varepsilon\delta}(x) = p_0(x) + \varepsilon \sum_{i=1}^{d} \pi^i \left(x, \frac{x}{\varepsilon}\right) \left(f_i - \frac{\partial p_0}{\partial x_i} - (K^{-1}s^\delta)_i\right). \tag{2.25}$$

Using the Darcy relations (2.17) and taking the y average we obtain

$$\left\langle \mathcal{V}^{\varepsilon\delta} \right\rangle_{Y^x} = \xi - s^\delta \ , \ \left\langle \mathcal{P}^{\varepsilon\delta} \right\rangle_{Y^x} = p_0.$$

Thus, using the properties of $s^\delta, \zeta^\varepsilon$, for $x \in \partial\Omega$ we have $\mathcal{V}^{\varepsilon\delta} = \left\langle \mathcal{V}^{\varepsilon\delta} \right\rangle_{Y^x} = 0$ and $\mathcal{P}^{\varepsilon\delta} = \left\langle \mathcal{P}^{\varepsilon\delta} \right\rangle_{Y^x} = p_0$. Thus, we have a velocity boundary corrector that has vanishing trace. We must show that the boundary correctors are sufficiently close to the fine-scale velocity and pressure. The boundary correctors are close to the first order correctors by construction as they only differ, in a smooth enough manner, on a small

domain near the boundary. A simple triangle inequality argument will complete the proof of our main result.

We will use these quantities and estimates extensively throughout the proof of our main result. It will be useful for us then to introduce the notation that

$$A_i^\delta(x) = \left(f_i - \frac{\partial p_0}{\partial x_i} - (K^{-1}s^\delta)_i \right), \tag{2.26}$$

and then we summarize a few key estimates. We have from (2.22) that for $0 < l \leq 3$

$$\left\| D^l A^\delta \right\|_{L^q(\mathcal{F}_\varepsilon)} \leq C\delta^{1/q-l}, \tag{2.27}$$

where, $q \in [1, \infty]$ if $d = 2$ and $q = 2$ for $d = 3$. In addition, using (2.23) and the fact that $|\text{supp}(\zeta^\varepsilon)| = O(\varepsilon)$, we have the estimate for derivatives of the cut-off function in $L^q(\mathcal{F}_\varepsilon)$ given by

$$\left\| D^l \zeta^\varepsilon \right\|_{L^q(\mathcal{F}_\varepsilon)} \leq C|\text{supp}(\zeta^\varepsilon)|^{1/q} \left\| D^l \zeta^\varepsilon \right\|_{L^\infty(\mathcal{F}_\varepsilon)} \leq C\varepsilon^{1/q-l}. \tag{2.28}$$

b. Proof of Theorem II.1

Now that we have constructed our boundary correctors we will show that, for a good choice in δ, the boundary correctors are close to the fine-scale velocity and pressure $(v_\varepsilon, p_\varepsilon)$ in the slowly varying domain $\mathcal{F}_\varepsilon$. As noted prior we proceed in the same way as [24], but here we must adapt parts of the proof to account for the new β term. First, we have the following lemma for the divergence of the boundary corrector to the velocity.

Lemma II.3. Let $(\mathcal{V}^{\varepsilon\delta}, \mathcal{P}^{\varepsilon\delta})$ be given by (2.24),(2.25). Then, for $q \in [1, \infty]$ if $d = 2$ and $q = 2$ for $d = 3$, we have the estimate

$$\left\| \text{div} \left(\mathcal{V}^{\varepsilon\delta} \right) \right\|_{L^q(\mathcal{F}_\varepsilon)} \leq C\delta^{-1} \left(\varepsilon^{1/q} + \varepsilon\delta^{1/q-1} \right). \tag{2.29}$$

Proof. Taking the divergence of the corrector (2.24) using the two-scale divergence $\operatorname{div}(\cdot) \to \operatorname{div}_x(\cdot) + \frac{1}{\varepsilon}\operatorname{div}_y(\cdot)$ and noting that $\operatorname{div}_y(w) = 0$ we obtain

$$\begin{aligned}\operatorname{div}\left(\mathcal{V}^{\varepsilon\delta}\right) = &\sum_{i,j}^{d}\left(\frac{\partial w_j^i}{\partial x_j}A_i^\delta + w_j^i\frac{\partial A_i^\delta}{\partial x_j}\right)\\ &+\sum_{i,j=1}^{d}\frac{\partial \beta_j^i}{\partial y_j}(1-\zeta^\varepsilon)A_i^\delta + \sum_{i,j=1}^{d}\operatorname{div}_y\left(\gamma^{ij}\right)(1-\zeta^\varepsilon)\frac{\partial A_i^\delta}{\partial x_j}\\ &+\varepsilon\left(\sum_{i=1}^{d}\operatorname{div}_x\left(\beta^i(1-\zeta^\varepsilon)A_i^\delta\right) + \sum_{i,j=1}^{d}\operatorname{div}_x\left(\gamma^{ij}(1-\zeta^\varepsilon)\frac{\partial A_i^\delta}{\partial x_j}\right)\right),\end{aligned}$$

here A_i^δ is given by 2.26. From the relations (2.17) and the divergence free nature of s^δ we see that

$$\begin{aligned}0 &= \sum_{i,j=1}^{d}\frac{\partial}{\partial x_j}\left(K_{ij}\left(f_i - \frac{\partial p_0}{\partial x_i} - (K^{-1}s^\delta)_i\right)\right)\\ &= \sum_{i,j=1}^{d}\frac{\partial}{\partial x_j}\left(K_{ij}A_i^\delta\right) = \sum_{i,j=1}^{d}\left(\frac{\partial K_{ij}}{\partial x_j}A_i^\delta + K_{ij}\frac{\partial A_i^\delta}{\partial x_j}\right).\end{aligned} \tag{2.30}$$

Using the higher order cell equations in (2.18a),(2.19a) to relate derivatives of β, γ to w and its derivative, then multiplying (2.30) by $|Y_{\mathcal{F}}^x|^{-1}$ and using this to simplify we obtain

$$\begin{aligned}\operatorname{div}\left(\mathcal{V}^{\varepsilon\delta}\right) = &\sum_{i,j=1}^{d}\left(\frac{\partial w_j^i}{\partial x_j} - |Y_{\mathcal{F}}^x|^{-1}\frac{\partial K_{ij}}{\partial x_j}\right)A_i^\delta\zeta^\varepsilon + \sum_{i,j=1}^{d}\left(w_j^i - |Y_{\mathcal{F}}^x|^{-1}K_{ij}\right)\frac{\partial A_i^\delta}{\partial x_j}\zeta^\varepsilon\\ &+\varepsilon\left(\sum_{i=1}^{d}\operatorname{div}_x\left(\beta^i(1-\zeta^\varepsilon)A_i^\delta\right) + \sum_{i,j=1}^{d}\operatorname{div}_x\left(\gamma^{ij}(1-\zeta^\varepsilon)\frac{\partial A_i^\delta}{\partial x_j}\right)\right).\end{aligned}$$

We write $\operatorname{div}\left(\mathcal{V}^{\varepsilon\delta}\right) = \mathcal{O}_1 + \varepsilon\mathcal{O}_2 + \varepsilon\mathcal{O}_3$ splitting the $x-$divergence of the terms involving γ, β into two pieces $\varepsilon\mathcal{O}_2$ and $\varepsilon\mathcal{O}_3$. We write $\mathcal{O}_1$ as

$$\begin{aligned}\mathcal{O}_1 = &\sum_{i,j=1}^{d}\left(\frac{\partial w_j^i}{\partial x_j} - |Y_{\mathcal{F}}^x|^{-1}\frac{\partial K_{ij}}{\partial x_j}\right)A_i^\delta\zeta^\varepsilon \\ &+ \sum_{i,j=1}^{d}\left(w_j^i - |Y_{\mathcal{F}}^x|^{-1}K_{ij}\right)\frac{\partial A_i^\delta}{\partial x_j}\zeta^\varepsilon. \end{aligned} \tag{2.31}$$

For the next group of terms

$$\varepsilon\mathcal{O}_2 = \varepsilon\sum_{i,j=1}^{d}\left(\frac{\partial\beta_j^i}{\partial x_j}(1-\zeta^\varepsilon)A_i^\delta - \beta_j^i\nabla_x\zeta^\varepsilon A_i^\delta + \beta_j^i(1-\zeta^\varepsilon)\frac{\partial A_i^\delta}{\partial x_j}\right), \tag{2.32}$$

and the last term

$$\begin{aligned}\varepsilon\mathcal{O}_3 = &\varepsilon\sum_{i,j=1}^{d}\left(\left(\operatorname{div}_x\left(\gamma^{ij}\right)(1-\zeta^\varepsilon) - \gamma^{ij}\nabla_x\zeta^\varepsilon\right)\frac{\partial A_i^\delta}{\partial x_j}\right) \\ &+ \varepsilon\sum_{i,j=1}^{d}\gamma^{ij}(1-\zeta^\varepsilon)\nabla_x\frac{\partial A_i^\delta}{\partial x_j}. \end{aligned} \tag{2.33}$$

Now we wish to compute the L^q norm of the divergence of the velocity corrector

$$\left\|\operatorname{div}\left(\mathcal{V}^{\varepsilon\delta}\right)\right\|_{L^q(\mathcal{F}_\varepsilon)} = \left\|\mathcal{O}_1 + \varepsilon\mathcal{O}_2 + \varepsilon\mathcal{O}_3\right\|_{L^q(\mathcal{F}_\varepsilon)}.$$

Using (2.27),(2.28) and estimates of w, K and their derivatives

$$\left\|\mathcal{O}_1\right\|_{L^q(\mathcal{F}_\varepsilon)} \leq C\left(\varepsilon^{1/q}\delta^{1/q-1} + \varepsilon^{1/q}\delta^{1/q}\right).$$

Noting that $|\operatorname{supp}(1-\zeta^\varepsilon)| = O(1)$ independent of ε. Again, using (2.27-2.28) and the estimates for β, γ, and its derivatives, we have in a similar fashion

$$\left\|\varepsilon\mathcal{O}_2\right\|_{L^q(\mathcal{F}_\varepsilon)} \leq C\left(\varepsilon\delta^{1/q} + \varepsilon^{1/q}\delta^{1/q} + \varepsilon\delta^{1/q-1}\right),$$

and

$$\|\varepsilon \mathcal{O}_3\|_{L^q(\mathcal{F}_\varepsilon)} \leq C\left(\varepsilon\delta^{1/q-1} + \varepsilon^{1/q}\delta^{1/q-1} + \varepsilon\delta^{1/q-2}\right).$$

We combine these estimates and obtain

$$\left\|\mathrm{div}\left(\mathcal{V}^{\varepsilon\delta}\right)\right\|_{L^q(\mathcal{F}_\varepsilon)} \leq C\left(\varepsilon\delta^{1/q-2} + \varepsilon^{1/q}\delta^{1/q-1}\right).$$

Q.E.D.

Remark Note that the main elements of slowly varying geometry comes into play with the x-dependent permeability K. Thus, the need for relation (2.30) and the x-dependent w necessitates the estimate (2.32) involving β.

For the following estimates we will need the well known Poincare Inequality, cf. [9, 33], for perforated domains.

Lemma II.4. Let $\mathcal{F}_\varepsilon$ be a perforated domain with period size ε and $\phi \in H_0^1(\mathcal{F}_\varepsilon)$ then we have

$$\|\phi\|_{L^2(\mathcal{F}_\varepsilon)} \leq \varepsilon C \|\nabla\phi\|_{L^2(\mathcal{F}_\varepsilon)}. \tag{2.34}$$

Proof. See [9, 33].

Q.E.D.

We now wish to estimate the $H^{-1}(\mathcal{F}_\varepsilon)$ norm of the residual function

$$\Psi^\varepsilon = \Delta\mathcal{V}^{\varepsilon\delta} - \varepsilon^{-2}\nabla\mathcal{P}^{\varepsilon\delta} + \varepsilon^{-2}f,$$

and summarize the result in the next lemma. In the proof of this lemma we do not use the two-scale derivatives, so the scaling of the quantities must be carefully scrutinized. It is important to also note that for $d = 3$, we construct s^δ in the Lemma II.2 for the case of $q = 2$ only. However, the following results hold for both $d = 2, 3$ as we are concerned with $q = 2$ for our main result Theorem II.1.

Lemma II.5. Let $(\mathcal{V}^{\varepsilon\delta}, \mathcal{P}^{\varepsilon\delta})$ be given by (2.24),(2.25). We have the estimate

$$\|\Psi^{\varepsilon}\|_{H^{-1}(\mathcal{F}_{\varepsilon})} \leq C\left(\varepsilon^{-1}\delta^{1/2} + \delta^{-1/2} + \varepsilon\delta^{-3/2}\right). \tag{2.35}$$

Proof. For any function $\phi \in H_0^1(\mathcal{F}_{\varepsilon})$ we have

$$\langle \Psi^{\varepsilon} | \phi \rangle = \int_{\mathcal{F}_{\varepsilon}} \left(\Delta \mathcal{V}^{\varepsilon\delta} - \varepsilon^{-2}\nabla \mathcal{P}^{\varepsilon\delta} + \varepsilon^{-2} f\right)\phi. \tag{2.36}$$

Integrating the Laplacian term by parts we have

$$\begin{aligned}\int_{\mathcal{F}_{\varepsilon}} \Delta \mathcal{V}^{\varepsilon\delta}\phi = &\sum_{i=1}^{d} \int_{\mathcal{F}_{\varepsilon}} \Delta\left(w^i A_i^{\delta}\right)\phi \\ &- \varepsilon \sum_{i,j=1}^{d} \int_{\mathcal{F}_{\varepsilon}} \nabla\left(\gamma^{ij}(1-\zeta^{\varepsilon})\frac{\partial A_i^{\delta}}{\partial x_j}\right)\nabla\phi \\ &- \varepsilon \sum_{i=1}^{d} \int_{\mathcal{F}_{\varepsilon}} \nabla\left(\beta^i(1-\zeta^{\varepsilon})A_i^{\delta}\right)\nabla\phi.\end{aligned}$$

Rearranging the terms and using the integrated Laplacian above we may write the inner product as

$$\begin{aligned}\langle \Psi^{\varepsilon} | \phi \rangle = &\sum_{i=1}^{d} \int_{\mathcal{F}_{\varepsilon}} \left(\Delta w^i - \varepsilon^{-1}\nabla \pi^i\right) A_i^{\delta}\phi - \varepsilon^{-2}\int_{\mathcal{F}_{\varepsilon}} (\nabla p_0 - f)\phi \\ &+ \int_{\mathcal{F}_{\varepsilon}} \Psi_2^{\varepsilon}\phi - \int_{\mathcal{F}_{\varepsilon}} \nabla\Psi_3^{\varepsilon}\nabla\phi - \int_{\mathcal{F}_{\varepsilon}} \nabla\Psi_4^{\varepsilon}\nabla\phi,\end{aligned}$$

where

$$\Psi_2^{\varepsilon} = \sum_{i=1}^{d} \left(\left(2\nabla w^i - \varepsilon^{-1}\pi^i\right)\nabla A_i^{\delta} + w^i \Delta A_i^{\delta}\right),$$

and

$$\Psi_3^{\varepsilon} = \varepsilon \sum_{i,j=1}^{d} \gamma^{ij}(1-\zeta^{\varepsilon})\frac{\partial A_i^{\delta}}{\partial x_j},$$

and the term due to slowly varying geometry

$$\Psi_4^\varepsilon = \varepsilon \sum_{i=1}^{d} \beta^i (1-\zeta^\varepsilon) A_i^\delta.$$

Since the derivatives are not two-scale derivatives we note that after taking a derivative of an oscillatory function we get a negative exponential power of ε^{-1}. Thus, we have $(\Delta w^i - \varepsilon^{-1}\nabla\pi^i) = O(\varepsilon^{-2})$ and so using (2.27) and (2.34), and the Cauchy-Schwarz inequality,

$$\begin{aligned}
&\left| \sum_{i=1}^{d} \int_{\mathcal{F}_\varepsilon} \left(\Delta w^i - \varepsilon^{-1}\nabla\pi^i\right) A_i^\delta \phi - \varepsilon^{-2} \int_{\mathcal{F}_\varepsilon} (\nabla p_0 - f)\phi \right| \\
&\leq C \left| \int_{\mathcal{F}_\varepsilon} \left(-\varepsilon^{-2}(f - \nabla p_0 - (K^{-1}s^\delta))\phi - \varepsilon^{-2}(\nabla p_0 - f)\phi\right) \right| \\
&\leq C\varepsilon^{-1}\delta^{1/2} \left\|\nabla\phi\right\|_{L^2(\mathcal{F}_\varepsilon)}.
\end{aligned}$$

Now for the second term, using the fact that $(2\nabla w^i - \varepsilon^{-1}\pi^i) = O(\varepsilon^{-1})$ and again equations (2.27) and (2.34) we obtain

$$\begin{aligned}
\left| \int_{\mathcal{F}_\varepsilon} \Psi_2^\varepsilon \phi \right| &\leq \sum_{i=1}^{d} \left| \int_{\mathcal{F}_\varepsilon} \left(\left(2\nabla w^i - \varepsilon^{-1}\pi^i\right) \nabla A_i^\delta \phi + w^i \Delta A_i^\delta \phi\right) \right| \\
&\leq C\delta^{-1/2} \left(1 + \varepsilon\delta^{-1}\right) \left\|\nabla\phi\right\|_{L^2(\mathcal{F}_\varepsilon)}.
\end{aligned}$$

For the next two terms we have the ζ^ε terms and will need the estimates (2.27),(2.28) and noting $\nabla\gamma = O(\varepsilon^{-1})$ we have

$$\begin{aligned}
\left| \int_{\mathcal{F}_\varepsilon} \nabla\Psi_3^\varepsilon \nabla\phi \right| &\leq \varepsilon \sum_{i,j=1}^{d} \left| \int_{\mathcal{F}_\varepsilon} \nabla \left(\gamma^{ij}(1-\zeta^\varepsilon)\frac{\partial A_i^\delta}{\partial x_j}\right) \nabla\phi \right| \\
&\leq C \left(\delta^{-1/2} + \varepsilon^{1/2}\delta^{-1/2} + \varepsilon\delta^{-3/2}\right) \left\|\nabla\phi\right\|_{L^2(\mathcal{F}_\varepsilon)}.
\end{aligned}$$

We have the new term Ψ_4^ε involving β and its derivatives that results from slowly varying geometry. Note that here too we have $\nabla\beta = O(\varepsilon^{-1})$ again estimating in a

similar way as the previous term using (2.27),(2.28) we compute

$$\left| \int_{\mathcal{F}_\varepsilon} \nabla \Psi_4^\varepsilon \nabla \phi \right| \leq \varepsilon \sum_{i=1}^{d} \left| \int_{\mathcal{F}_\varepsilon} \nabla \left(\beta^i (1-\zeta^\varepsilon) A_i^\delta \right) \nabla \phi \right|$$
$$\leq C \left(\delta^{1/2} + \varepsilon^{1/2} \delta^{1/2} + \varepsilon \delta^{-1/2} \right) \|\nabla \phi\|_{L^2(\mathcal{F}_\varepsilon)}. \tag{2.37}$$

Using the fact that ε^{-1} is sufficiently large so that $\delta^{1/2} < C\varepsilon^{-1}\delta^{1/2}$, $\varepsilon^{1/2}\delta^{1/2} < C\varepsilon^{-1}\delta^{1/2}$, and $\varepsilon\delta^{-1/2} < C\delta^{-1/2}$ we are able to bound the estimate (2.37) with the other terms in the inner product. Combining all these estimates together we obtain the result

$$\left| \langle \Psi^\varepsilon | \phi \rangle \right| \leq \left| \int_{\mathcal{F}_\varepsilon} -\varepsilon^{-2}(f - \nabla p_0 - K^{-1} s^\delta)\phi + \varepsilon^{-2}(f - \nabla p_0)\phi \right|$$
$$+ \left| \int_{\mathcal{F}_\varepsilon} \Psi_2^\varepsilon \phi \right| + \left| \int_{\mathcal{F}_\varepsilon} \nabla \Psi_3^\varepsilon \nabla \phi \right| + \left| \int_{\mathcal{F}_\varepsilon} \nabla \Psi_4^\varepsilon \nabla \phi \right|$$
$$\leq C \left(\varepsilon^{-1}\delta^{1/2} + \delta^{-1/2} + \varepsilon \delta^{-3/2} \right) \|\nabla \phi\|_{L^2(\mathcal{F}_\varepsilon)}.$$

Taking the supremum over all $\phi \in H_0^1(\mathcal{F}_\varepsilon)$ we obtain our norm estimate.

Q.E.D.

We are almost in a position to prove our main result. We denote the differences as $z_\varepsilon = v_\varepsilon/\varepsilon^2 - \mathcal{V}^{\varepsilon\delta}$ and $\Xi_\varepsilon = p_\varepsilon - \mathcal{P}^{\varepsilon\delta}$. The differences satisfy the Stokes equation with scaled ε^2 residual

$$-\varepsilon^2 \Delta z_\varepsilon + \nabla \Xi_\varepsilon = \varepsilon^2 \Psi^\varepsilon.$$

After extending z_ε by zero into the solid domain $\mathcal{S}_\varepsilon$, and using the pressure extension methods by Tartar [35] we have the following lemma.

Lemma II.6. There exists a pressure extension of Ξ_ε to $\tilde{\Xi}_\varepsilon \in L_0^2(\Omega)$ such that

$$\left\| \tilde{\Xi}_\varepsilon \right\|_{L_0^2(\Omega)} \leq C\varepsilon \left(\|\Psi^\varepsilon\|_{H^{-1}(\mathcal{F}_\varepsilon)} + \|\nabla z_\varepsilon\|_{L^2(\mathcal{F}_\varepsilon)} \right). \tag{2.38}$$

Proof. See [20].

Q.E.D.

Corollary II.7. We recall the following estimates

$$\|\nabla z_\varepsilon\|_{L^2(\mathcal{F}_\varepsilon)} \leq C\left(\|\Psi^\varepsilon\|_{H^{-1}(\mathcal{F}_\varepsilon)} + \varepsilon^{-1}\left\|\text{div}\left(\mathcal{V}^{\varepsilon\delta}\right)\right\|_{L^2(\mathcal{F}_\varepsilon)}\right), \tag{2.39}$$

$$\|z_\varepsilon\|_{H(\Omega,\text{div})} \leq C\left(\varepsilon\|\Psi^\varepsilon\|_{H^{-1}(\mathcal{F}_\varepsilon)} + \left\|\text{div}\left(\mathcal{V}^{\varepsilon\delta}\right)\right\|_{L^2(\mathcal{F}_\varepsilon)}\right). \tag{2.40}$$

We now have all the auxiliary results needed to state and prove a theorem concerning the closeness of the boundary correctors to $(v_\varepsilon, p_\varepsilon)$.

Theorem II.8. Let $(v_\varepsilon, p_\varepsilon)$ be solutions to (2.2) in the slowly varying domain $\mathcal{F}_\varepsilon$. Let $\mathcal{V}^{\varepsilon\delta}$ be given by (2.24) and the macroscopic pressure p_0 as in (2.17). Then,

$$\left\|v_\varepsilon/\varepsilon^2 - \mathcal{V}^{\varepsilon\delta}\right\|_{H(\Omega,\text{div})} \leq C\varepsilon^{1/6}, \tag{2.41}$$

$$||p_\varepsilon - p_0||_{L^2_0(\Omega)} \leq C\varepsilon^{1/6}. \tag{2.42}$$

Proof. Once we insert (2.29) and (2.35) into (2.40) we obtain the result

$$\begin{aligned}\left\|v_\varepsilon/\varepsilon^2 - \mathcal{V}^{\varepsilon\delta}\right\|_{H(\Omega,\text{div})} &\leq C\left(\varepsilon\|\Psi^\varepsilon\|_{H^{-1}(\mathcal{F}_\varepsilon)} + \left\|\text{div}\left(\mathcal{V}^{\varepsilon\delta}\right)\right\|_{L^2(\mathcal{F}_\varepsilon)}\right)\\ &= C\left(\delta^{1/2} + \varepsilon\delta^{-1/2} + \varepsilon^2\delta^{-3/2} + \delta^{-1}\varepsilon^{1/2} + \varepsilon\delta^{-3/2}\right).\end{aligned}$$

Choosing $\delta >> \varepsilon$ and so $\delta = \varepsilon^\alpha$ implies

$$\left\|v_\varepsilon/\varepsilon^2 - \mathcal{V}^{\varepsilon\delta}\right\|_{H(\Omega,\text{div})} \leq C\left(\varepsilon^{\alpha/2} + \varepsilon^{1-3\alpha/2} + \varepsilon^{1/2-\alpha}\right).$$

Letting $\alpha = 1/3$ we obtain our result. For the pressure estimate we plug (2.39) into (2.38) and repeat the argument above. We obtain the desired estimate on the pressure error.

Q.E.D.

Proof of Theorem II.1. We now have all the ingredients needed to prove our main result. Noting that the first order corrector $v_0 + \varepsilon v_1$ and $\mathcal{V}^{\varepsilon\delta}$ are close, order $\varepsilon^{1/6}$ or better by construction, and combining this with the results in Theorem II.8 we have via a simple triangle inequality

$$\begin{aligned} &\left\|v_\varepsilon/\varepsilon^2 - (v_0 + \varepsilon v_1)\right\|_{H(\Omega,\mathrm{div})} \\ &\leq \left\|v_\varepsilon/\varepsilon^2 - \mathcal{V}^{\varepsilon\delta}\right\|_{H(\Omega,\mathrm{div})} + \left\|\mathcal{V}^{\varepsilon\delta} - (v_0 + \varepsilon v_1)\right\|_{H(\Omega,\mathrm{div})} \qquad \leq C\varepsilon^{1/6}. \end{aligned} \tag{2.43}$$

Again, for the pressure estimate we plug (2.39) into (2.38) and repeat the argument above. We obtain the desired estimate on the pressure error.

Q.E.D.

C. Moving Averages Homogenization Scheme

In this section we present two numerical examples, that illustrate the convergence results obtained in Theorem II.1. First, we discuss some aspects of implementing a moving averages homogenization.

1. Numerical Implementation of a Moving Averages Homogenization

In periodic media, one has to compute a set of cell problem solutions at a single spatial location. Using these solutions, the upscaled permeability tensor is computed that is constant throughout the macroscopic domain Ω. Moreover, assuming the coarse pressure p is sufficiently smooth, correctors based on the expansion (2.4) naturally inherit the same regularity as the cell solutions.

The moving averages homogenization scheme generates a variable $K(x)$. Its values at any given x is computed by averaging the solution of the cell problem

solution (2.14). In practice, one cannot compute $K(x)$ everywhere for all $x \in \Omega$ and there is no need for such expensive computations. Depending on the discretization of (2.17) the values of $K(x)$ are needed at specific integration points.

In order to have a consistent interpolation scheme for $K(x)$ which also generates an approximation to downscaled quantities, we consider a generic conforming grid $\mathcal{T}_H$ over Ω and a conforming finite element discretization with nodal basis functions $\{\theta_i\}_{i=1}^N$ of polynomial order α. Denote the corresponding nodes by x_i, e.g., $\theta_i(x_i) = 1$ and zero for any other node. Now, one can compute $K(x_i)$ and use the FEM space to interpolate it elsewhere, e.g., $K(x) \approx \sum_{i=1}^N K(x_i)\theta_i(x)$.

One can also construct downscaled quantities. Take, for example v_0 defined in (2.13). First, fix x_j, compute $w^i(x_j, y)$, and extend it periodically into all neighboring cells. Then, construct the approximation $\hat{v}_0$ as follows:

$$\hat{v}_0 = \sum_{j=1}^{N} \theta_j(x) \left(\sum_{i=1}^{d} w^i(x_j, y) \left(f_i - \frac{\partial p_0}{\partial x_i} \right) \right). \tag{2.44}$$

Observe that $\{\theta_i\}_{i=1}^N$ is a partition of unity. One can in fact use any other suitable partition of unity over $\mathcal{T}_H$, leading to different downscaling projections.

In this work we use the simplest possible choice for $\mathcal{T}_H$ and $\{\theta\}_{i=1}^N$. Given a regular partition of Ω into cells $\{\varepsilon Y^i\}_{i=1}^N$ with $Y^i = Y_{\mathcal{F}}^i \cup Y_{\mathcal{S}}^i$ (see equation (2.1)), $\mathcal{T}_H$ is the staggered grid, e.g., its vertices are the centers of εY^i. In 2D this means a rectangular grid with vertices at $(\varepsilon(0.5+i), \varepsilon(0.5+j))$, $i, j = 1, \ldots, 1/\varepsilon$. We use the standard bilinear finite element basis functions as $\{\theta_i\}_{i=1}^N$.

2. A Synthetic Geometry

Here, we consider a periodic array of elliptical inclusions with slowly varying major and minor axis lengths. The inclusions populate a unit-sized macroscopic domain

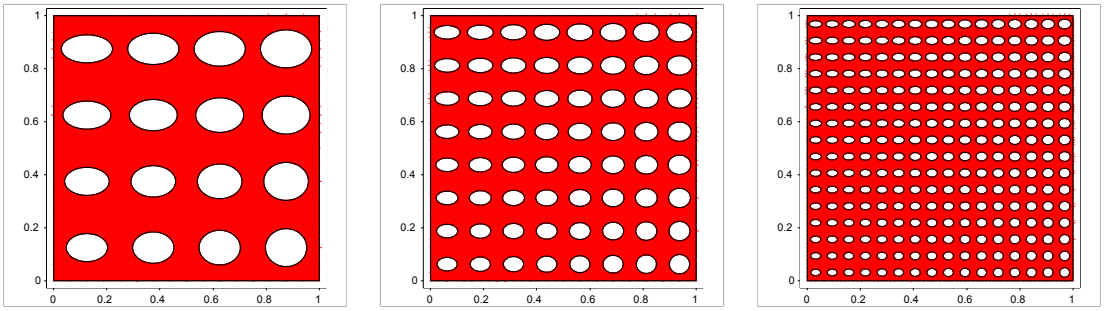

(a) $\varepsilon = 1/4$ (b) $\varepsilon = 1/8$ (c) $\varepsilon = 1/16$

Fig. 1. A series of slowly changing elliptical inclusions.

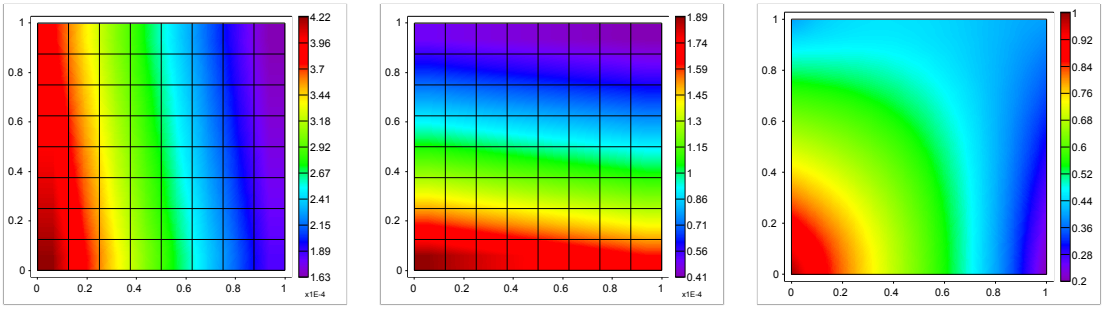

(a) K_{11} (b) K_{22} (c) Coarse pressure

Fig. 2. Upscaled permeability tensor (a, b) and coarse pressure (c) ($\varepsilon = 1/8$).

$\Omega = [0, 1]^2$. The centers of the inclusions are regularly spaced in both directions with step $1/\varepsilon$. Both axes of each inclusion are aligned with the coordinate directions. The major and minor axis lengths vary as follows: the x-axis has radius $0.3 + y/10$ and the y-axis has radius $0.2 + x/10$, where x and y are the coordinates of the inclusions' center (Figure 1). We observe the upscaled permeabilities $K11$ and $K22$ and coarse scale pressure in Figure 2.

We solve the Stokes equations (2.2) on a sequence of domains with $\varepsilon^{-1} = 4, 8, 16, 32, 64$. The fine-scale solutions are obtained using the $\mathbb{P}_2/\mathbb{P}_1$ Taylor-Hood triangular finite element, cf. e.g., [5]. The macroscopic problems are solved using standard quadratic triangular finite elements. For all cases, the following fine-scale

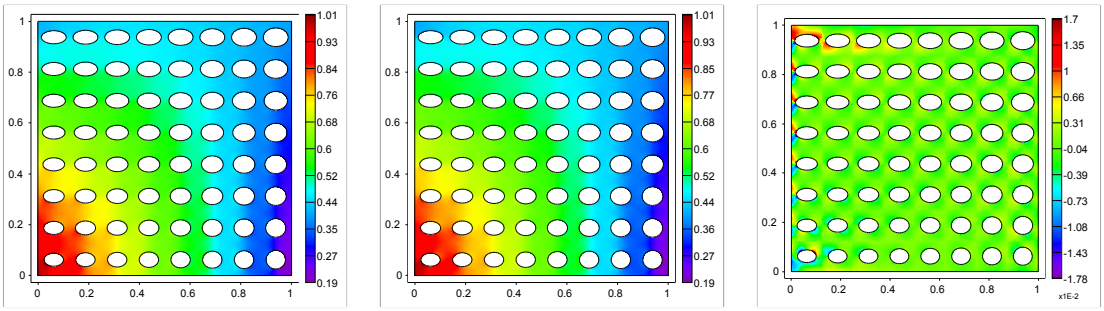

(a) Fine-scale pressure (b) Downscaled pressure (c) Error

Fig. 3. Fine-scale pressure obtained via DNS (a), downscaled pressure (b) and error (c) ($\varepsilon = 1/8$).

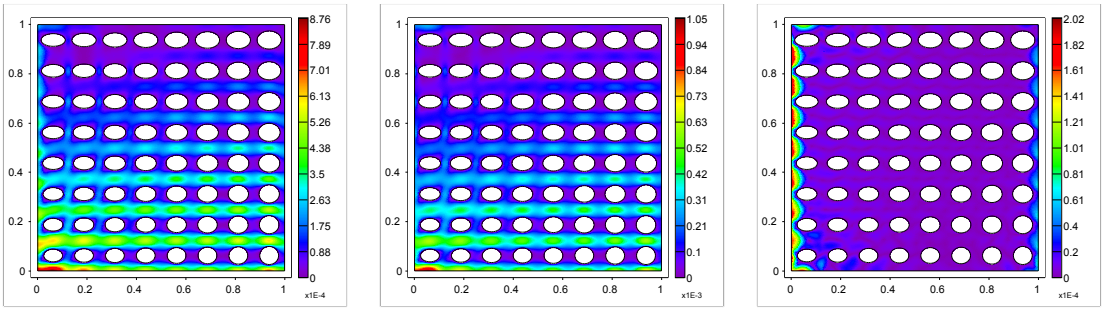

(a) Fine-scale velocity (b) Downscaled velocity (c) Error

Fig. 4. Fine-scale velocity (magnitude) obtained via DNS (a), downscaled velocity (b) and error (c) ($\varepsilon = 1/8$).

boundary value problem is considered: at $x = 0$, the pressure is set to $p = 1 - 0.6y$ and at $x = 1$ it is $p = 0.2(1 + y)$. At the top ($y = 1$) and bottom ($y = 0$) of the macroscopic domains we apply symmetry boundary conditions, e.g., $v_2 = 0$. Naturally, at the interface of each inclusion, no slip boundary conditions are applied. In all cases, the fluid viscosity is set to $\mu = 1$. Typical fine-scale velocity and pressure profiles for $\varepsilon = 8^{-1}$ are shown in Figures 3 and 4, respectively. We observe that there is very little qualitative difference between the DNS and downscaled approximations. The error is primarily concentrated at the $x = 0$ boundary.

Simultaneously we have homogenized each of the above problems. The homogenization is performed at the centers of each cell $(\varepsilon(0.5+i), \varepsilon(0.5+j))$, $i, j = 1, \ldots, 1/\varepsilon$, and the permeability computed and interpolated bilinearly in between.The interpolated $K(x)$ field and the computed coarse pressure for the case of $\varepsilon = 1/8$ are shown in Figure 2. We observe a varying permeability field. The slowly varying geometry has a noticeable effect on the macroscopic pressure distribution.

The downscaling is performed at the center of each cell. This defines pointwise values for velocity and pressure at each center $(\varepsilon(0.5+i), \varepsilon(0.5+j))$, $i, j = 1, \ldots, 1/\varepsilon$. Values at intermediate locations are then constructed by interpolating neighboring solutions via a partition of unity. The resulting downscaled fields are compared against a direct numerical simulation over the entire fine-scale domain. The results are reported in Table I. We observe better than theoretical convergence rates.

3. A Geometry Driven by Fluid-Structure Interaction

In this example we homogenize the Stokes equation over a fine-scale domain, associated with a Fluid-Structure Interaction problem. Fluid-Structure problems are examples of a process that can generate slowly changing geometries. We briefly describe this first.

Table I. Relative error in downscaled fields for elliptical obstacle geometry. All norms are computed over the fine-scale fluid domain $\mathcal{F}_\varepsilon$.

ε^{-1}	Velocity			Pressure	
	L^2	H^1	L^∞	L^2	H^1
4	$1.66\varepsilon{-}1$	$2.34\varepsilon{-}1$	0.27	$1.14\varepsilon{-}2$	$2.96\varepsilon{-}1$
8	$1.22\varepsilon{-}1$	$1.66\varepsilon{-}1$	0.23	$3.68\varepsilon{-}3$	$2.06\varepsilon{-}1$
16	$8.79\varepsilon{-}2$	$1.27\varepsilon{-}1$	0.20	$1.17\varepsilon{-}3$	$1.39\varepsilon{-}1$
32	$6.26\varepsilon{-}2$	$8.44\varepsilon{-}2$	0.18	$3.88\varepsilon{-}4$	$1.08\varepsilon{-}1$
64	$4.45\varepsilon{-}2$	$6.13\varepsilon{-}2$	0.16	$1.54\varepsilon{-}4$	$9.16\varepsilon{-}2$

a. Static Fluid-Structure Interaction

In an FSI problem, one has two domains, a fluid $\mathcal{F}_\varepsilon$ and a solid $\mathcal{S}_\varepsilon$. The solid is assumed deformable, and we assume linearized elasticity. The fluid is a Newtonian one, subject to the Stokes approximation. The solid deforms due to stresses at the interface Γ_ε with the fluid. We consider the stationary FSI problem, e.g., the fluid velocity has reached a stationary regime, while the solid deformation is steady state. In such a regime, the fluid is described by the Stokes equation (2.2) with no slip conditions on Γ_ε. The solid on the other hand is described on the reference domain $\mathcal{S}_\varepsilon^\#$, which we assume periodic. The deformation has the form (2.11). In this set-up the appropriate stress measure in the solid is the Piola-Kirchoff stress. It is denoted by S and is assumed a known function of the linearized strain $e(u_\varepsilon)$. With this the FSI problem is compactly written as follows: Find the interface Γ_ε, fluid velocity and pressure v_ε, p_ε, and the solid displacement u_ε, such that

$$\Gamma_\varepsilon = \left\{ p + u_\varepsilon(p) | \ \forall \ p \in \Gamma_\varepsilon^\# \right\}, \tag{2.45}$$

the Stokes equation (2.2), which we restate for clarity and assume general viscosity μ, is satisfied in the a-priori unknown domain $\mathcal{F}_\varepsilon$, that is

$$-\mu\Delta v_\varepsilon + \nabla p_\varepsilon = f, \qquad \nabla\cdot v_\varepsilon = 0 \qquad \text{in } \mathcal{F}_\varepsilon, \tag{2.46}$$

the balance of linear momentum in the solid holds

$$-\nabla\cdot S\left(e\left(u_\varepsilon\right)\right) = f_0 \qquad \text{in } \mathcal{S}_\varepsilon^{\#}, \tag{2.47}$$

here $S(e(u_\varepsilon))$ is the Piola-Kirkoff tensor. In our case, this will be the linear elastic tensor. Finally, the continuity of traction across the interface also holds

$$\det(\nabla u_\varepsilon + I)\left(p_\varepsilon I - 2\mu D\left(v_\varepsilon\right)\right)\left(\nabla u_\varepsilon + I\right)^{-T} n_0 = S\left(e\left(u_\varepsilon\right)\right) n_0 \qquad \text{on } \Gamma_\varepsilon^{\#}, \tag{2.48}$$

where I is the identity matrix and n_0 is the unit normal on $\Gamma_\varepsilon^{\#}$. In the last equation, $D(v_\varepsilon) = \frac{1}{2}\left(\nabla v_\varepsilon(x) + \nabla v_\varepsilon(x)^T\right)$. The left hand side is the fluid stress mapped back to the reference configuration and the right hand side is the solid stress. Note that this coupling condition makes the FSI problems nonlinear, regardless of the constitutive law employed for the solid.

b. Implementation of Method on FSI Geometry

To generate a series of fine-scale fluid geometries, we mimic a fractured porous medium geometry. We consider a reference solid domain $\mathcal{S}_\varepsilon^{\#}$ consisting of square obstacles of dimension 0.95ε. In the reference domain these obstacles are periodically arranged and each is supported rigidly at its center. The fluid occupies the remaining pore-space, e.g., $\mathcal{F}_\varepsilon^{\#} = [0,1]^2 \setminus \mathcal{S}_\varepsilon^{\#}$. This pore-space is a set of horizontal and vertical fractures of aperture 0.5. We assume linear isotropic solid with Young's modulus $E = 4$ and Poisson ration $\nu = 0.3$. The fluid has viscosity $\mu = 0.1$. The flow is driven by a pressure $p = 1 - 0.8y$ specified at $x = 0$ and $p = 0.2(1 + y)$ at $x = 1$. We also

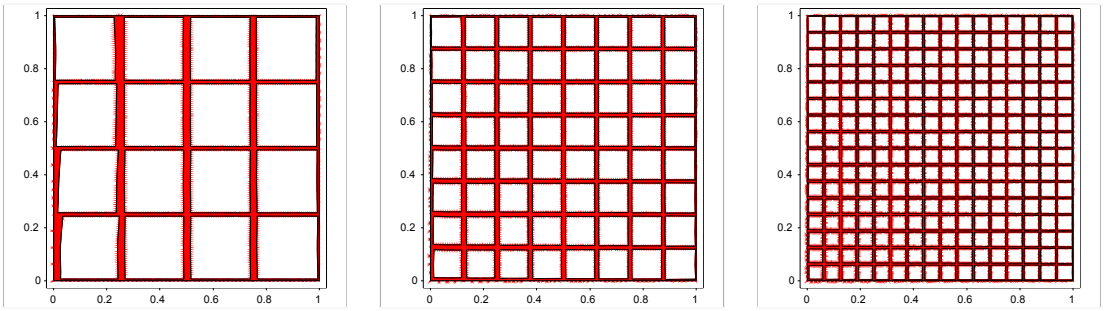

(a) $\varepsilon = 1/4$ (b) $\varepsilon = 1/8$ (c) $\varepsilon = 1/16$

Fig. 5. A series of fine-scale domains obtained by solving a Fluid-Structure Interaction problem. Colored in red is the deformed pore space $\mathcal{F}_\varepsilon$.

apply symmetric boundary conditions at $y = 0$ and $y = 1$.

This set-up leads to a significant deformation of the pore-space as shown in Figure 5. To solve the FSI problem numerically, we use a simple iterative procedure described in [19, 30]. Observe that the deformed shape of each solid inclusion is no longer a square. In fact all symmetry is lost and each inclusion differs from its neighbors. Compared to the reference geometry, the pore-space is significantly changed. Along the length of each channel, the aperture changes by up to two times from left to right.

Once the FSI problem is solved, we extract the fluid domain and perform the same type of calculations as in the previous elliptical geometry example. Typical fine-scale pressures and velocity fields (the 8×8 case) are shown in Figures 6 and 7, respectively. The error between the fine-scaled and downscaled quantities is reported in Table II. The same general observations regarding the convergence of the downscaled solutions can be made as in the previous example. The error in pressure has a more complicated structure than the elliptical obstacles, but the downscaled velocity remains close to the fine-scale velocity field.

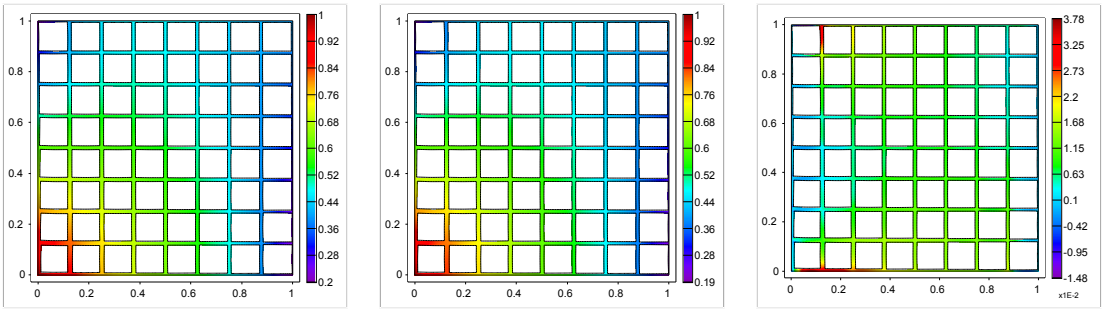

(a) Fine-scale pressure (b) Downscaled pressure (c) Error

Fig. 6. Fine-scale pressure obtained via DNS (a), downscaled pressure (b) and error (c) ($\varepsilon = 1/8$).

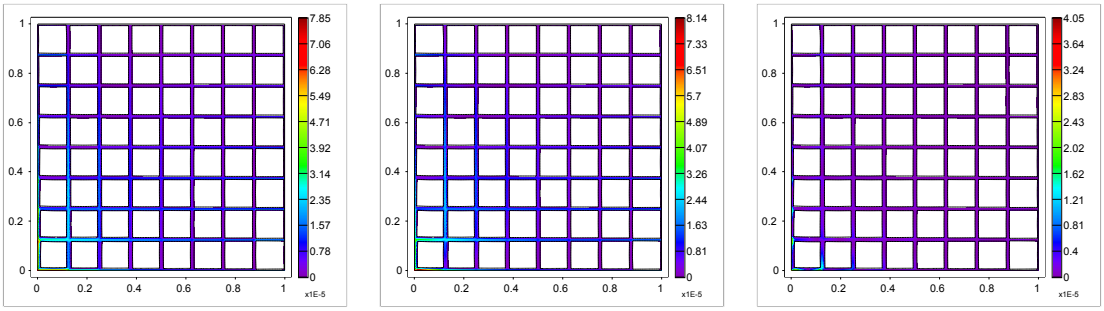

(a) Fine-scale velocity (b) Downscaled velocity (c) Error

Fig. 7. Fine-scale velocity (magnitude) obtained via DNS (a), downscaled velocity (b) and error (c) ($\varepsilon = 1/8$).

Table II. Relative error in downscaled fields for fluid-structure interaction geometry. All norms are computed over the fine-scale fluid domain $\mathcal{F}_\varepsilon$.

ε^{-1}	Velocity			Pressure	
	L^2	H^1	L^∞	L^2	H^1
4	0.554	0.5904	0.749	$3.61\varepsilon{-}2$	0.887
8	0.195	0.2509	0.516	$1.89\varepsilon{-}2$	0.267
16	0.106	0.1634	0.359	$5.07\varepsilon{-}3$	0.199

CHAPTER III

NONLINEAR HOMOGENIZATION OF FLUID-STRUCTURE INTERACTION

In the previous chapter, we discussed homogenization of Stokes flow in domains that are slowly varying. We are given a domain that was initially periodic, then through some *a-priori* known physical process the domain becomes slowly varying. The example of prime importance being that of Fluid-Structure Interaction. This is essentially a decoupled homogenization process. For example, in [32], the fluid and mechanics solves are computed iteratively which leads to an effective decoupled multiscale algorithm. We will now consider a fully coupled homogenization procedure.

In this chapter, we consider the coupling of Stokes fluid flow ([36]) with that of linear elastic mechanics ([17]) of a connected solid structure pore network with initially periodic microstructure. We may consider more complicated consitutive relations for the solid material, but we restrict our attention to linear elasticity for simplicity. The difficulties in modeling such interaction is two fold. First the complicated microstructure of the fluid-solid material makes exact resolution of all phenomena not possible and often undesirable. An "upscaled" or averaged description is more feasible and desirable. Second, classically the governing equations for each respective domain are presented in different coordinate systems.

The fluid flow equations are presented in the Eulerian description or current configuration. This is natural for fast flowing materials as one wants to know the fluid velocity at a certain point in space and time. On the other hand solid mechanics is presented in the fixed frame Lagrange description. In the theory of solid mechanics the solid domain has some reference configuration and we wish to model the deformation from that initial reference configuration to some deformed configuration. When coupling these two processes this coordinate difference presents a challenge both in

numerical solution of the FSI problem and properly homogenizing and upscaling the physics in a complicated microstructure.

It is advantageous to have both equations in the fixed reference frame for our application. This formulation is the so called Arbitrary Lagrangian-Eulerian (ALE) framework. ([15]). Once we represent the governing equations in the reference configuration by this approach, both the fluid flow and solid mechanics are in the same periodic reference domain. This periodicity will allow us justify formal asymptotic expansions, as in [33], to derive local cell problems and global upscaled macroscopic equations for the deformable porous media.

The Chapter is organized as follows. First, we present the necessary background where we develop the fine-scale FSI model cf. [32]. Then, we recall the periodic homogenization of the linear infinitesimal pore-scale Biot model as in [8]. We then homogenize the nonlinear fine-scale FSI model via. the use of the ALE formulation. From here nonlinear Biot equations are derived. Finally, we present simplifications of the nonlinear model and a related numerical example.

A. Background

In this section, we provide the background needed to develop a homogenized model of FSI. We first present the background material of the fine-scale FSI model. We present the fluid equations in the moving Eulerian frame and then, the solid mechanics equations in fixed Lagrangian frame. The models are coupled at the fluid-solid interface. The interface velocities interface must be continuous. Similarly, the traction at the interface must be continuous.

We then recall homogenization of the linear problem. In the case of nontrivial pore-scale deformation, the continuity of traction boundary condition is the primary

source of the nonlineary. In the linear case, the equations are presented in a unified fixed frame. The traction boundary condition becomes is linear. In this setting, we apply two-scale asymptotic techniques. We derive fluid and solid auxiliary cell problems that depend on geometry only. After averaging, we obtain the linear form of the macroscale Biot equations.

1. Fine-Scale FSI Problem

We begin with some notation. We assume that there is an initial reference domain $\Omega \subset \mathbb{R}^d$. Contained in the reference domain there is solid pore network with $\mathcal{S}_\varepsilon$ with characteristic pore size ε. The pores can exhibit complex geometries. Inside the pore-space is the initial fluid domain $\mathcal{F}_\varepsilon = \Omega \backslash \mathcal{S}_\varepsilon$. We assume the fluid domain is connected so that the flow will be nontrivial. The initial fluid solid interface $\Gamma_\varepsilon = \mathcal{F}_\varepsilon \cap \mathcal{S}_\varepsilon$. We denote the coordinates of the initial reference configuration by x.

We assume that there is a smooth deformation of the medium. Indeed, we let $X_\varepsilon(x,t) : \Omega \to \Omega(t)$, be the deformation of the initial reference domain to the deformed current domain at time t. The current interface at time t is given by

$$\Gamma_\varepsilon(t) = \{X_\varepsilon(x,t) | x \in \Gamma_\varepsilon\},$$

and, similarly, the current fluid and solid domains are given by $\mathcal{F}_\varepsilon(t) = X_\varepsilon(\mathcal{F}_\varepsilon, t)$ and $\mathcal{S}_\varepsilon(t) = X_\varepsilon(\mathcal{S}_\varepsilon, t)$. In general, X_ε can arise from various coupled phenomena, however, we focus our attention on mechanical based deformation. In the mechanics setting, we may write the deformation as $X_\varepsilon(x,t) = x + u_\epsilon(x,t)$, where $u_\varepsilon(x,t)$ is the solid displacement. The displacement can be computed by solving an elasticity problem with nonlinear interface to be described below. This deformation defines a coordinate system in X for the Eulerian or current configuration.

We begin by presenting the incompressible Navier-Stokes equations. These equa-

tions are naturally presented in the current or Eulerian configuration. Scaling of physicical quantities will be very important for us here. We assume the microstructure is scaled in such a way that the full time derivative term, the nonlinear convective term, is of order ε^2 cf. [21]. The assumption is physically viable for creeping flow in complex pore geometries. The fluid pore space is assumed to be occupied with a Newtonian fluid with viscosity μ. Such a fluid satisfies the equation of motion

$$\mathrm{div}_X(\widetilde{T}_\varepsilon^f) = \varepsilon^2 \frac{d\tilde{v}_\varepsilon}{dt} + \tilde{f} \text{ in } \mathcal{F}_\varepsilon(t), \tag{3.1}$$

where the Cauchy fluid stress tensor given by

$$\widetilde{T}_\varepsilon^f = -\tilde{p}_\varepsilon(X,t)I + \mu\left(\nabla_X \tilde{v}_\varepsilon(X,t) + \nabla_X \tilde{v}_\varepsilon(X,t)^T\right). \tag{3.2}$$

Here $(\tilde{v}_\varepsilon, \tilde{p}_\varepsilon)$, are fluid velocity and pore pressure. We use the notation that$\tilde{}$denotes quantities presented in the current Eulerian frame. Expanding the time derivative yields the more familiar nonlinear convective term. The conservation of linear momentum and conservation of mass are given by

$$-\nabla_X \tilde{p}_\varepsilon + \mu \Delta_X \tilde{v}_\varepsilon = \varepsilon^2 \left(\partial_t \tilde{v}_\varepsilon + \tilde{v}_\varepsilon \cdot \nabla_X \tilde{v}_\varepsilon\right) + \tilde{f} \text{ in } \mathcal{F}_\varepsilon(t), \tag{3.3a}$$

$$\mathrm{div}_X(\tilde{v}_\varepsilon) = 0 \text{ in } \mathcal{F}_\varepsilon(t). \tag{3.3b}$$

Note here that we use a different sign convention for the Stokes equations in this chapter. Due to the conservation fo mass, or incompressibility condition, the divergence of the transposed velocity gradient vanishes as $\mathrm{div}_X(\nabla_X \tilde{v}_\varepsilon^T) = \nabla_X(\mathrm{div}_X(\tilde{v}_\varepsilon)) = 0$. On the interface we suppose the boundary condition

$$\tilde{v}_\varepsilon^f = \varepsilon^2 \tilde{v}_\varepsilon^s \text{ on } \Gamma_\varepsilon(t). \tag{3.4}$$

This condition states that the velocity of the fluid $\tilde{v}_\varepsilon^f$ and velocity of the scaled solid

velocity $\varepsilon^2 \tilde{v}_\varepsilon^s$ should be equal on the interface.

For our investigation, we assume that the solid material has a linear elastic constitutive law. This may be relaxed to more general materials with more complicated constitutive laws however linear elastic allows for a clearer presentation. These equations are presented in the initial fixed Lagrangian configuration Ω with coordinates x. The solid skeleton satisfies equations of quasi-static equilibrium

$$-\mathrm{div}_x \left(Ce(u_\varepsilon)\right) = b \text{ in } \mathcal{S}_\varepsilon, \tag{3.5}$$

where $e(u_\epsilon) = \frac{1}{2}\left(\nabla u_\varepsilon + \nabla u_\varepsilon^T\right)$ is the symmetric strain tensor and C is the symmetric four-tensor associated with linear elasticity. We require that the normal components of the fluid stress tensor and solid stress tensor be equal on the initial interface Γ_ε. However, the Cauchy fluid stress tensor $\widetilde{T}_\epsilon^f$ is presented in the Eulerian configuration, and the Piola-Kirchhoff solid stress tensor $Ce(u_\varepsilon)$ is presented in the initial Lagrangian configuration. We may represent the Cauchy stress tensor in the Lagrangian configuration via the Piola transformation. The interface condition becomes

$$Ce(u_\varepsilon)n_0 = T_\varepsilon^f G_\varepsilon n_0 \text{ on } \Gamma_\varepsilon. \tag{3.6}$$

Here $G_\varepsilon = \det\left(I + \nabla_x u_\varepsilon\right)\left(I + \nabla_x u_\varepsilon\right)^{-T}$ is the Piola transformation and n_0 is the unit normal on the interface Γ_ε. Let the deformation gradient and Jacobian be denoted $F_\varepsilon = I + \nabla_x u_\varepsilon$, and $J_\varepsilon = \det\left(I + \nabla_x u_\varepsilon\right)$, respectively. By a simple application of the chain rule we see that $\nabla_X \tilde{v}_\varepsilon = \nabla_x v_\varepsilon F_\varepsilon^{-1}$ and hence the Cauchy fluid stress in the reference configuration can be expressed as $T_\varepsilon^f = -p_\varepsilon I + \mu\left(\nabla_x v_\varepsilon F_\varepsilon^{-1} + (\nabla_x v_\varepsilon F_\varepsilon^{-1})^T\right)$

We summarize the model here. Putting this formulation all together we can write the full time dependent FSI problem in the two coordinate systems. The fully

coupled fine-scale FSI problem can be written as

$$-\nabla_X \tilde{p}_\varepsilon + \mu \Delta_X \tilde{v}_\varepsilon = \varepsilon^2(\partial_t \tilde{v}_\varepsilon + \tilde{v}_\varepsilon \cdot \nabla_X \tilde{v}_\varepsilon) + \tilde{f} \qquad \text{in } \mathcal{F}_\epsilon(t), \tag{3.7a}$$

$$\operatorname{div}_X(\tilde{v}_\varepsilon) = 0 \qquad \text{in } \mathcal{F}_\epsilon(t), \tag{3.7b}$$

$$\tilde{v}_\varepsilon^f = \varepsilon^2 \tilde{v}_\varepsilon^s \qquad \text{on } \Gamma_\epsilon(t), \tag{3.7c}$$

$$-\operatorname{div}_x(Ce(u_\varepsilon)) = b \qquad \text{in } \mathcal{S}_\varepsilon, \tag{3.7d}$$

$$Ce(u_\varepsilon)n_0 = T_\varepsilon^f G_\varepsilon n_0 \qquad \text{on } \Gamma_\varepsilon. \tag{3.7e}$$

The equations are coupled at the current interface $\Gamma_\varepsilon(t)$ by continuity of velocities (3.7c) and at the reference interface Γ_ε by continuity of normal stress (3.7e).

Remark When we wish to represent a quantity $\tilde{\phi}(X,t)$ in the Eulerian or current configuration in the reference configuration we write

$$\phi(x,t) = \tilde{\phi}(X(x,t),t).$$

The tilde above a quantity will always denote quantities in the current deformed configuration. Throughout the main portion of this work we will work mainly in the Lagrangian or reference configuration. We use the simpler notation without the tilde in this configuration. Note that this is different than the notation used in Chapter II, where we used the superscript # to denote the periodic fixed frame and no superscript to denote the deformed frame. We will continue to use this notation throughout the rest of the document.

2. Linear Biot Model

The classical model of soil consolidation and geomechanics is given by the Biot model first proposed in [4]. Later, by utilizing mathematical homogenization techniques in [8], the authors were able to derive the Biot equations. This is accomplished by

assuming the microstructure undergoes infinitesimal deformation only. We briefly recall these ideas here, so that we may relate our work with that of the classical Biot model.

In the infinitesimal pore scale deformation setting, the fine-scale equations (3.7) simplify. Note, locally, the domains remains fixed. Thus, the interface condition (3.7e) becomes linear. More precisely, the condition simplifies to

$$Ce(u_\varepsilon)n_0 = T_\varepsilon^f n_0, \tag{3.8}$$

where T_ε^f is of the form (3.2). In this setting, we will not longer need to differentiate between frames, so we will drop the $\tilde{}$ notation.

We assume a bit more structure of our media. We assume solid and fluid domains are decomposed into a set of unit cells $\varepsilon\{Y_{\mathcal{S}}^i\}_{i=1}^N$ and $\varepsilon\{Y_{\mathcal{F}}^i\}_{i=1}^N$, respectively and ε is the characteristic pore size. Assume further, that the media is periodic. In this case, each cell will be a translation of a single unit cell. That is, $Y_{\mathcal{S}}^i = Y_{\mathcal{S}} + k_i$ and $Y_{\mathcal{F}}^i = Y_{\mathcal{S}} + k_i$ are unit-sized domains, for $k_i \in \mathbb{Z}^d$ corresponding to $i = 1, \ldots, N$. With this notation we may decompose the solid and fluid domains as

$$\mathcal{S}_\varepsilon = \left(\bigcup_{k_i \in \mathbb{Z}^d} \varepsilon\left(Y_{\mathcal{S}} + k_i\right) \right) \cap \Omega, \qquad \mathcal{F}_\varepsilon = \left(\bigcup_{k_i \in \mathbb{Z}^d} \varepsilon\left(Y_{\mathcal{F}} + k_i\right) \right) \cap \Omega. \tag{3.9}$$

We denote the unit cell by $Y = Y_{\mathcal{S}} \cup Y_{\mathcal{F}}$ and denote by $Y_\Gamma = \bar{Y}_{\mathcal{S}} \cup \bar{Y}_{\mathcal{F}}$ the fluid-solid interface on the unit cell.

We apply the method of asymptotic two-scale expansions ([8, 33]) to the fine-scale equations under the infinitesimal pore scale deformation assumption. We assume the following ansatz for the expansion of our physical quantities. For the displacement we suppose

$$u_\varepsilon(x,t) = u_0(x,t) + \varepsilon u_1(x,y,t) + \cdots . \tag{3.10}$$

For pressure and velocity we expand as

$$p_\varepsilon(x,t) = p_0(x,t) + \varepsilon p_1(x,y,t) + \cdots,$$
$$v_\varepsilon(x,y,t) = \varepsilon^2 v_0(x,y,t) + \varepsilon^3 v_1(x,y,t) + \cdots, \tag{3.11}$$

where $y = x/\varepsilon$ is the fast variable. The derivative of such two-scale functions transform as $\nabla \to \nabla_x + \frac{1}{\varepsilon}\nabla_y$. We apply the above expansions to the fine-scale model under infinitesimal pore-scale deformation conditions, and collect terms in ε. We arrive at the cell problem

$$-\nabla_y p_1 + \mu \Delta_y v_0 = \nabla_x p_0 + f \text{ in } Y_{\mathcal{F}},$$
$$\operatorname{div}_y(v_0) = 0 \text{ in } Y_{\mathcal{F}}.$$

where v_0 and p_1 are $y-$periodic, we also require $v_0 = \partial_t u_0$ on Y_Γ and $\langle p_1 \rangle_Y = 0$. We use linearity in the slow variable x and the fact that $\partial_t u_0$ depends on x to simplify this cell problems further. We may write

$$v_0 = w\left(\nabla_x p_0 + f\right) + \partial_t u_0, \tag{3.12a}$$
$$p_1 = \pi\left(\nabla_x p_0 + f\right), \tag{3.12b}$$

where (w^i, π^i), $i = 1, \ldots, d,$, are the solutions to the Stokes cell equations

$$-\nabla_y \pi^i + \mu \Delta_y w^i = e_i \text{ in } Y_{\mathcal{F}}, \tag{3.13a}$$
$$\operatorname{div}_y(w^i) = 0 \text{ in } Y_{\mathcal{F}}, \tag{3.13b}$$

with w^i and π^i being $y-$periodic, and $\langle \pi^i \rangle_Y = 0$, with the boundary condition $w^i = 0$ on Y_Γ. Similarly, for the elasticity equations, we may write

$$u_1 = -p_0 Q + e_x(u_0) R, \tag{3.14}$$

where $e_y(\cdot) = \frac{1}{2}\left(\nabla_y(\cdot) + \nabla_y(\cdot)^T\right)$ and (Q, R) are the solutions to the elasticity cell equations

$$-\mathrm{div}_y\left(C(I + e_y(R))\right) = 0 \text{ in } Y_{\mathcal{S}}, \tag{3.15a}$$

$$C(I + e_y(R))n_0 = 0 \text{ on } Y_\Gamma, \tag{3.15b}$$

and

$$-\mathrm{div}_y\left(Ce_y(Q)\right) = 0 \text{ in } Y_{\mathcal{S}}, \tag{3.16a}$$

$$Ce_y(Q)n_0 = In_0 \text{ on } Y_\Gamma, \tag{3.16b}$$

where R and Q, are y-periodic and vanish on the interface Y_Γ. The macroscopic Biot equations may now be derived. Let $\langle\cdot\rangle_Y$ be the y-average over the cell Y

$$\langle\cdot\rangle_Y = \frac{1}{|Y|}\int_Y \cdot dy.$$

In addition, we let $\langle\cdot\rangle_{Y_{\mathcal{S}}}$ and $\langle\cdot\rangle_{Y_{\mathcal{F}}}$ be the restriction of the integrand to solid and fluid cells respectively. We consider the next order ε of the incompressibility condition. Taking the average, using (3.12a) and (3.14), and the velocity interface condition we obtain we obtain

$$\begin{aligned}
&\mathrm{div}_x\left(\langle v_0\rangle_Y\right) + \langle \mathrm{div}_y\left(v_1\right)\rangle_Y = \mathrm{div}_x\left(\langle v_0\rangle_Y\right) + \frac{1}{|Y|}\int_{Y_\Gamma} v_1 \cdot n_0 dy \\
&= \mathrm{div}_x\left(\langle w\rangle_Y\left(\nabla_x p_0 + f\right) + \langle \partial_t u_0\rangle_{Y_{\mathcal{S}}}\right) + \frac{1}{|Y|}\int_{Y_\Gamma} \partial_t u_1 \cdot n_0 dy \\
&= \mathrm{div}_x\left(\langle w\rangle_Y\left(\nabla_x p_0 + f\right)\right) \\
&+ \partial_t e_x(u_0)\left((1-\phi)I + \frac{1}{|Y|}\int_{Y_\Gamma} R \cdot n_0 dy\right) - \partial_t p_0 \frac{1}{|Y|}\int_{Y_\Gamma} Q \cdot n_0 dy,
\end{aligned}$$

where $(1-\phi) = \frac{|Y_{\mathcal{S}}|}{|Y|}$ is the solid phase porosity. Applying the divergence theorem to

the interface integrals terms, this time on the solid domain, we obtain

$$\begin{aligned}
&\operatorname{div}_x\left(\langle w\rangle_Y\left(\nabla_x p_0+f\right)\right)\\
&+\partial_t e_x(u_0)\left((1-\phi)I-\frac{1}{|Y|}\int_{Y_{\mathcal{S}}}\operatorname{div}_y(R)dy\right)+\partial_t p_0\frac{1}{|Y|}\int_{Y_{\mathcal{S}}}\operatorname{div}_y(Q)dy\\
&=\operatorname{div}_x\left(K\left(\nabla_x p_0+f\right)\right)+\left((1-\phi)I-A\right)\partial_t e_x(u_0)+B\partial_t p_0=0 \text{ in } \Omega, \qquad (3.17)
\end{aligned}$$

where $K=\langle w\rangle_Y, A=\langle \operatorname{div}_y(R)\rangle_{Y_{\mathcal{S}}}$, and $B=\langle \operatorname{div}_y(Q)\rangle_{Y_{\mathcal{S}}}$. Above is the linear Biot fluid equation. Similarly for elasticity, we collect the next order in ε of the expansion of the elasticity equations. Averaging over y, using the expansion for (3.14), and the linearized interface condition, (3.8), we obtain

$$\begin{aligned}
&-\operatorname{div}_x\left(\langle Ce_x(u_0)+Ce_y(u_1)\rangle_Y\right)-\langle \operatorname{div}_y(Ce_x(u_1))\rangle_Y\\
&=-\operatorname{div}_x\left(\langle C(I+e_y(R))\rangle_Y e_x(u_0)-\langle Ce_y(Q)\rangle_Y p_0\right)\\
&-\frac{1}{|Y|}\int_{Y_\Gamma}(-p_1I+\mu\nabla_y v_0+\nabla_y v_0^T)n_0dy.
\end{aligned}$$

Applying the divergence theorem, this time on the fluid part, and using the fluid cell equations, we simplify the interface integral term

$$\begin{aligned}
&-\operatorname{div}_x\left(\langle C(I+e_y(R))\rangle_Y e_x(u_0)-\langle Ce_y(Q)\rangle_Y p_0\right)+\frac{1}{|Y|}\int_{Y_{\mathcal{F}}}(-\nabla_y p_1+\mu\Delta_y v_0)dy\\
&=-\operatorname{div}_x\left(\langle C(I+e_y(R))\rangle_Y e_x(u_0)-\langle Ce_y(Q)\rangle_Y p_0\right)+\phi(\nabla_x p_0+f)\\
&=-\operatorname{div}_x\left(C^*e_x(u_0)-\alpha^*p_0\right)+\phi f=b \text{ in } \Omega, \qquad (3.18)
\end{aligned}$$

where $\phi=\frac{|Y_{\mathcal{F}}|}{|Y|}$ is the porosity, and $C^*=\langle C(I+e_y(R))\rangle_Y$ and $\alpha^*=\langle Ce_y(Q)\rangle_Y+\phi$. The above equation is the solid mechanics equation of the linear Biot equation.

B. Homogenization of FSI in the ALE Formulation

Due to the differences in coordinate systems, applying two-scale asymptotic techniques of [33, 34] to the nonlinear fine-scale equations (3.7) is challenging. Applying the asymptotic techniques formally to (3.7) does not yield a coherent understanding of the relationship between microscale and macroscale quantities. The domain's periodicity is also broken. We are able to successfully apply asymptotic techniques to the linearized model via the infinitesimal pore-scale deformation assumption in Section 2. In the linear setting, these problems do not arise.

By utilizing the Arbitrary Lagrange-Eulerian formulation, we will obtain FSI equations in a unified periodic domain. In the unified periodic domain, we apply asymptotic techniques. From here we will derive auxiliary cell equations that relate the macroscale information to the microscale. The cell equations are more complex as they do not decouple from macroscale quantities. Then, we obtain homogenized nonlinear macroscale equations analogous to the classical Biot equations (3.17) and (3.18). However, the effective coefficients will depend nonlinearly on the macroscopic variables.

1. FSI in the Arbitrary Lagrange-Eulerian Formulation

In this section we apply a coordinate transform to Navier-Stokes equations (3.7a) and (3.7b), and represent the fluid equations in the so called Arbitrary Lagrange-Eulerian (ALE) formulation. This unified coordinate formulation will allow us to apply two-scale asymptotic expansion techniques, when we consider an initially periodic domain.

Using the Piola transform integral formulas cf. [17], we see that for the time-independent part of (3.7a) and (3.7b) can written using the Cauchy stress tensor notation. For an arbitrary $\mathcal{P}_\varepsilon(t) \subset \mathcal{F}_\varepsilon(t)$, using the divergence theorem on (3.7a) and

changing coordinates to the initial reference frame we have for

$$\int_{\mathcal{P}_\varepsilon(t)} (\mathrm{div}_X(\widetilde{T}_\varepsilon^f) - \tilde{f}) dV_X = \int_{\partial\mathcal{P}_\varepsilon(t)} \widetilde{T}_\varepsilon^f n dA_X - \int_{\mathcal{P}_\varepsilon(t)} \tilde{f} dV_X$$
$$= \int_{\partial\mathcal{P}_\varepsilon} T_\varepsilon^f G_\varepsilon n_0 dA_x - \int_{\mathcal{P}_\varepsilon} J_\varepsilon f dV_x = \int_{\mathcal{P}_\varepsilon} (\mathrm{div}_x(T_\varepsilon^f G_\varepsilon) - J_\varepsilon f) dV_x.$$

For the incompressibility equation (3.7b) we proceed similarly

$$\int_{\mathcal{P}_\varepsilon(t)} \mathrm{div}_X(\tilde{v}_\varepsilon) dV_X = \int_{\partial\mathcal{P}_\varepsilon(t)} \tilde{v}_\varepsilon \cdot n dA_X = \int_{\partial\mathcal{P}_\varepsilon} v_\varepsilon \cdot (G_\varepsilon n_0) dA_x$$
$$= \int_{\partial\mathcal{P}_\varepsilon} (G_\varepsilon^T v_\varepsilon) \cdot n_0 dA_x = \int_{\mathcal{P}_\varepsilon} \mathrm{div}_x(G_\varepsilon^T v_\varepsilon) dV = 0.$$

For the convective term we use the identities as in [15], we obtain

$$\partial_t \tilde{v}_\varepsilon = \partial_t v_\varepsilon - (F_\varepsilon^{-1} \partial_t X_\varepsilon \nabla_x v_\varepsilon),$$
$$\frac{d\tilde{v}_\varepsilon}{dt} = \partial_t v_\varepsilon + (F_\varepsilon^{-1}(v_\varepsilon - \partial_t X_\varepsilon) \nabla_x v_\varepsilon).$$

Integrating over $\mathcal{P}_\varepsilon(t)$, and changing coordinates we obtain

$$\int_{\mathcal{P}_\varepsilon(t)} \left(\frac{d\tilde{v}_\varepsilon}{dt} \right) dV_X = \int_{\mathcal{P}_\varepsilon} \left(\partial_t v_\varepsilon + (F_\varepsilon^{-1}(v_\varepsilon - \partial_t X_\varepsilon) \nabla_x v_\varepsilon) \right) J_\varepsilon dV_x.$$

The full time derivative term will play no explicit role in our analysis as it is scaled as ε^2, but we write it here for completeness. The velocity interface condition is much more transparent in this frame as the condition $\tilde{v}_\varepsilon^f = \varepsilon^2 \tilde{v}_\varepsilon^s$ on $\Gamma_\varepsilon(t)$ becomes $v_\varepsilon = \varepsilon^2 \partial_t u_\varepsilon$ on Γ_ε in the Lagrangian coordinates. The ε^2 scaling is introduced on the solid velocity to match the scaling of the fluid velocity. In addition, noting gradients transform as $\nabla_X \tilde{v}_\varepsilon = \nabla_x v_\varepsilon F_\varepsilon^{-1}$. We let $H_\varepsilon = F_\varepsilon^{-1} G_\varepsilon$, using this tensor notation we see that

$$T_\varepsilon^f G_\varepsilon = -p_\varepsilon G_\varepsilon + \mu(\nabla_x v_\varepsilon H_\varepsilon + (\nabla_x v_\varepsilon H_\varepsilon)^T).$$

Note that after taking the divergence of $T_\varepsilon^f G_\varepsilon$ the transpose velocity term vanishes as

in the Eulerian frame. This, again, is due to the modified incompressibility condition. Combining the above integral identities, we obtain the full FSI in the Lagrangian reference formulation. We reformulate the coupled FSI problem (3.7) in the ALE as

$$-\nabla_x(p_\varepsilon G_\varepsilon) + \mu \mathrm{div}_x(\nabla_x v_\varepsilon H_\varepsilon) = \left(\varepsilon^2 \frac{\partial v_\varepsilon}{\partial t} + f\right) J_\varepsilon \qquad \text{in } \mathcal{F}_\epsilon, \tag{3.19a}$$

$$\mathrm{div}_x(G_\varepsilon^T v_\varepsilon) = 0 \qquad \text{in } \mathcal{F}_\varepsilon, \tag{3.19b}$$

$$v_\varepsilon = \varepsilon^2 \partial_t u_\varepsilon \qquad \text{on } \Gamma_\varepsilon, \tag{3.19c}$$

$$-\mathrm{div}_x(Ce(u_\varepsilon)) = b \qquad \text{in } \mathcal{S}_\varepsilon, \tag{3.19d}$$

$$Ce(u_\varepsilon)n_0 = T_\varepsilon^f G_\varepsilon n_0 \qquad \text{on } \Gamma_\varepsilon, \tag{3.19e}$$

where we denote $\frac{\partial v_\varepsilon}{\partial t} = (\partial_t v_\varepsilon + (F_\varepsilon^{-1}(v_\varepsilon - \partial_t X_\varepsilon)\nabla_x v_\varepsilon))$ to be the convective time derivative term in the reference configuration.

2. Auxiliary Cell Equations

We are now in a position to apply the two-scale asymptotic expansion to the FSI equations in the ALE formulation (3.19). We suppose the fluid $\mathcal{F}_\varepsilon$ and solid $\mathcal{S}_\varepsilon$ domains have periodic structure as in (3.9). We expand $u_\varepsilon, p_\varepsilon$, and v_ε as in (3.10) and (3.11). Since the deformation gradient, Jacobian, and related tensors depend on $\nabla_x u_\varepsilon$, we write the two-scale expansions for these quantities. Note that the deformation gradient expands as $F_\varepsilon = I + \nabla_x u_\varepsilon = (I + \nabla_x u_0 + \nabla_y u_1) + \varepsilon(\nabla_x u_1)$. Thus, we expand the deformation gradient and Jacobian as

$$\begin{aligned} F_\varepsilon(x,y,t) &= F_0(x,y,t) + \varepsilon F_1(x,y,t), \\ J_\varepsilon(x,y,t) &= J_0(x,y,t) + \varepsilon J_1(x,y,t), \end{aligned} \tag{3.20}$$

and similarly for the higher order tensors

$$G_\varepsilon(x,y,t) = G_0(x,y,t) + \varepsilon G_1(x,y,t),$$
$$H_\varepsilon(x,y,t) = H_0(x,y,t) + \varepsilon H_1(x,y,t). \tag{3.21}$$

a. Stokes Cell Equations

We begin with the fluid equations. Applying the expansions (3.10-3.11), and (3.20-3.21) into the conservation of momentum (3.19a) along with the two-scale expansion for the differential operators we obtain

$$\begin{aligned} &-\left(\mathrm{div}_x + \frac{1}{\varepsilon}\mathrm{div}_y\right)\left((p_0 + \varepsilon p_1 \cdots)\left(G_0 + \varepsilon G_1 + \cdots\right)\right) \\ &+\mu\left(\mathrm{div}_x + \frac{1}{\varepsilon}\mathrm{div}_y\right)\Bigg[\left(\left(\nabla_x + \frac{1}{\varepsilon}\nabla_y\right)\left(\varepsilon^2 v_0 + \varepsilon^3 v_1 \cdots\right)\right) \\ &\times\left(H_0 + \varepsilon H_1 + \cdots\right)\Bigg] = f\left(J_0 + \varepsilon J_1 \cdots\right) + O(\varepsilon^2), \end{aligned}$$

and for the conservation of mass equation (3.19b)

$$\left(\mathrm{div}_x + \frac{1}{\varepsilon}\mathrm{div}_y\right)\left(\left(G_0^T + \varepsilon G_1^T + \cdots\right)\left(v_0 + \cdots\right)\right) = 0. \tag{3.22}$$

Note that here we suppress the time derivative and nonlinear convective terms as these quantities are of order ε^2. Collecting the ε^0 terms from conservation of momentum we have

$$\begin{aligned} -\mathrm{div}_x\left(p_0 G_0\right) - \mathrm{div}_y(p_0 G_1) - \mathrm{div}_y(p_1 G_0) \\ +\mu\mathrm{div}_y\left(\nabla_y v_0 H_0\right) = f J_0, \end{aligned} \tag{3.23}$$

and the ε^1 terms from the conservation of mass equation

$$\mathrm{div}_y\left(G_0^T v_0\right) = 0. \tag{3.24}$$

We may simplify (3.23) by noting that G_ε is divergence free via the identity

$$\int_{\mathcal{P}_\varepsilon} \mathrm{div}_x(G_\varepsilon) dV_x = \int_{\partial\mathcal{P}_\varepsilon} G_\varepsilon \cdot n_0 dA_x$$
$$= \int_{\partial\mathcal{P}_\varepsilon(t)} I \cdot n dA_X = \int_{\mathcal{P}_\varepsilon(t)} \mathrm{div}_X(I) dV_X = 0.$$

From here we see that the tensor G_ε satisfies $\mathrm{div}_x(G_\varepsilon) = 0$. Using the asymptotic expansions (3.21) we obtain

$$\left(\mathrm{div}_x + \frac{1}{\varepsilon}\mathrm{div}_y\right)(G_0 + \varepsilon G_1 + \cdots) = 0.$$

Gathering similar terms in ε terms we see that for ε^{-1}

$$\mathrm{div}_y(G_0) = 0,$$

and for ε^0

$$\mathrm{div}_x(G_0) + \mathrm{div}_y(G_1) = 0.$$

Using these identities we deduce

$$-\mathrm{div}_x(p_0 G_0) - \mathrm{div}_y(p_0 G_1) - \mathrm{div}_y(p_1 G_0)$$
$$= -G_0 \nabla_x p_0 - G_0 \nabla_y p_1.$$

Using the above identity we simplify (3.23) along with the incompressibility equation (3.24), we write the cell problem for the modified Stokes equations as

$$-G_0 \nabla_y p_1 + \mu \mathrm{div}_y(\nabla_y v_0 H_0) = G_0 \nabla_x p_0 + f J_0, \qquad \text{in } Y_\mathcal{F}, \tag{3.25a}$$
$$\mathrm{div}_y(G_0^T v_0) = 0 \qquad \text{in } Y_\mathcal{F}, \tag{3.25b}$$

where v_0 and p_1 are $y-$periodic, we also require $v_0 = \partial_t u_0$ on Y_Γ and $\langle p_1 \rangle_Y = 0$. We, again, use linearity in the slow variable x and the x dependence of $\partial_t u_0$ to simplify

this cell problems further. Indeed, we write

$$v_0 = w_1 \nabla_x p_0 + w_2 f + \partial_t u_0, \tag{3.26a}$$

$$p_1 = \pi_1 \nabla_x p_0 + \pi_2 f, \tag{3.26b}$$

where (w_j^i, π_j^i), $i = 1, \ldots, d$, and $j = 1, 2$, are the solutions to the two sets of modified Stokes cell equations

$$-G_0 \nabla_y \pi_1^i + \mu \mathrm{div}_y \left(\nabla_y w_1^i H_0 \right) = G_0 e_i \text{ in } Y_{\mathcal{F}}, \tag{3.27a}$$

$$\mathrm{div}_y (G_0^T w_1^i) = 0 \text{ in } Y_{\mathcal{F}}, \tag{3.27b}$$

and for the second cell

$$-G_0 \nabla_y \pi_2^i + \mu \mathrm{div}_y \left(\nabla_y w_2^i H_0 \right) = J_0 e_i \text{ in } Y_{\mathcal{F}}, \tag{3.28a}$$

$$\mathrm{div}_y (G_0^T w_2^i) = 0 \text{ in } Y_{\mathcal{F}}, \tag{3.28b}$$

with w_j^i and π_j^i being $y-$periodic, $w_j^i = 0$ on Y_Γ and $\left\langle \pi_j^i \right\rangle_Y = 0$ for $j = 1, 2$.

b. Elasticity Cell Equation

We now apply the two-scale expansions to the elasticity equations (3.19d) and (3.19e). This procedure is similar to the methods used in elliptic problems in perforated domains c.f. [9] and references therein. Using (3.10),(3.11) and (3.20),(3.21) and the two-scale differential operators, into (3.19d) we obtain

$$-\left(\mathrm{div}_x + \frac{1}{\varepsilon} \mathrm{div}_y \right) \left(C \left(e_x + \frac{1}{\varepsilon} e_y \right) (u_0 + e u_1 + \cdots) \right) = b. \tag{3.29}$$

For the interface stress tensor condition (3.19e) we have

$$\begin{aligned}\left(C\left(e_x(\cdot)+\frac{1}{\varepsilon}e_y(\cdot)\right)(u_0+eu_1+\cdots)\right)n_0 = \\ \Bigg(-(p_0+\varepsilon p_1+\cdots)(G_0+\varepsilon G_1+\cdots) \\ +\mu\Bigg[\left(\nabla_x+\frac{1}{\varepsilon}\nabla_y\right)\left(\left(\varepsilon^2 v_0+\cdots\right)(H_0+\cdots)\right)+ \\ \left(\left(\nabla_x+\frac{1}{\varepsilon}\nabla_y\right)\left(\left(\varepsilon^2 v_0+\cdots\right)(H_0+\cdots)\right)\right)^T\Bigg]\Bigg)n_0.\end{aligned}$$

Collecting ε^{-1} terms of the elasticity problem and the ε^0 terms of the interface condition we obtain the elasticity cell problem

$$-\mathrm{div}_y\left(C\left(e_x(u_0)+e_y(u_1)\right)\right)=0 \text{ in } Y_{\mathcal{S}}, \tag{3.30a}$$

$$C\left(e_x(u_0)+e_y(u_1)\right)n_0 = -p_0 G_0\left(\nabla_x u_0, \nabla_y u_1\right)n_0 \text{ on } Y_\Gamma. \tag{3.30b}$$

and we require u_1 to be $y-$periodic. We emphasize the dependence on $(\nabla_x u_0, \nabla_y u_1)$ in the tensor G_0 as this will be crucial in understanding the relationship of macroscale and microscale variables.

Remark Note that the velocity terms on the interface condition are all of order ε. Hence the fluid shear stress, from the fluid velocity gradients, plays no part in the elasticity cell problem but will be important in higher order cell equations.

3. Homogenized Equations

In this section, we use the auxiliary cell problems to derive macroscale homogenized equations. We begin with the homogenization of the fluid equations. Here we develop a generalization of (3.17). Then, we turn our attention to the solid equations and present the corresponding generalization of (3.18).

a. Macroscopic Fluid Equation

We are now in a position to derive the macroscopic fluid equation. Returning to the incompressibility equation (3.22) collecting the ε^0 terms we obtain

$$\mathrm{div}_x(G_0^T v_0) + \mathrm{div}_y(G_0^T v_1) + \mathrm{div}_y(G_1^T v_0) = 0.$$

Then, after taking the average of the above equation we obtain

$$\mathrm{div}_x\left(\left\langle G_0^T v_0\right\rangle_Y\right) + \left\langle \mathrm{div}_y(G_0^T v_1)\right\rangle_Y + \left\langle \mathrm{div}_y(G_1^T v_0)\right\rangle_Y = 0.$$

Using the divergence theorem in the y variable and by $y-$periodicity we have an integral over Y_Γ. From (3.19c) and the expansions (3.10-3.11) we have $v_i = \partial_t u_i$ for $i = 0, 1$, on Y_Γ. Thus, we obtain

$$\begin{aligned}
&\mathrm{div}_x\left(\left\langle G_0^T v_0\right\rangle_Y\right) + \frac{1}{|Y|}\int_{Y_\Gamma}(G_0^T v_1)n_0 dy + \frac{1}{|Y|}\int_{Y_\Gamma}(G_1^T v_0)n_0 dy \\
&= \mathrm{div}_x\left(\left\langle G_0^T v_0\right\rangle_Y\right) + \frac{1}{|Y|}\int_{Y_\Gamma}(G_0^T \partial_t u_1)n_0 dy + \frac{1}{|Y|}\int_{Y_\Gamma}(G_1^T \partial_t u_0)n_0 dy.
\end{aligned}$$

Using the divergence theorem, this time over the solid cell domain $Y_\mathcal{S}$, and noting the minus sign from the change in normal vectors $n_0 \to -n_0$, we obtain

$$\begin{aligned}
&\mathrm{div}_x\left(\left\langle G_0^T v_0\right\rangle_Y\right) - \frac{1}{|Y|}\int_{Y_\mathcal{S}}\left(\mathrm{div}_y\left(G_0^T \partial_t u_1\right) + \mathrm{div}_y\left(G_1^T \partial_t u_0\right)\right) dy \\
&= \mathrm{div}_x\left(\left\langle G_0^T v_0\right\rangle_Y\right) - \frac{1}{|Y|}\int_{Y_\mathcal{S}}\left(\mathrm{div}_y\left(G_0^T \partial_t u_1\right) - \mathrm{div}_x\left(G_0^T\right)\partial_t u_0\right) dy \\
&= \mathrm{div}_x\left(\left\langle G_0^T v_0\right\rangle_Y\right) - \frac{1}{|Y|}\int_{Y_\mathcal{S}}\mathrm{div}_y\left(G_0^T \partial_t u_1\right) dy + \mathrm{div}_x\left(\frac{1}{|Y|}\int_{Y_\mathcal{S}} G_0^T dy\right)\partial_t u_0.
\end{aligned} \tag{3.31}$$

Note here we used the identity $\mathrm{div}_x\left(G_0^T\right) + \mathrm{div}_y\left(G_1^T\right) = 0$.

Note that the dependence of the tensor $G_0 = G_0(\nabla_x u_0, \nabla_y u_1)$. The elasticity

cell problem (3.30), depends on the macroscopic quantities $(p_0, \nabla_x u_0)$, hence $u_1 = u_1(p_0, \nabla_x u_0)$. Thus, the other tensors, J_0, F_0, G_0 and H_0 also depend on $(p_0, \nabla_x u_0)$. Returning to the fluid cell , we see that the cell velocity v_0 depends on $(p_0, \nabla_x u_0)$ nonlinearly and linearly on $\nabla_x p_0$ and $\partial_t u_0$. With this view in mind we let

$$u_1 = N(p_0, \nabla_x u_0), \tag{3.32}$$

here N satisfies (3.30), where we view $(p_0, \nabla_x u_0)$ as inputs into the equations cf. [12]. By applying a formal chain rule in time we have

$$\frac{\partial N}{\partial t} = \left(\frac{\partial N}{\partial \nabla_x u_0}\right) \partial_t \nabla_x u_0 + \left(\frac{\partial N}{\partial p_0}\right) \partial_t p_0.$$

We formally define the effective quantities

$$A^*(p_0, \nabla_x u_0) = \left\langle \operatorname{div}_y \left(G_0^T \frac{\partial N}{\partial \nabla_x u_0} \right) \right\rangle_{Y_S}, \tag{3.33a}$$

$$B^*(p_0, \nabla_x u_0) = -\left\langle \operatorname{div}_y \left(G_0^T \frac{\partial N}{\partial p_0} \right) \right\rangle_{Y_S}, \tag{3.33b}$$

$$K^*(p_0, \nabla_x u_0) = \left\langle G_0^T w_1 \right\rangle_Y, J^*(p_0, \nabla_x u_0) = \left\langle G_0^T w_2 \right\rangle_Y, \tag{3.33c}$$

$$D^*(p_0, \nabla_x u_0) = \left\langle G_0^T \right\rangle_{Y_S}. \tag{3.33d}$$

Applying this notation to (3.31) and using the expansion (3.26a), we obtain a generalization of the Biot fluid equation (3.17)

$$\begin{aligned} &\operatorname{div}_x \left(K^*(p_0, \nabla_x u_0) \nabla_x p_0 + J^*(p_0, \nabla_x u_0) f + D^*(p_0, \nabla_x u_0) \partial_t u_0 \right) \\ &- A^*(p_0, \nabla_x u_0) \partial_t \nabla_x u_0 + B^*(p_0, \nabla_x u_0) \partial_t p_0 + \operatorname{div}_x \left(D^*(p_0, \nabla_x u_0) \right) \partial_t u_0 = 0 \text{ in } \Omega. \end{aligned} \tag{3.34}$$

We may return to the linear Biot fluid equation (3.17). Indeed, linearizing, we have J_0, F_0, G_0 and $H_0 \to I$. We may write u_1 as in (3.14) and A^*, B^* are as in the linear setting. We reduce to a single cell equation (3.13) and $K^* = J^* = \langle w \rangle_Y$. Finally,

$D^* = (1-\phi)I$. and the $\partial_t u_0$ term vanishes for constant porosity.

b. Macroscopic Elasticity Equation

To complete the asymptotic expansion of the FSI in the reference configuration we return to the expansion (3.29). We will derive the homogenized elasticity equations. Collecting the ε^0 we have

$$-\mathrm{div}_x\left(Ce_x(u_0) + Ce_y(u_1)\right) - \mathrm{div}_y\left(Ce_x(u_1)\right) = b.$$

Taking the y-average and using the fact that u_1 is y-periodic, the second divergence in y becomes a boundary integral after an application of the divergence theorem, we obtain

$$\begin{aligned} -\mathrm{div}_x\left(\langle Ce_x(u_0) + Ce_y(N(p_0, \nabla_x u_0))\rangle_Y\right) - \int_{Y_\Gamma} Ce_x(N(p_0, \nabla_x u_0))n_0 dy \\ = -\mathrm{div}_x\left(\langle Ce_x(u_0) + Ce_y(N(p_0, \nabla_x u_0))\rangle_Y\right) \\ -\frac{1}{|Y|}\int_{Y_\Gamma}(-p_1 G_0 - p_0 G_1 + \mu\nabla_y v_0 H_0 + (\nabla_y v_0 H_0)^T)n_0 dy. \end{aligned}$$

Here we used the next ε order of the expansion for the normal stresses on the interface. Applying the divergence theorem to the boundary term and using (3.23) (and subsequent simplifications) we obtain

$$\begin{aligned} &-\mathrm{div}_x\left(\langle Ce_x(u_0) + Ce_y(N(p_0, \nabla_x u_0))\rangle_Y\right) + \frac{1}{|Y|}\int_{Y_\mathcal{F}}(-G_0\nabla_y p_1 + \mu\mathrm{div}_y\left(\nabla_y v_0 H_0\right))dy \\ &= -\mathrm{div}_x\left(\langle Ce_x(u_0) + Ce_y(N(p_0, \nabla_x u_0))\rangle_Y\right) + \frac{1}{|Y|}\int_{Y_\mathcal{F}} G_0 dy \nabla_x p_0 + \frac{1}{|Y|}\int_{Y_\mathcal{F}} J_0 dy f. \end{aligned}$$

We define the modified porosities $\phi_1(p_0, \nabla_x u_0) = \langle G_0 \rangle_{Y_\mathcal{F}}, \phi_2(p_0, \nabla_x u_0) = \langle J_0 \rangle_{Y_\mathcal{F}}$. and, we obtain

$$\begin{aligned} &- \operatorname{div}_x \left(\langle Ce_x(u_0) + Ce_y(N(p_0, \nabla_x u_0)) \rangle_Y \right) \\ &+ \phi_1(p_0, \nabla_x u_0) \nabla_x p_0 + \phi_2(p_0, \nabla_x u_0) f = b \text{ in } \Omega. \end{aligned} \tag{3.35}$$

Recall, we write $u_1 = N(p_0, \nabla_x u_0)$, satisfying (3.30), as to emphasize dependence on the macroscale quantities. Again, if we linearize the tensors to identity, we obtain u_1 as in (3.14). In addition the modified porosities equal true porosity, $\phi_1 = \phi_2 = \phi$ and we return to (3.18).

C. Simplifications of the Model

In this section we consider various simplifications of the homogenized FSI model. We attempt to better connect the nonlinear Biot equations in Section B to the linear model in Section 2. In addition, we use the simplifications to design future effective computational techniques.

We first note, in two dimensions the form of G_0 is linear with respect to $\nabla_x u_0$ and $\nabla_y u_1$. This simpler form of the tensor G_0 will allow us to greatly simplify the elasticity cell problems (3.30). In this case, we are able to obtain cell problems that are nonlinearly coupled only to the macroscopic pressure p_0. After a simple linearization of the Piola tensor, we are able to accomplish this in three dimensions.

We then present a simple hierarchy of models based on simplifications of the elasticity cell equations. We show by subsequent assumptions on the deformation we are able to obtain simpler models. Ultimately, fully decoupling from the mechanics equation, where we obtain a Darcy type law with coefficients only depending on the pressure.

1. Elasticity Cell Linearization

We begin by noting a simple fact of the leading order of Piola transform G_0. In two dimensions G_0 can be written as

$$G_0^{2D} = \begin{bmatrix} \frac{\partial u_0^{(2)}}{\partial x_2} + \frac{\partial u_1^{(2)}}{\partial y_2} + 1 & -\frac{\partial u_0^{(2)}}{\partial x_1} - \frac{\partial u_1^{(2)}}{\partial y_1} \\ -\frac{\partial u_0^{(1)}}{\partial x_2} - \frac{\partial u_1^{(1)}}{\partial y_2} & \frac{\partial u_0^{(1)}}{\partial x_1} + \frac{\partial u_1^{(1)}}{\partial y_1} + 1 \end{bmatrix}. \tag{3.36}$$

We define an indexing 4-tensor D_{ijkl} as $D_{1122} = D_{2211} = 1$ and $D_{1221} = D_{2112} = -1$ and $D_{ijkl} = 0$ elsewhere. We see that

$$D\Big(\nabla_x u_0 + \nabla_y u_1\Big) = \begin{bmatrix} \frac{\partial u_0^{(2)}}{\partial x_2} + \frac{\partial u_1^{(2)}}{\partial y_2} & -\frac{\partial u_0^{(2)}}{\partial x_1} - \frac{\partial u_1^{(2)}}{\partial y_1} \\ -\frac{\partial u_0^{(1)}}{\partial x_2} - \frac{\partial u_1^{(1)}}{\partial y_2} & \frac{\partial u_0^{(1)}}{\partial x_1} + \frac{\partial u_1^{(1)}}{\partial y_1} \end{bmatrix}. \tag{3.37}$$

and so

$$G_0^{2D}(\nabla_x u_0, \nabla_y u_1) = D\left(\nabla_x u_0 + \nabla_y u_1\right) + I. \tag{3.38}$$

We will need to simplify our notation and change the presentation of the problem. Note that for the elasticity cell problem we may re-index the equations and use the symmetry relation $C_{ijkl} = C_{ijlk}$. We obtain

$$-\mathrm{div}_y\left(C(e_x(u_0) + e_y(u_1))\right) = -\mathrm{div}_y\left(C(\nabla_x u_0 + \nabla_y u_1)\right) = 0.$$

Using (3.38), into this modified version of (3.30) we obtain

$$-\mathrm{div}_y\left(C(\nabla_x u_0 + \nabla_y u_1)\right) = 0 \text{ in } Y_{\mathcal{S}}, \tag{3.39a}$$

$$\left(C + p_0 D\right)(\nabla_x u_0 + \nabla_y u_1) n_0 = -p_0 I n_0 \text{ on } Y_\Gamma. \tag{3.39b}$$

Letting

$$u_1 = \nabla_x u_0 R_{p_0} - p_0 Q_{p_0}, \tag{3.40}$$

be an expansion for the first order corrector, we obtain two cell problems

$$-\mathrm{div}_y\left(C(I+\nabla_y R_{p_0})\right)=0 \text{ in } Y_{\mathcal{S}}, \tag{3.41a}$$

$$\left(C+p_0 D\right)\left(I+\nabla_y R_{p_0}\right)n_0=0 \text{ on } Y_\Gamma, \tag{3.41b}$$

and

$$-\mathrm{div}_y\left(C(\nabla_y Q_{p_0})\right)=0 \text{ in } Y_{\mathcal{S}}, \tag{3.42a}$$

$$\left(C+p_0 D\right)\left(\nabla_y Q_{p_0}\right)n_0=In_0 \text{ on } Y_\Gamma, \tag{3.42b}$$

where $R_{p_0}Q_{p_0}$, are y-periodic and vanish on the interface Y_Γ. We now can construct the displacement up to first order as $u_\varepsilon = u_0 + \varepsilon(\nabla_x u_0 R_{p_0} - p_0 Q_{p_0})$. We see that the above cell equations are completely decoupled from $\nabla_x u_0$.

We are able to generalize the ideas from the above two dimensional setting to three dimensions. This is accomplished by a linearization of the Piola tensor G_0 with respect to $\nabla_x u_0$ and $\nabla_y u_1$. In this way we obtain an expression for the similar to (3.38). Note, in three dimensions

$$G_0^{3D} = G_0^L + O(\nabla u_\varepsilon^2).$$

Here, we write the linear part as

$$G_0^L = I+$$
$$\begin{bmatrix} \frac{\partial u_0^{(2)}}{\partial x_2}+\frac{\partial u_0^{(3)}}{\partial x_3}+\frac{\partial u_1^{(2)}}{\partial y_2}+\frac{\partial u_1^{(3)}}{\partial y_3} & -\frac{\partial u_0^{(2)}}{\partial x_1}-\frac{\partial u_1^{(2)}}{\partial y_1} & -\frac{\partial u_0^{(3)}}{\partial x_1}-\frac{\partial u_1^{(3)}}{\partial y_1} \\ -\frac{\partial u_0^{(1)}}{\partial x_2}-\frac{\partial u_1^{(1)}}{\partial y_2} & \frac{\partial u_0^{(1)}}{\partial x_1}+\frac{\partial u_0^{(3)}}{\partial x_3}+\frac{\partial u_1^{(1)}}{\partial y_1}+\frac{\partial u_1^{(3)}}{\partial y_3} & -\frac{\partial u_0^{(3)}}{\partial x_2}-\frac{\partial u_1^{(3)}}{\partial y_2} \\ -\frac{\partial u_0^{(1)}}{\partial x_3}-\frac{\partial u_1^{(1)}}{\partial y_3} & -\frac{\partial u_0^{(2)}}{\partial x_3}-\frac{\partial u_1^{(2)}}{\partial y_3} & \frac{\partial u_0^{(1)}}{\partial x_1}+\frac{\partial u_0^{(2)}}{\partial x_2}+\frac{\partial u_1^{(1)}}{\partial y_1}+\frac{\partial u_1^{(2)}}{\partial y_2} \end{bmatrix}.$$

Thus we see that the linear part in three dimensions has a similar form to (3.38). We

let D^{3D} be the indexing 4-tensors such that we write the linearized Piola tensor as

$$G_0^L(\nabla_x u_0, \nabla_y u_1) = D^{3D}\left(\nabla_x u_0 + \nabla_y u_1\right) + I. \tag{3.43}$$

We see that we may expand u_1 as (3.40), and we obtain structurally similar cell equations as (3.41) and (3.42), although with the three dimensional 4-tensor D^{3D}. We will drop the superscript when there is no ambiguity. With this linearization we are able to decouple the gradient of the macro displacement, $\nabla_x u_0$, from elasticity cell equations as in the two dimensional setting.

The equation (3.35) may now be simplified. For simplicity, in this section we assume no body forces, i.e. $f = b = 0$. First, note that using (3.40) and (3.43), we obtain for modified porosity

$$\begin{aligned}\phi_1(p_0, \nabla_x u_0) = \frac{1}{|Y|}\int_{Y_{\mathcal{F}}} G_0 dy = \phi_1(p_0, \nabla_x u_0) &= \frac{1}{|Y|}\int_{Y_{\mathcal{F}}} \left(D\left(\nabla_x u_0 + \nabla_y u_1\right) + I\right) dy \\ &= D\nabla_x u_0\left(I + \langle \nabla_y R_{p_0}\rangle_{Y_{\mathcal{F}}}\right) - p_0 D\langle \nabla_y Q_{p_0}\rangle_{Y_{\mathcal{F}}} + \phi. \end{aligned} \tag{3.44}$$

Using the expansion (3.40) into (3.35) and applying the above expression for ϕ_1, we obtain

$$-\mathrm{div}_x\left(\langle C(I + e_y(R_{p_0}))\rangle_Y \nabla_x u_0 - p_0\langle C e_y(Q_{p_0})\rangle_Y\right) + \phi_1(p_0, \nabla_x u_0)\nabla_x p_0 = 0.$$

Here we have a more clear picture of the macroscale elasticity equation. In addition, we have decoupled $\nabla_x u_0$ from the elasticity cell equations.

2. Hierarchy of Models

In this section, we use the above formulation. That is, we assume that we have linearized the Piola Tensor to arrive at the above cell problems and expansions for u_1. We present a hierarchy of models based on this linearization. This hierarchy is

presented so that we may obtain simpler models and use these simplifications in our numerical example.

a. Full Model with Linearized Piola Tensor

In the full model, we assume that the displacement is of the form $u_\varepsilon = u_0 + \varepsilon(\nabla_x u_0 R_{p_0} - p_0 Q_{p_0})$. Thus the fluid and solid equations can be expressed as

$$\begin{aligned}
&\mathrm{div}_x \left(K^*\left(p_0, \nabla_x u_0\right) \nabla_x p_0\right) + \left(D^*\left(p_0, \nabla_x u_0\right) - A^*(p_0, \nabla_x u_0)\right)\partial_t \nabla_x u_0, \\
&+ B^*(p_0, \nabla_x u_0)\partial_t p_0 + 2\mathrm{div}_x \left(D^*(p_0, \nabla_x u_0)\right) \partial_t u_0 = 0 \\
&- \mathrm{div}_x \left(\langle C(I + e_y(R_{p_0}))\rangle_Y \nabla_x u_0 - p_0 \langle C e_y(Q_{p_0})\rangle_Y\right) + \phi_1(p_0, \nabla_x u_0)\nabla_x p_0 = 0
\end{aligned}$$

b. Negligible Cell Strain: $\nabla_y R_{p_0} = 0$

Here we will still have a macroscopic solid equation, but the elasticity equation will have a simplified form. In addition, we need only solve one elasticity cell equation (3.42). We let the displacement be given by $u_\varepsilon = u_0 - \varepsilon p_0 Q_{p_0}$. The fluid and solid equations are given by

$$\begin{aligned}
&\mathrm{div}_x \left(K^*\left(p_0, \nabla_x u_0\right) \nabla_x p_0\right) + \left(D^*\left(p_0, \nabla_x u_0\right) - A^*(p_0, \nabla_x u_0)\right)\partial_t \nabla_x u_0 \\
&+ B^*(p_0, \nabla_x u_0)\partial_t p_0 + 2\mathrm{div}_x \left(D^*(p_0, \nabla_x u_0)\right) \partial_t u_0 = 0, \\
&- \mathrm{div}_x \left(\langle C\rangle_Y \nabla_x u_0 - p_0 \langle C e_y(Q_{p_0})\rangle_Y\right) + \phi_1(p_0, \nabla_x u_0)\nabla_x p_0 = 0
\end{aligned}$$

where, ϕ_1 is given by (3.44), but with $\nabla_y R_{p_0} = 0$.

c. No Macroscopic displacement $u_0 = 0$

In the simplest case we assume that there is no macroscale displacement. Thus, $u_\varepsilon = -\varepsilon p_0 Q_{p_0}$, where Q_{p_0} is a solution to a cell problem of the form (3.42). Then,

the solid equation vanishes and we have pure pressure nonlinear diffusion.

$$\mathrm{div}_x \left(K^* \left(p_0 \right) \nabla_x p_0 \right) + B^*(p_0) \partial_t p_0 = 0$$

In the next section, we will present numerics based on this simplification. This simplification implies that the macroscopic parameters depend only on pressure p_0. Hence, we may create one parameter tables based on this simplification.

d. Numerical Application

In this section, we discuss a numerical example. For simplicity we shall use the simplest model where the macroscopic quantities depend only on macroscopic pressure. This corresponds to a pore pressure driven deformation. The extension to including displacement gradient dependence on the macroscopic quantities is the subject of future research.

As noted prior, we can view the cell problems (3.25) and (3.30) as parameterized by the macroscopic quantities $(p_0, \nabla_x u_0)$. Note that if we have no macroscopic displacement on the cell level, $e_x(u_0) = 0$, the elasticity cell equation becomes

$$-\mathrm{div}_y \left(C \left(e_y(u_1) \right) \right) = 0 \text{ in } Y_{\mathcal{S}}, \tag{3.45a}$$

$$C \left(e_y(u_1) \right) n_0 = -p_0 G_0 \left(\nabla_y u_1 \right) n_0 \text{ on } Y_\Gamma. \tag{3.45b}$$

Linearizing as before we write $G_0 = D \nabla_y u_1 + I$. Letting

$$u_1 = -p_0 Q_{p_0}, \tag{3.46}$$

where Q_{p_0} satisfies

$$-\mathrm{div}_y \left(C(\nabla_y Q_{p_0}) \right) = 0 \text{ in } Y_{\mathcal{S}}, \tag{3.47a}$$

$$\left(C + p_0 D \right) \left(\nabla_y Q_{p_0} \right) n_0 = I n_0 \text{ on } Y_\Gamma. \tag{3.47b}$$

Thus, given a value of macroscopic pressure, we can compute the cell quantity Q_{p_0} and thus the deformation u_1 given by (3.46). Recall, since $u_0 = 0$, we have $u_\varepsilon = \varepsilon u_1 = -\varepsilon p_0 Q_{p_0}$. From here we may compute a tabular function of Permeability K and Biot constant α^* given a macroscopic pressure.

Indeed, we compute $\alpha^* = \langle Q_{p_0} \rangle_Y + \phi$ given a macroscopic pressure and corresponding cell solution. From here we may construct the deformation of the cell for this given pressure by the relation (3.46). Then, by solving a local Stokes cell equation, we compute K. In this way we arrive at a table.

We implement this procedure on a test cell geometry. In Figure 8(a), we observe a simple fluid cell geometry. In Figure 8(b), the corresponding solid geometry of the microstructure. Given a pressure we construct the displacement using (3.46). Such an example of the solid cell displacement can be seen in Figure 9(a). We implement this procedure for varying values of p_0 and subsequently compute values of α^* and K. The results can be observed in Table III. We see there is a weak dependence on the pressure for the Biot constant α^* and a stronger dependence on the pressure for permeability K.

Now that we have tabular values of macroscopic quantities α^*, K, they can be utilized in computation of nonlinear Biot equations. For example, if we assume time independence and a fixed elasticity tensor C, we arrive at the following Biot equations

$$-\mathrm{div}(K(p_0)\nabla p_0) = f, \tag{3.48}$$

$$-\mathrm{div}\left(Ce(u_0) - \alpha^*(p_0)\right) = b. \tag{3.49}$$

For the above equations one can envision an iterative numerical procedure to calculate the solutions of such equations. This will be the subject of future numerical investigations. In addition one can consider more complicated cell dependency, such

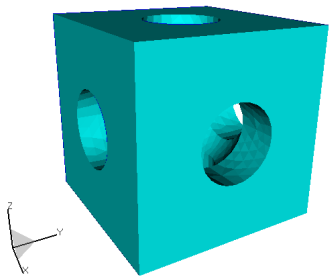

(a) Fluid Cell

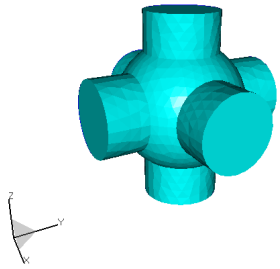

(b) Solid Cell

Fig. 8. Test cell geometry.

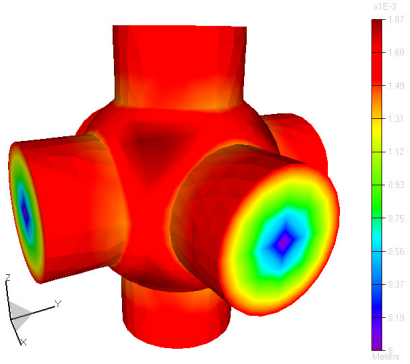

(a) Solid Displacement

Fig. 9. Solid displacement given by $u_\varepsilon = -\varepsilon p_0 Q_{p_0}$.

as depending on both macroscopic pressure and, for example, volumetric strain or directional strain etc.

Table III. Table of Biot coefficient and permeability for various values of pressure.

p_0	α	K
0.001	0.192793	0.0914
0.01	0.192263	0.0929
0.1	0.186783	0.1137

CHAPTER IV

MULTISCALE HIERARCHICAL FINITE ELEMENT METHODS FOR STOKES EQUATIONS

In the previous chapter, we introduced the concept of the Stokes equations in the Arbitrary Lagrange-Eulerian. We will now use this formulation to develop an efficient algorithm for computing the permeability tensor throughout complicated slowly varying media. As in Chapter II, we return to a setting where we have decoupled fluid flow and solid mechanics. A fully coupled hierarchical finite element algorithm is the topic for future research.

A. Introduction

As noted in earlier chapters, direct numerical simulation (DNS) of fluid flow in complex geometries with many scales is often not feasible and an effective or homogenized description is more desirable. To construct the homogenized equations, effective properties must be computed. Computation of effective properties for non-periodic microstructures can be prohibitively expensive as many local cell problems must be solved for different macroscopic points. The local problems may also exhibit complex geometries and scale disparity making them computationally expensive. When the microstructure varies slowly, we develop an efficient numerical method for two-scales that achieves essentially the same accuracy as that for the full resolution solve of every local cell problem. In this method, we build a dense hierarchy of macroscopic grid-points and a corresponding nested sequence of approximation spaces. Essentially, solutions computed in high accuracy approximation spaces at select points in the hierarchy are used as corrections for the error of the lower accuracy approximation spaces at nearby macroscopic points. We give a brief overview of slowly varying

media and formal Stokes homogenization in such domains. We present a general outline of the algorithm and list reasonable and easily verifiable assumptions on the partial differential equations, geometry, and approximation spaces. With these assumptions, we achieve the same accuracy as the full solve. By full solve we mean we use a high accuracy finite element space at all the points. To demonstrate the elements of the proof of the error estimate, we use a hierarchy of macro-grid points in $[0,1]^2$ and Finite Element (FE) approximation spaces in $[0,1]^2$. We apply this algorithm to Stokes equations in a slowly porous medium where the microstructure is obtained from a reference periodic domain by a known smooth map. Using the Arbitrary Lagrange-Eulerian (ALE) formulation of the Stokes equations cf. [15], we obtain modified Stokes equations with varying coefficients in the periodic domain. We show that the algorithm can be utilized in this setting. Finally, we implement the algorithm on the modified Stokes equations, using a simple stretch deformation mapping, and compute the effective permeability. We show that our efficient computation is of the same order as the full solve.

In this chapter we again consider creeping flow of an incompressible Newtonian fluid in a complex microstructure that is slowly varying. We develop a novel and efficient two-scale Finite Element Method (FEM) to compute solutions to the auxiliary cell equations. These cell problems relate the micro-scale information to the macro-scale or effective description. In turn, we are able to construct a numerical approximation to the homogenized equations in slowly varying geometries. In this method, we are able to reuse previously computed information from nearby cell equations to obtain a more accurate solution at a reduced computational cost. Our main goal of the chapter is to show that we obtain the same order of accuracy with our algorithm as the much more costly full solve.

Recall, in the event that the media is periodic, analytical techniques and com-

putational algorithms for Stokes homogenization are well studied. Using the method of two-scale asymptotic expansion [33, 34], the authors develop a formal justification for the homogenization of Stokes equations in perforated domains. First, auxiliary cell equations are deduced then, after averaging, the solutions are used to construct the homogenized Darcy equation [10]. In the periodic setting, the cell equations completely uncouple from macro-scale variables and only depend on the cell pore geometry. This fact, along with periodicity, results in a single set of cell equations that must be computed to construct the homogenized equations. In slowly varying media this is not the case, as the geometry changes a new set of cell equations must be calculated. This is often also true for elliptic problems with highly oscillatory coefficients [1]. For example, in two-scale diffusion problems, the diffusivity tensor may depend on both macro- and micro-scales. For each macroscopic point a corresponding set of cell equations must be computed.

In practice, we cannot compute a set of cell equations for each macroscopic point. In [7], the topic of Chapter II, the authors develop a moving averages homogenization algorithm, a numerical technique to construct the homogenized Darcy equation in slowly varying media. By computing the set of cell problems at many select macroscopic points using a standard FEM and interpolating the result, a numerical approximation to the homogenized equation is obtained. This approach, although successful in its task, can be improved upon in a number of ways. Each of the cell equations are computed using the same order of accuracy and must be re-meshed for each unique geometry. This can be computationally expensive, especially in cases where the cell geometry is very complicated. Even though the geometry is slowly varying and there is little change from RVE to RVE, information from nearby cells cannot be reused without sampling errors from interpolating solutions with differing meshes. Since the geometries vary little, there is some redundancy in re-calculating cell problems in

nearby RVEs. In this work, we develop techniques to circumvent these difficulties.

The idea of the algorithm is as follows. We first develop an algorithm that yields a hierarchy of grids, with specified qualities, in the macroscopic variable. Traditionally, we would solve a set of cell problems at all these macroscopic grid points with the same accuracy as in the method of moving averages [7]. In our proposed framework, we build a corresponding nested collection of finite element (FE) approximation spaces with varying orders of accuracy to compute cell equations. With some macro-grids we compute very accurate cell solutions, and with more refined macro-grids (closer grid-spacing) we compute cell solutions with less accuracy. We use local information from nearby higher accuracy solutions as known "right-hand-side data" to correct the lower accuracy solves. These ideas have been used successfully for elliptic problems. In the case where a high dimensional homogenized equation is available, the sparse tensor product discretization approach developed in [18] computes the solution to the effective equation and the corrector with an essentially equal complexity to that for solving a single macroscopic PDE and achieves essentially equal accuracy as the full solve, without forming the effective equation explicitly. As for the Stokes equations, for the elliptic problem considered in [18], if the effective coefficient is of interest, it can be computed efficiently with much reduced complexity by our method.

Often, slowly varying media arises from coupled physical processes. In this work, we assume the mapping from the initial periodic (reference) configuration to the slowly varying (current) configuration is known. For example, in iterative FSI, fluid equations are solved then normal stresses at the interface are passed to the solid mechanics equations. The displacement of the solid is computed and fluid equations are solved again in the newly deformed domain c.f [32]. At each iteration step, the deformation from the reference to the current configuration is computed by composing displacements of each iteration. With this information, we are able to reformulate the

Stokes equations in a slowly varying domain to modified Stokes equations with tensor coefficients in the initial periodic domain. In the context of FSI, this reformulation is referred to as the Arbitrary Lagrange-Eulerian (ALE) formulation of the Stokes equations cf. [14, 15]. For the full time dependent model we refer to Chapter III. The periodic ALE formulation allows us to construct a nested collection of FE spaces. The geometry does not change, but instead the tensor coefficients vary. In this formulation, we are able to prove with reasonable and easily verifiable assumptions, that our algorithm produces essentially the same order of accuracy as the full solve with much reduced complexity.

The organization of the chapter is as follows. First, we motivate the need for an efficient multiscale algorithm in slowly varying media. We begin by giving a summary of formal homogenization of Stokes equations in such media. This will serve to introduce terminology used throughout the work and highlight advantages of reformulating the problem in the ALE. Then, an overview of the solution approach and computational algorithm is presented in general terms. We outline physically reasonable and easily verifiable abstract mathematical assumptions on the microstructure geometry, variational equations, and FE approximation spaces. These assumptions will guarantee that our algorithm has the same order of accuracy as the full solve, but at less computational cost. We prove this for a two-dimensional hierarchy of macro-grids to illustrate the main ideas of the proof. Then, we reformulate the Stokes equations from the slowly varying geometry to the periodic ALE formulation. We verify that the abstract assumptions outlined in the abstract formulation hold assuming the geometry is slowly varying. Hence, our efficient multiscale algorithm will be applicable in this setting. Finally, we apply our algorithm to a constructed example where initially periodic media with square inclusions is deformed via a horizontal stretch. We show that our algorithm is the same order of accuracy as the full fine mesh solve by

comparing permeabilities or, averaged cell velocity solutions.

B. Background and Overview of Algorithm

In this section we briefly recall exposition of slowly varying domains given in Chapter II, formal Stokes homogenization in such media, and an overview of our efficient multiscale FE algorithm. We introduce periodic perforated domains and then, after applying a mapping, we obtain the slowly varying domain. This mapping is an *a-priori* known quantity computed from another coupled process such as FSI deformation or chemical degradation, etc. [29, 32]. Unlike in Chapter III, we assume that the fluid flow is time independent and decoupled from the mechanics. This can be achieved via an iterative scheme. The homogenization background will serve to motivate our algorithm and give definitions to general terminology used throughout the chapter. We follow the presentation of this material given in [7]. To this end, we introduce the fine-scale Stokes operator, and then via formal two-scale asymptotic expansions [33], we arrive at the auxiliary cell operator. From here we can construct the homogenized equations.

We are then in a position to give an overview for our algorithm. First, we highlight the challenges in the numerical homogenization of the equations presented in the following section. The primary challenge being, due to the changing pore geometry, we must solve many sets of cell problems at various points in the domain. A synopsis of the algorithm approach is given. We outline the requisite properties of the hierarchy of macro-grids and corresponding nested sequence of FE approximation spaces. We then state the procedure required to obtain the desired order of accuracy.

1. Notation, Slowly Varying Media, and Homogenization of Stokes Flow

We begin with some basic notation. Let the macroscopic domain Ω be an open bounded subset of $\mathbb{R}^d$. We assume that the domain is periodically perforated by an open solid microstructure denoted $\mathcal{S}_\varepsilon$. The solid surrounds a connected fluid pore-space denoted by $\mathcal{F}_\varepsilon$. That is, $\Omega = \mathcal{F}_\varepsilon \cup \mathcal{S}_\varepsilon$ and $\mathcal{F}_\varepsilon \cap \mathcal{S}_\varepsilon = \emptyset$. The interface between the two media is denoted as $\Gamma_\varepsilon = \bar{\mathcal{F}}_\varepsilon \cap \bar{\mathcal{S}}_\varepsilon$. Furthermore, we assume that the media has an additional structure. The two domains are decomposed into a set of unit cells $\varepsilon \{Y_\mathcal{F}^i\}_{i=1}^N$ and $\varepsilon \{Y_\mathcal{S}^i\}_{i=1}^N$, respectively, and ε is the characteristic pore size. That is, $Y_\mathcal{S}^i$ and $Y_\mathcal{F}^i$, $i = 1, \ldots, N$, are unit-sized domains and

$$\mathcal{F}_\varepsilon = \left(\bigcup_{i=1}^N \varepsilon Y_\mathcal{F}^i \right) \cap \Omega, \qquad \mathcal{S}_\varepsilon = \left(\bigcup_{i=1}^N \varepsilon Y_\mathcal{S}^i \right) \cap \Omega. \tag{4.1}$$

Since the domain is assumed to be periodic, each of the cells differ only by a translation. That is, $Y_\mathcal{F}^i = Y_\mathcal{F} + k_i$ and $Y_\mathcal{S}^i = Y_\mathcal{S} + k_i$, where $k_i \in \mathbb{Z}^d$ corresponds to the i-th cell. We denote the entire unit cell as $Y = Y_\mathcal{F} \cup Y_\mathcal{S}$ and the cell interface Y_Γ.

Let $\widetilde{X}_\varepsilon : \Omega \to \widetilde{\Omega}_\varepsilon$ be a smooth map of the periodic domain to the deformed domain $\widetilde{\Omega}_\varepsilon$. In this chapter, we assume that the deformation has reached a steady-state. We denote $\widetilde{X}_\varepsilon$ as the steady-state deformation. Consequently, we may define the steady-state deformed fluid, solid, and interface as $\widetilde{\mathcal{F}}_\varepsilon = \widetilde{X}_\varepsilon(\mathcal{F}_\varepsilon)$, $\widetilde{\mathcal{S}}_\varepsilon = \widetilde{X}_\varepsilon(\mathcal{S}_\varepsilon)$, and $\widetilde{\Gamma}_\varepsilon = \widetilde{X}_\varepsilon(\Gamma_\varepsilon)$, respectively. In this chapter, we denote the coordinates of the periodic geometry by x and the slowly varying geometry by $\tilde{x}$. We denote physical quantities in the slowly varying geometry with a $\widetilde{\ }$. Again, as in Chapter III, we will work mainly in the periodic reference domain and not use the $\widetilde{\ }$ notation for most of the chapter. An example of two domains can be seen in Figure 10, where $\Omega = [0,1]^2$ and $\varepsilon = 1/4$. Each unit cell is now deformed, so we define a moving representative volume element (RVE). For each $\tilde{x} \in \widetilde{\Omega}$ the fluid and solid cell domains contained in a RVE are

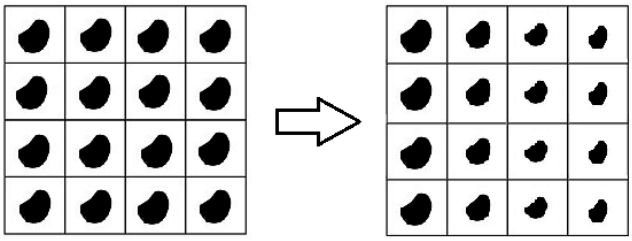

Fig. 10. Mapping from periodic $\Omega = \mathcal{F}_\varepsilon \cup \mathcal{S}_\varepsilon$ to slowly varying $\widetilde{\Omega}_\varepsilon = \widetilde{\mathcal{F}}_\varepsilon \cup \widetilde{\mathcal{S}}_\varepsilon$ by $\widetilde{X}_\varepsilon$. The fluid and solid are white and black, respectively, in both domains.

denoted by $Y^{\tilde{x}}_{\widetilde{\mathcal{S}}}$ and $Y^{\tilde{x}}_{\widetilde{\mathcal{F}}}$, and the interface by $Y^{\tilde{x}}_{\widetilde{\Gamma}}$. The deformation creates a natural correspondence between translated periodic cells and deformed cells. We view the slowly varying RVEs as the image of the mapping $\widetilde{X}_\varepsilon$ restricted to translated periodic cells. That is, $\varepsilon Y^{\tilde{x}}_{\widetilde{\mathcal{F}}} = \widetilde{X}_\varepsilon(\varepsilon\,(Y_{\mathcal{F}} + k_x))$ and $\varepsilon Y^{\tilde{x}}_{\widetilde{\mathcal{S}}} = \widetilde{X}_\varepsilon(\varepsilon\,(Y_{\mathcal{S}} + k_x))$, where $k_x \in \mathbb{Z}^d$ corresponds to the RVE at $x \in \Omega$ in the periodic domain. Thus, the deformed fluid and solid space are given by

$$\widetilde{\mathcal{F}}_\varepsilon = \bigcup_{\tilde{x}\in\widetilde{\Omega}} \varepsilon Y^{\tilde{x}}_{\widetilde{\mathcal{F}}}, \qquad\qquad \widetilde{\mathcal{S}}_\varepsilon = \bigcup_{\tilde{x}\in\widetilde{\Omega}} \varepsilon Y^{\tilde{x}}_{\widetilde{\mathcal{S}}}.$$

Remark Recalling the formal definition of slowly varying media given in [7], we say a medium is slowly varying if nearby RVE pore geometry differs slightly. More precisely, we say that $\widetilde{\Omega}_\varepsilon$ is slowly varying if the map $\widetilde{X}_\varepsilon$ is such that if $\tilde{x}, \tilde{x}' \in \widetilde{\Omega}_\varepsilon$ and $\|\tilde{x} - \tilde{x}'\| < O(\varepsilon)$ then,

$$|(Y^{\tilde{x}}_{\widetilde{\mathcal{F}}} \cup Y^{\tilde{x}'}_{\widetilde{\mathcal{F}}})\backslash(Y^{\tilde{x}}_{\widetilde{\mathcal{F}}} \cap Y^{\tilde{x}'}_{\widetilde{\mathcal{F}}})| < O(\varepsilon).$$

In this work, we will need to make more concrete assumptions on the mapping $\widetilde{X}_\varepsilon$. Indeed, we will require that the mapping and its gradient be sufficiently smooth and Lipschitz continuous with respect to the macroscopic (slow) variables.

Representative volume elements contain a representative sample of small scale

information. At each of these points, local problems are solved. For complex microstructure this can be very computationally expensive. To resolve local flow properties, Stokes equations are solved in the RVEs assuming periodic boundary conditions. These boundary conditions assume that, near a fixed macroscopic point, the microstructure is periodic.

For the sake of clarity and In the following we recall the homogenization procedure of Chapter II. We recall a formal derivation of this type of procedure by two-scale asymptotic expansions for Stokes flow in slowly varying domains. This will serve to introduce general terminology and motivate our algorithm.

We suppose that we have an incompressible Newtonian fluid in the pore-space with viscosity μ. The fine-scale pressure and velocity are denoted $\widetilde{p}_\varepsilon$ and $\widetilde{v}_\varepsilon$, respectively. The flow of such a fluid at creeping velocities is governed by the Stokes approximation [36]. The conservation of linear momentum and conservation of mass then reads

$$-\nabla\widetilde{p}_\varepsilon + \mu\Delta\widetilde{v}_\varepsilon = \widetilde{f} \text{ in } \widetilde{\mathcal{F}}_\varepsilon, \tag{4.2a}$$

$$\nabla\cdot\widetilde{v}_\varepsilon = 0 \text{ in } \widetilde{\mathcal{F}}_\varepsilon, \tag{4.2b}$$

and we assume the boundary condition $\widetilde{v}_\varepsilon = 0$ on $\widetilde{\Gamma}_\varepsilon$. For convenience in notation for what follows, we let $\widetilde{\mathcal{L}}_\varepsilon\left(\tilde{x}, \frac{\tilde{x}}{\varepsilon}\right)$ denote the above fine-scale Stokes operator. Using the two-scale expansions first proposed in [34], pressure and velocity are expanded as

$$\widetilde{v}_\varepsilon(\tilde{x}) = \varepsilon^2\left(\widetilde{v}_0(\tilde{x},\tilde{y}) + \varepsilon\widetilde{v}_1(\tilde{x},\tilde{y}) + \cdots\right), \tag{4.3a}$$

$$\widetilde{p}_\varepsilon(\tilde{x}) = \widetilde{p}_0(\tilde{x}) + \varepsilon\widetilde{p}_1(\tilde{x},\tilde{y}) + \cdots, \tag{4.3b}$$

where $\tilde{y} = \tilde{x}/\varepsilon$ is the fast variable and derivatives behave as $\nabla \to \nabla_{\tilde{x}} + \frac{1}{\varepsilon}\nabla_{\tilde{y}}$. The cell problems are now stated for a given spatial position. Fixing $\tilde{x}$ and substituting the

expansions (4.3) into the Stokes equations (4.2), gathering ε^0 terms in the conservation of linear momentum and ε^{-1} terms in the incompressibility equation, one obtains

$$-\nabla_{\tilde{y}}\widetilde{p}_1(\tilde{x},\tilde{y}) + \Delta_{\tilde{y}}\widetilde{v}_0(\tilde{x},\tilde{y}) = \widetilde{f}(\tilde{x}) + \nabla_{\tilde{x}}\widetilde{p}_0(\tilde{x}) \qquad \text{in } Y^{\tilde{x}}_{\widetilde{\mathcal{F}}}, \tag{4.4a}$$

$$\nabla_{\tilde{y}} \cdot \widetilde{v}_0(\tilde{x},\tilde{y}) = 0 \qquad \text{in } Y^{\tilde{x}}_{\widetilde{\mathcal{F}}}, \tag{4.4b}$$

where $\widetilde{v}_0$ and $\widetilde{p}_1$ are $\tilde{y}-$periodic also require $\widetilde{v}_0 = 0$ on $Y^{\tilde{x}}_{\widetilde{\Gamma}}$ and $\langle \widetilde{p}_1 \rangle_{Y^{\tilde{x}}} = 0$. Here, $\langle \cdot \rangle_{Y^{\tilde{x}}}$ is the average over the unit cell centered at $\tilde{x}$ given by

$$\langle \cdot \rangle_{Y^{\tilde{x}}} = \frac{1}{\left|Y^{\tilde{x}}\right|} \int_{Y^{\tilde{x}}} \cdot \, d\tilde{y}. \tag{4.5}$$

Next, due to linearity of (4.4) and the right-hand-side being a function of the slow variable $\tilde{x}$ only, one has

$$\widetilde{v}_0(\tilde{x},\tilde{y}) = \widetilde{w}(\tilde{x},\tilde{y}) \cdot \left(\widetilde{f}(\tilde{x}) + \nabla_{\tilde{x}}\widetilde{p}_0(\tilde{x}) \right), \tag{4.6a}$$

$$\widetilde{p}_1(\tilde{x},\tilde{y}) = \widetilde{\pi}(\tilde{x},\tilde{y}) \cdot \left(\widetilde{f}(\tilde{x}) + \nabla_{\tilde{x}}\widetilde{p}_0(\tilde{x}) \right), \tag{4.6b}$$

where $(\widetilde{w}^i(\tilde{x},\tilde{y}), \widetilde{\pi}^i(\tilde{x},\tilde{y}))$, $i = 1, \ldots, d$ are the solutions to the auxiliary cell equations

$$-\nabla_{\tilde{y}}\widetilde{\pi}^i + \mu\Delta_{\tilde{y}}\widetilde{w}^i = e_i \text{ in } Y^{\tilde{x}}_{\widetilde{\mathcal{F}}}, \tag{4.7a}$$

$$\operatorname{div}_{\tilde{y}}\left(\widetilde{w}^i\right) = 0 \text{ in } Y^{\tilde{x}}_{\widetilde{\mathcal{F}}}, \tag{4.7b}$$

with $\widetilde{w}^i$ and $\widetilde{\pi}^i$ being $\tilde{y}-$periodic, $\widetilde{w}^i = 0$ on $Y^{\tilde{x}}_{\widetilde{\Gamma}}$ and $\langle \pi^i \rangle_{Y^{\tilde{x}}} = 0$. Here, e_i is the i-th standard unit vector in $\mathbb{R}^d$. Again, for convenience in presentation in the following we denote the above Stokes cell operator as $\widetilde{\mathcal{L}}_{\tilde{y}}(\tilde{x})$. Now, to relate these cell problems to the classical Darcy equation [10], one inserts (4.3a) into the conservation of mass of the fine-scale operator (4.2) and, by collecting ε^0 terms, we obtain

$$\nabla_{\tilde{x}} \cdot \widetilde{v}_0 + \nabla_{\tilde{y}} \cdot \widetilde{v}_1 = 0 \text{ in } \widetilde{\mathcal{F}}_\varepsilon. \tag{4.8}$$

We fix $\tilde{x}$ and integrate over the cell $Y_{\widetilde{\mathcal{F}}}^{\tilde{x}}$. Using the divergence theorem, the fact that $\widetilde{v}_1$ has zero trace on $Y_\Gamma^{\tilde{x}}$, $\tilde{y}-$periodicity, and (4.6a), one obtains the homogenized macroscopic equation of Darcy type

$$\nabla_{\tilde{x}} \cdot \left(\widetilde{K}(\tilde{x}) \left(\nabla_{\tilde{x}} \widetilde{p}_0(\tilde{x}) + \widetilde{f}(\tilde{x}) \right) \right) = 0 \text{ in } \widetilde{\Omega}, \tag{4.9}$$

where the $\tilde{x}$-dependent permeability is defined as $\widetilde{K}_{ij}(\tilde{x}) := \int_{Y_{\widetilde{\mathcal{F}}}^{\tilde{x}}} \widetilde{w}^{ij}(\tilde{x}, \tilde{y}) d\tilde{y}$ and we define the Darcy velocity $\widetilde{\xi} = \widetilde{K}(\tilde{x}) \left(\widetilde{f}(\tilde{x}) + \nabla_{\tilde{x}} \widetilde{p}_0(\tilde{x}) \right)$. We require the boundary condition $\widetilde{\xi} \cdot \widetilde{\nu} = 0$ on $\partial\widetilde{\Omega}$, where $\widetilde{\nu}$ is the outward normal. In what follows, we denote the above homogenized operator as $\widetilde{\mathcal{L}}(\tilde{x})$. Note that in the periodic setting we have only one cell geometry, and need only compute one set of cell equations (4.7). Thus, $\widetilde{K}(\tilde{x}) = \widetilde{K}$ is constant and does not depend on the slow variable.

Remark In addition, we require that the mapping $\widetilde{X}_\varepsilon$ be smooth enough so that the asymptotic expansions (4.3) will yield correct cell equations (4.4) and that the permeability $\widetilde{K}(\tilde{x})$ is a sufficiently smooth enough function of the slow variable $\tilde{x}$. Formally speaking, the map does not change the microstructure from neighboring RVEs in a significant way and varies slowly.

2. Overview of the Algorithm

The main goal of employing the two-scale asymptotic expansion is to obtain effective homogenized macroscopic equations $\widetilde{\mathcal{L}}(\tilde{x})$ of the fine-scale equations $\widetilde{\mathcal{L}}_\varepsilon\left(\tilde{x}, \frac{\tilde{x}}{\varepsilon}\right)$, given here by (4.9), (4.2), respectively. In numerical homogenization, we wish to construct an approximation to the homogenized equations $\widetilde{\mathcal{L}}(\tilde{x})$ by computing solutions to auxiliary cell equations $\widetilde{\mathcal{L}}_{\tilde{y}}(\tilde{x})$, given here by (4.7). In the periodic setting, this is inexpensive as $\widetilde{\mathcal{L}}_{\tilde{y}}(\tilde{x}) = \widetilde{\mathcal{L}}_{\tilde{y}}$. In this section, we outline an efficient multiscale algorithm to compute the homogenized equations in slowly varying geometries.

The solution approach can be summarized as follows. Since we are given the mapping $\widetilde{X}_\varepsilon$ *a-priori*, we use it to reformulate Stokes equations in the periodic ALE formulation [14, 15]. This process transfers the information of the slowly varying geometry to tensor coefficients of the modified Stokes equations. Then, we apply the two-scale asymptotic expansion homogenization technique to the modified Stokes equations $\mathcal{L}_\varepsilon\left(x, \frac{x}{\varepsilon}\right)$. This yields the cell equations $\mathcal{L}_y(x)$ and, subsequently, the homogenized equations $\mathcal{L}(x)$. We are then able work in fixed cell domains $Y_\mathcal{F}$ as opposed to $Y_{\widetilde{\mathcal{F}}}^{\tilde{x}}$ for many values of $\tilde{x}$. This fixed domain approach simplifies the analysis and allows for information from nearby RVEs to be used in an effective way. The approach may be summed up in the following diagram

$$\begin{array}{ccccc} \widetilde{\mathcal{L}}_\varepsilon\left(\tilde{x}, \frac{\tilde{x}}{\varepsilon}\right) & \xrightarrow{\text{Two-Scale}} & \widetilde{\mathcal{L}}_{\tilde{y}}(\tilde{x}) & \xrightarrow{\text{Averaging}} & \widetilde{\mathcal{L}}(\tilde{x}) \\ \downarrow & & \text{Reformulate Equations in Periodic Domain} & & \uparrow \\ \mathcal{L}_\varepsilon\left(x, \frac{x}{\varepsilon}\right) & \xrightarrow{\text{Two-Scale}} & \mathcal{L}_y(x) & \xrightarrow{\text{Averaging}} & \mathcal{L}(x). \end{array}$$

In later sections, we present explicit expressions for the operators $\mathcal{L}_\varepsilon\left(x, \frac{x}{\varepsilon}\right), \mathcal{L}_y(x)$, and, $\mathcal{L}(x)$ and in the Appendix we derive the equations by two-scale expansion for the steady-state Stokes equations.

First, some mathematical preliminaries. We keep the presentation abstract in the interest of generality because the methods here may be used for a wide class of two-scale linear partial differential operators. Let $\mathcal{V}$ and $\mathcal{W}$ be two Hilbert spaces for functions of y in the cell domain $Y \subset \mathbb{R}^d$ and $\mathcal{V}'$ and $\mathcal{W}'$, their respective dual spaces. Let f be a map in $\mathcal{W}'$. For each x in the macroscopic domain $\Omega \subset \mathbb{R}^d$, we consider the problem of a linear partial differential equation in y: Find $v \in \mathcal{V}$ such that

$$\mathcal{L}_y(x)\, v(x, y) = f(y),$$

and integrating we obtain the corresponding weak variational form

$$\mathcal{A}_y(x)\left(v(x,\cdot),\phi\right) = (f,\phi)\,, \tag{4.10}$$

for $\phi \in \mathcal{W}$. Here, $\mathcal{A}_y(x)(\cdot,\cdot)$ is the bilinear form corresponding to the linear partial differential operator $\mathcal{L}_y(x)$ and $(\cdot,\cdot)$ denotes the duality pairing $(\cdot,\cdot)_{\mathcal{W}',\mathcal{W}}$.

Remark Note here for the Stokes cell equations $v(x,y)$ will have components related to velocity and pressure, more precisely, $v(x,y) = (w(x,y),\pi(x,y))$ given by (4.7) (in the current slowly varying configuration). In addition, the spaces we will need are the same for both the solution and test spaces $\mathcal{V} = \mathcal{W}$, hence $\mathcal{V}' = \mathcal{W}'$. We will be more specific about the spaces in later sections. Finally, the domain Y below plays the role of the cell $Y_{\mathcal{F}}$ in our Stokes problem.

We make a general outline of the algorithm.

Step 1 : Build Nested FE Spaces. Fixing the macro-point $x \in \Omega$ we wish to find an approximation $v(x,\cdot) \in \mathcal{V}$, satisfying (4.10), using Galerkin FEM. To this end, we build a nested collection of FE spaces for the problem. We denote the nested solution spaces as $\mathcal{V}_0 \subset \mathcal{V}_1 \subset \cdots \subset \mathcal{V}_L \subset \mathcal{V}$ and the trial spaces $\mathcal{W}_0 \subset \mathcal{W}_1 \subset \cdots \subset \mathcal{W}_L \subset \mathcal{W}$, for L some fixed positive integer. We construct them so that the error between the correct solution $v(x,\cdot) \in \mathcal{V}$ and Galerkin FE approximation $\bar{v}(x,\cdot)$ decreases in a structured way. More precisely, for $\phi \in \mathcal{W}_{L-i}$, we solve for $\bar{v}(x,\cdot) \in \mathcal{V}_{L-i}$

$$\mathcal{A}_y(x)\left(\bar{v}(x,\cdot),\phi\right) = (f,\phi)\,, \tag{4.11}$$

where $\bar{v}(x,\cdot)$ satisfies the error condition

$$\|v(x,\cdot) - \bar{v}(x,\cdot)\|_{\mathcal{V}} \leq \inf_{\psi\in\mathcal{V}_{L-i}} \|v(x,\cdot) - \psi\|_{\mathcal{V}} \leq C\kappa^i h \,\|v(x,\cdot)\|_{\mathcal{U}}\,. \tag{4.12}$$

Here, h is the error in the finest approximation spaces $(\mathcal{V}_L,\mathcal{W}_L)$ and κ is the FE

coarsening factor. The space $\mathcal{U}$ is the regularity for the solution, standard in FEM error expression cf. [5]. Note that we are clearly limited in the amount of coarsening of our FE approximation spaces. That is, the coarsest error $\kappa^L h$ must still be able to resolve the scales on the cell domain for it to be a meaningful approximation.

Remark This coarsening may be accomplished by coarsening the mesh or conversely refining. In the numerical example in this work, we start with the lowest level space $\mathcal{V}_0$ and refine the mesh to build the collection of FEM spaces. This process can be seen in the figure on page 104.

Step 2 : Build Hierarchy of Macro-Grids. To choose judiciously at which macro-grid points we will solve with high accuracy and which to solve with lower accuracy correction terms, we must build a hierarchy of macro-grid points. First, we must build a nested macro-grid for Ω denoted

$$\mathcal{T}_0 \subset \mathcal{T}_1 \subset \cdots \subset \mathcal{T}_L \subset \Omega.$$

We construct this grid inductively as follows. Suppose we have an initial grid $\mathcal{T}_0$ with grid spacing H. By grid spacing we mean the distance between neighboring nodes is at most H. Proceeding inductively, we construct refinement of $\mathcal{T}_{i-1}$, namely $\mathcal{T}_i$ with grid spacing $H\kappa^{-i}$. Note that the refinement is inversely of the same order as the FE coarsening factor of the error expression (4.12) for the nested FE spaces.

We then define the dense hierarchy of macro-grids $\{S_0, S_1, \cdots, S_L\}$ inductively as $S_0 = \mathcal{T}_0$, $S_1 = \mathcal{T}_1 \backslash S_0$, and in general

$$S_i = \mathcal{T}_i \Big\backslash \left(\bigcup_{k<i} S_k \right).$$

We refer to the coarsest grid S_0 as the anchor points. We require that the hierarchy of macro-grids be dense. That is, we require that for each point $x \in S_i$, there exists

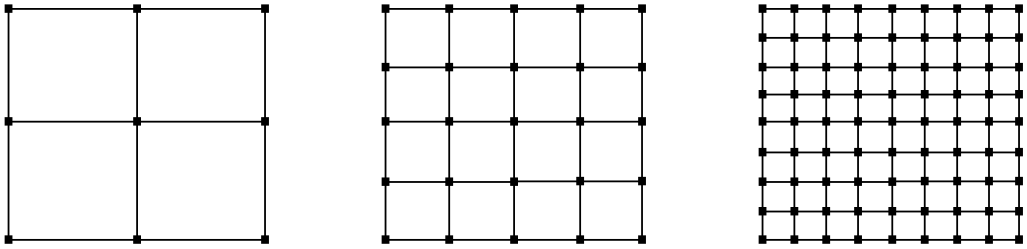

(a) $\mathcal{T}_0$ (b) $\mathcal{T}_1$ (c) $\mathcal{T}_2$

Fig. 11. 3-Level Nested Macro-grids

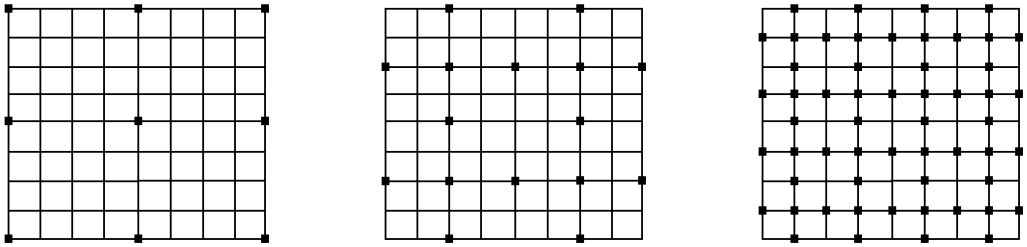

(a) S_0 (b) S_1 (c) S_2

Fig. 12. 3-Level Hierarchy of Macro-grids

at least one point $x' \in \bigcup_{k<i} S_k$ such that the dist $(x, x') < O(H\kappa^{-i})$. An example of a 3-level nested and corresponding hierarchy of macro-grids $\{(\mathcal{T}_i, \mathcal{S}_i)\}_{i=0}^{2}$, contained in $\Omega = [0,1]^2$, can be seen in Figures 11 and 12.

Step 3 : Calculating the Correction Term. We now relate the nested FE spaces and the hierarchy of macro-grids in an efficient computational scheme. We begin by solving at the so-called anchor points. At these points, we solve using the standard Galerkin FEM. Let $x \in S_0$, the most sparse macro-grid, then, we solve the corresponding cell problems in the space of highest accuracy. That is, we find

$\bar{v}(x,\cdot) \in \mathcal{V}_L$ that satisfies

$$\mathcal{A}_y(x)\left(\bar{v}(x,\cdot),\phi\right) = (f,\phi), \text{ for all } \phi \in \mathcal{W}_L. \tag{4.13}$$

We then proceed inductively for, $i = 1, \cdots, L$, let $x \in S_i$ and $\{x_1, x_2, \cdots, x_n\} \in (\bigcup_{k<i} S_k)$ be a collection of points sufficiently close to x. More precisely, the distance between x and $\{x_1, x_2, \cdots, x_n\}$ is less than $O\left(H\kappa^{-i}\right)$ for all points in the collection. There exists at least one such point in $(\bigcup_{k<i} S_k)$ since we constructed the hierarchy of grids in a dense way. We denote the i-th macro-grid interpolation as

$$I_i^x(v) = \sum_{j=1}^{n} c_j v(x_j,\cdot), \tag{4.14}$$

where the coefficients c_j determine the interpolation procedure. We also require $\sum_{j=1}^{n} c_j = 1$. Let $I_i^x(\bar{v}) = \sum_{j=1}^{n} c_j \bar{v}(x_j,\cdot)$ denote the macro-grid interpolation of Galerkin approximations. Recall, we assume that we have already computed $\{\bar{v}(x_j,\cdot)\}_{j=1}^{n}$ inductively. We solve for the correction term $\bar{v}_c(x,\cdot) \in \mathcal{V}_{L-i}$ so that

$$\mathcal{A}_y(x)\left(\bar{v}_c(x,\cdot),\phi\right) = (f,\phi) - \mathcal{A}_y(x)\left(I_i^x(\bar{v}),\phi\right),$$

for all $\phi \in \mathcal{W}_{L-i}$. Note that the right-hand-side term is known data from the previous finer accuracy solves at macro-grid points in $(\bigcup_{k<i} S_k)$. We solve for the correction term in a set of FE spaces $(\mathcal{V}_{L-i}, \mathcal{W}_{L-i})$ with coarser accuracy. Using both the correction term and the macro-grid interpolation term let

$$\bar{v}(x,\cdot) = \bar{v}_c(x,\cdot) + I_i^x(\bar{v}), \tag{4.15}$$

be an approximation for $v(x,\cdot)$. We will show in the abstract formulation that the approximation (4.15) for $v(x,\cdot)$ is of the same order accuracy as if we solved the standard way via (4.13) using the finest FE spaces $(\mathcal{V}_L, \mathcal{W}_L)$, at a reduced computational cost.

The simplest macro-grid interpolation scheme is that of a single point, $I_i^x(v) = v(x_1, \cdot)$ for some $x_1 \in (\bigcup_{k<i} S_k) \bigcap B_{H\kappa^{-i}}(x)$. Here, $B_{H\kappa^{-i}}(x)$ is an open ball in Ω centered at x with radius $H\kappa^{-i}$. Another, being the two point scheme. For some $x_1, x_2 \in (\bigcup_{k<i} S_k) \bigcap B_{H\kappa^{-i}}(x)$ we write $I_i^x(v) = \frac{1}{2}(v(x_1, \cdot) + v(x_2, \cdot))$ and so on.

Remark The relationship between the error coarsening factor κ of the nested FE spaces and the refinement of the hierarchy of macro-grids is critical. The coarser the FE spaces the closer the macro-grid points must be when calculating the correction term. Conversely, for very fine resolution FE solves, we use a sparser macro-grid. With this in mind, we see that Step 1 and Step 2 can be interchanged in order.

C. Abstract Formulation

In this section, we enumerate the assumptions and conditions required to guarantee our efficient multiscale algorithm will yield the same accuracy of the full solve. These assumptions on the variational form (4.10) are physically reasonable and easily verifiable. To illustrate the main of ideas of the proof of the error estimate, we proceed to build a nested collection of FE spaces and a corresponding hierarchy of macro-grids for $\Omega = [0, 1]^2$.

We show in Theorem IV.2 , without loss of generality, we are able to obtain the same order of accuracy as the full solve. For large domains with large variation in microstructure over the domain, we must resolve the local scales at many macroscopic points. We must solve many cell problems, each of which can be computationally expensive. Indeed, if we have $O(M)$ cell problems and in each cell we have $O(N)$ unknowns then, the total number of degrees of freedom for the full solve is $O(MN)$. Comparatively, the hierarchical solve will be that of one single set of cell equations or $O(N)$ degrees of freedom, a significant reduction. The computational complexity

is summarized in Theorem IV.3.

1. Assumptions on Operator

To ensure that our algorithm will give us the proper rate of convergence we must make a few abstract assumptions on the variational form (4.10). The first of which is a standard assumption. These conditions are the boundedness and so-called inf-sup conditions, and non-degeneracy cf. [13]. They guarantee the existence, uniqueness, and *a-priori* bounds for the solution.

Assumption C.1. There are positive constants α and β, independent of the nested FE spaces, so that for all $x \in \Omega$

$$\sup_{v\in\mathcal{V},w\in\mathcal{W}} \frac{|\mathcal{A}_y(x)(v,w)|}{\|v\|_{\mathcal{V}}\|w\|_{\mathcal{W}}} \leq \alpha < \infty, \tag{4.16a}$$

$$\inf_{0\neq v}\sup_{0\neq w} \frac{|\mathcal{A}_y(x)(v,w)|}{\|v\|_{\mathcal{V}}\|w\|_{\mathcal{W}}} \geq \beta > 0, \tag{4.16b}$$

$$\forall\, 0 \neq w \in \mathcal{W}: \ \sup_{v\in\mathcal{V}} |\mathcal{A}_y(x)(v,w)| > 0. \tag{4.16c}$$

With Assumption C.1, problem (4.10) has a unique solution v that satisfies the *a-priori* bounds

$$\|v\|_{\mathcal{V}} \leq \frac{1}{\beta}\|f\|_{\mathcal{W}'}.$$

To utilize information from solutions at other nearby macro-grid points, we must have some measure of how much the variational form may change from macro-point to macro-point in Ω. The following assumption that the variational form must be Lipschitz in x allows us to quantify this idea.

Assumption C.2. There exists a constant γ, independent of the nested FE spaces, so

that for all $x, x' \in \Omega$

$$|(\mathcal{A}_y(x) - \mathcal{A}_y(x'))(v, w)| \leq \gamma |x - x'| \|v\|_{\mathcal{V}} \|w\|_{\mathcal{W}}.$$

To assure accuracy of the finite element approximations we must assume regularity of the true solution and existence of a regularity space $\mathcal{U}$. For the canonical example, the Laplacian operator $-\Delta$ using linear Lagrange FE we have $\mathcal{V} = H^1(Y)$ and $\mathcal{U} = H^2(Y)$ [13]. We also have specific requirements on the FE error. We summarize this in an assumption.

Assumption C.3. There is a regularity space $\mathcal{U}$, containing $\mathcal{V}$, and a nested sequence of finite element spaces $\mathcal{V}_0 \subset \mathcal{V}_1 \subset \ldots \mathcal{V}_L \subset \mathcal{V}$ such that for all v in $\mathcal{U}$

$$\inf_{\psi \in \mathcal{V}_{L-i}} \|v - \psi\|_{\mathcal{V}} \leq \theta(1 + \frac{\alpha}{\beta})\kappa^i h \|v\|_{\mathcal{U}}, \tag{4.17}$$

where the constant θ only depends on the spaces $\mathcal{U}, \mathcal{V}$ and the domain Ω. The constants α and β are as in Assumption C.1. Here, h is the order of accuracy for the finest space $\mathcal{V}_L$ and κ the FE coarsening factor.

For the purpose of formulating the finite element approximations of (4.10), we assume that the boundedness, inf-sup, non-degeneracy conditions hold for the discrete problem, and the constants are independent of the nested FE spaces. This may be guaranteed by choosing proper stable FE spaces. For example, for Stokes equations we can use $\mathbb{P}_k/\mathbb{P}_{k-1}, k \geq 2$, Taylor-Hood elements cf. [13]. In the numerical example section, we use the stable element $\mathbb{P}_2/\mathbb{P}_0$ in the implementation of our algorithm. We summarize this requirement in an assumption.

Assumption C.4. There is a nested sequence of finite element spaces $\mathcal{W}_0 \subset \mathcal{W}_1 \subset$

$\ldots \subset \mathcal{W}_L \subset \mathcal{W}$, such that

$$\sup_{v\in\mathcal{V}_i, w\in\mathcal{W}_i} \frac{|\mathcal{A}_y(x)(v,w)|}{\|v\|_{\mathcal{V}}\|w\|_{\mathcal{W}}} \leq \alpha < \infty, \tag{4.18a}$$

$$\inf_{0\neq\mathcal{V}_i} \sup_{0\neq\mathcal{W}_i} \frac{|\mathcal{A}_y(x)(v,w)|}{\|v\|_{\mathcal{V}}\|w\|_{\mathcal{W}}} \geq \beta > 0, \tag{4.18b}$$

$$\forall\, 0 \neq w \in \mathcal{W}_i : \ \sup_{v\in\mathcal{V}_i} |\mathcal{A}_y(x)(v,w)| > 0, \tag{4.18c}$$

for, $i = 0, 1, \cdots, L$, and the spaces $\mathcal{V}_0 \subset \mathcal{V}_1 \subset \ldots \subset \mathcal{V}_L \subset \mathcal{V}$ are as in Assumption C.3. The constants α and β are the same as in Assumption C.2.

To ensure that our macro-grid interpolation (4.14) is close to the solution of (4.10), we assume the following regularity condition with respect to the macro-variable x. This assumption assumes a slow changing microstructure. With this regularity we can show by a simple Taylor expansion argument the following inequality.

Assumption C.5. The solution v of the problem (4.10) is in $C^1(\bar{\Omega})$ as a map from $v(x,\cdot) : \Omega \to \mathcal{U}$. Let $I_i^x(v)$ be the interpolating operator in (4.14), we then have

$$\|v(x,\cdot) - I_i^x(v)\|_{\mathcal{U}} \leq N \max_{j=1}^{n} \left(d(x, x_j)\right),$$

for some $N > 0$, independent of the nested FE spaces, and d is the standard Euclidean metric.

2. Proof of Main Theorem for Two Dimensional Macro-Grid

In this section we construct a rectangular hierarchy of macro-grids and corresponding nested FE spaces that satisfy the assumptions of the algorithm, where $\Omega = [0,1]^2$ and $Y = [0,1]^2$. We prove that using the assumptions on the variational form (4.10), we obtain the same order of convergence as the full solve. The proof generalized to $\Omega \subset \mathbb{R}^d$ and $Y \subset \mathbb{R}^d$ can be achieved in a similar manner. We proceed in this way with the intent to elucidate elements of the proof without a loss of generality.

We begin by outlining the FE spaces needed in the proof. Here, the explicit representation of the FE spaces are not so important, but the proper error bounds are crucial. Let $(\mathcal{V}_i, \mathcal{W}_i)_{i=1}^{L}$ be FE spaces over Y, satisfying the assumptions.Where $\mathcal{V}_0 = \mathcal{W}_0 = \emptyset$ for simplicity of notation of indices, as it is convenient here to re-index. Furthermore, let $v_i \in \mathcal{V}_i$ be such that

$$\mathcal{A}_y(x)\,(v_i(x,\cdot),\phi) = (f,\phi) \quad \forall \phi \in \mathcal{W}_i. \tag{4.19}$$

From Assumption C.4, this problem has a unique solution $v_i \in \mathcal{V}_i$. In addition, from Assumption C.3 we have the error estimate

$$\|v(x,\cdot) - v_i(x,\cdot)\|_{\mathcal{V}} \leq (1+\frac{\alpha}{\beta}) \inf_{\phi\in\mathcal{V}_i} \|v-\phi\|_{\mathcal{V}} \leq \theta(1+\frac{\alpha}{\beta})2^{-i}\|v\|_{\mathcal{U}}.$$

Here, we have that $h = 2^{-L}$ is the accuracy of the finest space $\mathcal{V}_L$ and $\kappa = 2$ is the FE coarsening factor. As v is a continuous map from Ω to $\mathcal{U}$, $\|v(x,\cdot)\|_{\mathcal{U}}$ is bounded uniformly for all $x \in \Omega$. Therefore, there is a constant M such that

$$\|v(x,\cdot) - v_i(x,\cdot)\|_{\mathcal{V}} \leq M2^{-i}, \tag{4.20}$$

for all $i = 1, \cdots L$, and all $x \in \Omega$.

For simplicity, in the following presentation, we assume that the macroscopic domain Ω is the closed cube $[0,1]^2 \subset \mathbb{R}^2$. In the interval $[0,1]$, let T_0 be the set $\{0, 1/2, 1\}$ and for $k \geq 1$, T_k be the set $\{(2j-1)2^{-(k+1)},\ j = 2^{-1}, 2^0, 2^1, \ldots, 2^k, (2^k + 2^{-1})\}$. We define the set $S_i \subset \Omega$ as

$$S_i = \{x = (x_1, x_2),\ x_k \in T_{i_k} :\ \max\{i_1, i_2\} = i\},$$

and let $S = \cup_{i=0}^{L-1} S_i$, where $S_L = \emptyset$ due to re-indexing. The first few of both nested and hierarchical macro-grids can be seen in Figures 11 and 12. Clearly, this hierarchy of macro-grids satisfies the grid spacing and density requirements. We will show with

the above hierarchy of macro-grids $\{S_i\}_{i=0}^{L-1}$ and nested FE spaces $(\mathcal{V}_i, \mathcal{W}_i)_{i=1}^{L}$ the algorithmyields equivalent accuracy as when using finest FE space $\mathcal{V}_L$ for all points S.

We begin by establishing standard Galerkin approximation at the anchor points as a base step to our induction. For each point $x \in S_0$, consider the Galerkin approximation (4.19) using the finest FE spaces $(\mathcal{V}_L, \mathcal{W}_L)$ we find the solution $\bar{v}(x,\cdot) \in \mathcal{V}_L$ such that

$$\|v(x,\cdot) - \bar{v}(x,\cdot)\|_{\mathcal{V}} \leq M 2^{-L}.$$

We then find the Galerkin approximations for (4.10) at other points $x \in S$ inductively as follows. Consider a point $x = (x_1, x_2)$ in S_i i.e. $x_1 \in T_{i_1}$ and $x_2 \in T_{i_2}$, $\max\{i_1, i_2\} = i$. Let $x_1 = (2j_1 - 1)2^{-i_1}$ and $x_2 = (2j_2 - 1)2^{-i_2}$. Let

$$\begin{aligned} x' &= (2(j_1-1)2^{-i_1}, (2j_2-1)2^{-i_2}) \quad \text{if } \ i_1 > i_2, \\ x' &= ((2j_1-1)2^{-i_1}, 2(j_2-1)2^{-i_2}) \quad \text{if } \ i_1 < i_2, \\ x' &= (2(j_1-1)2^{-i_1}, 2(j_2-1)2^{-i_2}) \quad \text{if } \ i_1 = i_2. \end{aligned}$$

It is clear that $x' \in S_{i'}$ where $i' < i$ and in any case $d(x, x') < \sqrt{2} \cdot 2^{-i}$. Assume that a Galerkin approximation $\bar{v}(x',\cdot) \in \mathcal{V}_{L-i'}$ has been computed for $v(x',\cdot)$. We consider the following problem: Find the correction term, $\bar{v}_c(x,\cdot) \in \mathcal{V}_{L-i}$ so that

$$\mathcal{A}_y(x)\left(\bar{v}_c(x,\cdot), \phi\right) = (f, \phi) - \mathcal{A}_y(x)\left(\bar{v}(x',\cdot), \phi\right), \tag{4.21}$$

for all $\phi \in \mathcal{W}_{L-i}$. Let the approximation for $v(x,\cdot)$ be given by

$$\bar{v}(x,\cdot) = \bar{v}_c(x,\cdot) + \bar{v}(x',\cdot).$$

Note here that we use the single point interpolation $I_i^x(v) = v(x',\cdot)$ as in (4.14). We

have the following proposition for $\bar{v}(x,\cdot)$ constructed in such a way.

Proposition IV.1. There is a positive constant c_i which only depends on the operator $\mathcal{L}_y$ and i so that

$$\|v(x,\cdot)-\bar{v}(x,\cdot)\|_{\mathcal{V}} \leq c_i 2^{-L}. \tag{4.22}$$

Proof We prove (4.22) by induction. The conclusion obviously holds for $i=0$. We assume that the conclusions hold for all $l<i$. Let $x\in S_i$ and $x'\in S_{i'}$, for $i'<i$, be as above and define the continuous correction term be given by

$$v_c(x,y)=v(x,y)-v(x',y).$$

Sufficient smoothness for $v(x,\cdot):\Omega\to\mathcal{U}$, is guaranteed from Assumption C.5 and, using $d(x,x')\leq\sqrt{2}\cdot 2^{-i}$, we have the estimate

$$\|v_c(x,\cdot)\|_{\mathcal{U}} \leq N d(x,x') \leq N 2^{-i}, \tag{4.23}$$

where we absorb the factor $\sqrt{2}$ into N. From the variational formulation on the continuous level we have

$$\mathcal{A}_y(x)\left(v_c(x,\cdot),\phi\right)=(f,\phi)-\mathcal{A}_y(x)\left(v(x',\cdot),\phi\right),$$

for all $\phi\in\mathcal{W}$. Recall that we have solved

$$\mathcal{A}_y(x')\left(v(x',\cdot),\phi\right)=(f,\phi),$$

from here we deduce that

$$\mathcal{A}_y(x)\left(v_c(x,\cdot),\phi\right)=-\left(\mathcal{A}_y(x)-\mathcal{A}_y(x')\right)\left(v(x',\cdot),\phi\right).$$

Let $\bar{\bar{v}}_c(x,\cdot)\in\mathcal{V}_{L-i}$ be such that

$$\mathcal{A}_y(x)\left(\bar{\bar{v}}_c(x,\cdot),\phi\right)=-\left(\mathcal{A}_y(x)-\mathcal{A}_y(x')\right)\left(v(x',\cdot),\phi\right), \text{for all } \phi\in\mathcal{W}_{L-i}. \tag{4.24}$$

From the Assumption C.4 and Cea's lemma [5], we obtain

$$\|v_c(x,\cdot) - \bar{\bar{v}}_c(x,\cdot)\|_{\mathcal{V}} \leq (1+\frac{\alpha}{\beta}) \inf_{\phi \in \mathcal{V}_{L-i}} \|v_c - \phi\|_{\mathcal{V}}.$$

From (4.17) and (4.23) we deduce that

$$\|v_c(x,\cdot) - \bar{\bar{v}}_c(x,\cdot)\|_{\mathcal{V}} \leq \theta(1+\frac{\alpha}{\beta})2^{i-L}(N2^{-i}) \leq \theta(1+\frac{\alpha}{\beta})N2^{-L}.$$

As $x' \in S_{i'}$, where $i' < i$, and so $\mathcal{V}_{L-i} \subset \mathcal{V}_{L-i'}$. Recall that we have previously computed $\bar{v}(x',\cdot) \in \mathcal{V}_{L-i'}$, a FE space with higher accuracy. Therefore, $\bar{v}(x',\cdot)$ will satisfy the variational form (4.19) over nested spaces with lower accuracy. More precisely, we will have

$$\mathcal{A}_y(x')\left(\bar{v}(x',\cdot),\phi\right) = (f,\phi), \text{ for all } \phi \in \mathcal{W}_{L-i}. \tag{4.25}$$

From (4.21) and (4.25) we deduce

$$\mathcal{A}_y(x)\left(\bar{v}_c(x,\cdot),\phi\right) = -\left(\mathcal{A}_y(x) - \mathcal{A}_y(x')\right)\left(\bar{v}(x',\cdot),\phi\right), \text{ for all } \phi \in \mathcal{W}_{L-i}. \tag{4.26}$$

Therefore, from Assumption C.4 and using (4.24) and (4.26)

$$\|\bar{\bar{v}}_c(x,\cdot) - \bar{v}_c(x,\cdot)\|_{\mathcal{V}} \leq \frac{1}{\beta}\| \left(\mathcal{A}_y(x) - \mathcal{A}_y(x')\right)\left(v(x',\cdot) - \bar{v}(x',\cdot)\right) \|_{\mathcal{W}'}.$$

Finally, using the Lipschitz Assumption C.2 we obtain

$$\begin{aligned}\| \left(\mathcal{A}_y(x) - \mathcal{A}_y(x')\right)\left(v(x',\cdot) - \bar{v}(x',\cdot)\right) \|_{\mathcal{W}'} &\leq \gamma|x-x'|\|v(x',\cdot) - \bar{v}(x',\cdot)\|_{\mathcal{V}} \\ &\leq \gamma(\sqrt{2}\cdot 2^{-i})(c_i 2^{-L}) \leq \sqrt{2}c_i\gamma 2^{-L-i}.\end{aligned}$$

Therefore

$$\|\bar{\bar{v}}_c(x,\cdot) - \bar{v}_c(x,\cdot)\|_{\mathcal{V}} \leq \frac{\sqrt{2}}{\beta}c_i\gamma 2^{-L-i}.$$

Thus, putting all the estimates together we obtain

$$\|v(x,\cdot)-\bar{v}(x,\cdot)\|_{\mathcal{V}} \le \|v_c(x,\cdot)-\bar{v}_c(x,\cdot)\|_{\mathcal{V}} + \|v(x',\cdot)-\bar{v}(x',\cdot)\|_{\mathcal{V}} \le c_{i+1}2^{-L},$$

where

$$c_{i+1} = c_i + \frac{\sqrt{2}}{\beta}c_i\gamma 2^{-i} + (1+\frac{\alpha}{\beta})\theta N. \tag{4.27}$$

□

We are now in the position to prove our main result.

Theorem IV.2. Let the assumptions of Proposition IV.1 hold. Furthermore, assume we have constructed $\bar{v}(x,\cdot)$ as above for $x \in S_i$. Then, for a sufficiently large constant c_* which only depends on the operator $\mathcal{L}_y$, we have the estimate

$$\|v(x,\cdot)-\bar{v}(x,\cdot)\|_{\mathcal{V}} \le c_*(i+1)2^{-L}.$$

Proof We choose a constant $\bar{i}$ independent of L such that $i2^{-i} < \beta/(2\sqrt{2}\gamma)$ for $i > \bar{i}$. Let

$$c_* = \max\{\max_{0\le i\le \bar{i}}\{c_i/i\}, 2(1+\frac{\alpha}{\beta})\theta N\},$$

where c_i is given by (4.27). We prove that

$$\|v(x,\cdot)-\bar{v}(x,\cdot)\|_{\mathcal{V}} \le c_*(i+1)2^{-L}, \tag{4.28}$$

by induction. This obviously holds for all $i \le \bar{i}$. We assume that the conclusions hold for all i. From (4.27), we deduce

$$c_{i+1} \le ic_* + \frac{\sqrt{2}\gamma}{\beta}\frac{\beta}{2\sqrt{2}\gamma}c_* + \frac{c_*}{2} \le (i+1)c_*.$$

The theorem is proved.

□

We also state a theorem on the computational complexity of our algorithm for

such a hierarchy of macro-grids and FE spaces given in this section.

Theorem IV.3. Suppose that we solve (4.10) for x in $S_0, S_1, \ldots, S_L$, the total number of degrees of freedom is $\mathcal{O}(L2^{2L})$ for the hierarchical solve. Comparatively, the number of degrees of freedom in the full solve is $\mathcal{O}((2^{2L})^2)$.

Proof First note that the dimension of $\mathcal{V}_{L-i}$ is $\mathcal{O}(2^{2(L-i)})$ and that the number of points in S_i is $\mathcal{O}(2^{2i})$. Therefore, the total number of degrees of freedom when solving (4.10) for all points in S_i is $\mathcal{O}(2^{2i})\mathcal{O}(2^{2L-2i}) = \mathcal{O}(2^{2L})$. Thus, the total number of degrees of freedom used when solving (4.10) for all points in $S_0, S_1, \ldots, S_L$ is $\mathcal{O}(L2^{2L})$. □

D. Application to the Stokes Equations

In this section, we apply the algorithm and methodology outlined in prior sections to the modified Stokes equations in the periodic domain. Here, we use the ALE formulation of the Stokes equations cf. [14, 15]. We will briefly present this reformulation in the periodic domain and will then apply the two-scale asymptotic expansion ([33]) to the steady-state modified equations as in Chapter III. This will allow for an easy application of our efficient algorithm. The details for the derivation of the steady-state ALE formulation and application of two-scale expansion can be found in the Appendix. We obtain auxiliary cell equations hence, the homogenized equations in the periodic ALE.

With the intention of developing a proper nested collection of FE spaces, we then introduce appropriate Sobolev spaces for the solutions. Then, the variational formulation of the cell equations is presented. We make basic assumptions on the smoothness properties of the mapping $\widetilde{X}_\varepsilon$ and the geometry of the cell equations. With these assumptions we verify that the conditions on the operator outlined in

prior sections are satisfied. Hence, given a hierarchy of macro-grids and corresponding nested collection of FE spaces, satisfying the abstract assumptions, we are able to obtain the error estimate given by Theorem IV.2.

1. Homogenization of Stokes Equations in the ALE formulation

In the slowly varying domains, there is variation of the cell geometry from RVE to RVE. When we reformulate the Stokes equations to the periodic domain, we encode this information into the tensor coefficients of the modified equations. We begin by reformulating the Stokes equations.

Recall, that the fine-scale Stokes equations (4.2) are represented in the slowly varying fluid domain $\widetilde{\mathcal{F}_\varepsilon} = \widetilde{X}_\varepsilon(\mathcal{F}_\varepsilon)$. Let $\mathcal{P}_\varepsilon \subset \mathcal{F}_\varepsilon$ be some open subset of the periodic fluid domain, and thus $\widetilde{X}_\varepsilon(\mathcal{P}_\varepsilon) = \widetilde{\mathcal{P}}_\varepsilon$. We rewrite the Stokes equations in integral form after the application of the divergence theorem as

$$\int_{\partial\widetilde{\mathcal{P}}_\varepsilon} (-\widetilde{p}_\varepsilon(\tilde{x})I + \mu\nabla_{\tilde{x}}\widetilde{v}_\varepsilon(\tilde{x})) \cdot \widetilde{n}(\tilde{x})d\tilde{x} = \int_{\widetilde{\mathcal{P}}_\varepsilon} \widetilde{f}(\tilde{x})d\tilde{x}, \tag{4.29a}$$

$$\int_{\partial\widetilde{\mathcal{P}}_\varepsilon} \widetilde{v}_\varepsilon(\tilde{x}) \cdot \widetilde{n}(\tilde{x})d\tilde{x} = 0. \tag{4.29b}$$

We make the change of variables $\tilde{x} \to \tilde{x}(x)$ and map back to the initial periodic fluid domain. If $\widetilde{\phi}(\tilde{x})$ is a physical quantity in the deformed (slowly varying) domain, then denote the pullback to the periodic domain $\phi(x) := \widetilde{\phi}(\tilde{x}(x))$. We need to define a few tensors. Let the mapping gradient and Jacobian be defined as

$$F_\varepsilon(x) = \nabla_x \widetilde{X}_\varepsilon(x) \ , \ J_\varepsilon(x) = \det(\nabla_x \widetilde{X}_\varepsilon(x)),$$

and related tensors

$$G_\varepsilon(x) = \det(F_\varepsilon(x))F_\varepsilon(x)^{-T} \ , \ H_\varepsilon(x) = F_\varepsilon^{-1}(x)G_\varepsilon(x).$$

We assume that the mapping is non degenerate, that is there exists a $c > 0$ such that $J_\varepsilon(x) > c > 0$ for all $x \in \Omega$. Hence, $F_\varepsilon(x)$ and related tensors will be invertible for all points in the domain. Noting that in this coordinate transformation, gradients are transformed as

$$\nabla_{\tilde{x}} \widetilde{v}_\varepsilon(\tilde{x}) = \nabla_x v_\varepsilon(x) F_\varepsilon^{-1}(x).$$

Let the surface normal on $\partial\widetilde{\mathcal{P}}_\varepsilon$ be $\widetilde{n}$ and the surface normal on $\partial\mathcal{P}_\varepsilon$ be n. The surface normals and volume elements transform as

$$\widetilde{n}(\tilde{x}) = F_\varepsilon^{-T}(x) n(x) \ , \ d\tilde{x} = J_\varepsilon(x) dx.$$

Using these transformations, we represent (4.29) in the periodic domain as

$$\int_{\partial\mathcal{P}_\varepsilon} (-p_\epsilon(x) G_\varepsilon(x) + \mu \nabla_x v_\varepsilon(x) H_\varepsilon(x)) \cdot n(x) dx = \int_{\mathcal{P}_\varepsilon} f(x) J_\varepsilon(x) dx,$$
$$\int_{\partial\mathcal{P}_\varepsilon} v_\varepsilon(x) \cdot G_\varepsilon(x) \cdot n dx = 0.$$

This is true for any $\mathcal{P}_\varepsilon \subset \mathcal{F}_\varepsilon$. We move to the divergence form of these equations, we obtain the modified Stokes equations in the periodic domain $\mathcal{F}_\varepsilon$

$$-\mathrm{div}_x \left(p_\varepsilon(x) G_\varepsilon(x)\right) + \mu \mathrm{div}_x (\nabla_x v_\varepsilon(x) H_\varepsilon(x)) = f(x) J_\varepsilon(x) \text{ in } \mathcal{F}_\varepsilon, \tag{4.30a}$$

$$\mathrm{div}_x (G_\varepsilon^T(x) v_\varepsilon) = 0 \text{ in } \mathcal{F}_\varepsilon, \tag{4.30b}$$

and we assume the boundary condition that $v_\varepsilon = 0$ on Γ_ε. This is a representation of the fine-scale Stokes operator we denoted earlier $\mathcal{L}_\varepsilon\left(x, \frac{x}{\varepsilon}\right)$. We apply the two-scale asymptotic expansions (4.42-4.46), given in the Appendix, and apply them to (4.30).

Gathering terms in ε we obtain the two auxiliary cell equations for $i = 1, \cdots, d$,

$$-G_0 \nabla_y \pi_1^i + \mu \mathrm{div}_y \left(\nabla_y w_1^i H_0 \right) = G_0 e_i \text{ in } Y_{\mathcal{F}}, \tag{4.31a}$$

$$\mathrm{div}_y (G_0^T w_1^i) = 0 \text{ in } Y_{\mathcal{F}}, \tag{4.31b}$$

and for the second cell equation

$$-G_0 \nabla_y \pi_2^i + \mu \mathrm{div}_y \left(\nabla_y w_2^i H_0 \right) = J_0 e_i \text{ in } Y_{\mathcal{F}}, \tag{4.32a}$$

$$\mathrm{div}_y (G_0^T w_2^i) = 0 \text{ in } Y_{\mathcal{F}}, \tag{4.32b}$$

with w_j^i and π_j^i being $y-$periodic, $w_j^i = 0$ on Y_Γ and $\left\langle \pi_j^i \right\rangle_Y = 0$. The two cell equations are a result of the representation (4.49) for p_1 and v_0. The above partial differential operator is the cell operator denoted $\mathcal{L}_y(x)$.

From the ε^0 order of the expansion of (4.30b) and averaging over $Y_{\mathcal{F}}$ we obtain a representation for the homogenized operator in the periodic domain $\mathcal{L}(x)$. The modified Darcy equation is given by

$$\nabla_x \cdot \left(K(x) \nabla_x p_0(x) + \bar{f}(x) \right) = 0 \text{ in } \Omega, \tag{4.33}$$

where

$$K(x) = \left\langle G_0^T(x,y) w_1(x,y) \right\rangle_Y \text{ and } \bar{f}(x) = \left\langle G_0^T(x,y) w_2(x,y) \right\rangle_Y f(x).$$

The modified Darcy velocity is given by $\xi = K(x) \nabla_x p_0(x) + \bar{f}(x)$. We also require the boundary conditions $\xi \cdot \nu = 0$ on $\partial\Omega$, where ν is the unit normal.

2. Variational Form and Verification of Algorithm Assumptions

In this section, we present definitions of appropriate Sobolev solution spaces. Then, we derive the corresponding variational form for the cell operator in the periodic

setting $\mathcal{L}_y(x)$ given by (4.31) and (4.32). We show that this variational form will satisfy the abstract assumptions.

We define the following Sobolev spaces. For the pressure related quantities let

$$(L^2_{\int=0}(Y_{\mathcal{F}}))^d = \{\zeta \in (L^2(Y_{\mathcal{F}}))^d : \frac{1}{|Y_{\mathcal{F}}|}\int_{Y_{\mathcal{F}}} \zeta dy = 0\},$$

and for the velocity related quantities

$$(H^1_{\#,0}(Y_{\mathcal{F}}))^{d\times d} = \{q \in (H^1(Y_{\mathcal{F}}))^{d\times d} : q = 0 \text{ on } Y_\Gamma \text{ and } q \text{ is } y-\text{periodic}\}.$$

Recall, we have the same solution and test space for our Stokes equations. Indeed, we let

$$\mathcal{V} = \mathcal{W} = (H^1_{\#,0}(Y_{\mathcal{F}}))^{d\times d} \times (L^2_{\int=0}(Y_{\mathcal{F}}))^d. \tag{4.34}$$

Remark For the rest of the chapter, when we state the spaces $\mathcal{V}, \mathcal{W}$, we will mean the above cross product of Sobolev spaces with $\mathcal{V} = \mathcal{W}$. Moreover, the spaces $\{\mathcal{V}_l = \mathcal{W}_l\}_{l=0}^L$ will be finite dimensional FE subspaces of $\mathcal{V}$ given by (4.34).

Multiplying both sides of equations (4.31) and (4.32), by test functions $(q(y), \zeta(y)) \in \mathcal{V}$ and integrating by parts we obtain a corresponding variational form for each $x \in \Omega$,

$$\begin{aligned}\mathcal{A}_y(x)\Big((w(x,y),\pi(x,y)),(q(y),\zeta(y))\Big) = \\ \int_{Y_{\mathcal{F}}} \big(\pi(x,y)\cdot \mathrm{div}_y(G_0^T(x,y)q(y)) - \mu(\nabla_y w(x,y)H_0(x,y)) : \nabla_y q(y)\big)\, dy \\ + \int_{Y_{\mathcal{F}}} \big(\zeta(y)\cdot \mathrm{div}_y(G_0^T(x,y)w(x,y))\big)\, dy.\end{aligned} \tag{4.35}$$

The cell problems (4.31) and (4.32) can then be written as the following two varia-

tional problems: Find $(w_j(x,y), \pi_j(x,y)) \in \mathcal{V}$, for $j = 1, 2$, such that

$$\mathcal{A}_y(x)\Big((w_1(x,y), \pi_1(x,y)), (q(y), \zeta(y))\Big) = \int_{Y_{\mathcal{F}}} G_0(x,y) : q(y)dy$$
$$\mathcal{A}_y(x)\Big((w_2(x,y), \pi_2(x,y)), (q(y), \zeta(y))\Big) = \int_{Y_{\mathcal{F}}} J_0(x,y)I : q(y)dy$$

for all $(q(y), \zeta(y)) \in \mathcal{V}$.

We will now state and prove a lemma that will allow us to use our efficient multiscale finite element algorithm. We verify the necessary abstract assumptions.

Lemma IV.4. Assume that Ω and $Y_{\mathcal{F}}$ are sufficiently smooth. Let the mapping be of the form $\widetilde{X}_\varepsilon(x) = \widetilde{X}_0(x) + \varepsilon\widetilde{X}_1(x,y)$ as in (4.41). Suppose the regularity $\widetilde{X}_0 \in C^2(\bar{\Omega})$ and $\widetilde{X}_1(x,y) \in C^2(\bar{\Omega} \times Y)$. Assume the mapping is non degenerate. There exists a $c > 0$, such that for all $x \in \Omega$, $J_\varepsilon(x) = \det(\nabla\widetilde{X}_\varepsilon(x)) > c > 0$ and $J_0(x,y) = \det(\nabla_x\widetilde{X}_0(x) + \nabla_y\widetilde{X}_1(x,y)) > c > 0$. Then, the variational form (4.35) satisfies the abstract assumptions, namely Assumption C.1 and Assumption C.2, required of $\mathcal{A}_y(x)$.

Proof First, we verify Assumption C.1. The boundedness condition (4.16a) is a simple consequence of the boundedness that the smooth matrix functions J_0, F_0, G_0, and H_0 are of class $C^1(\bar{\Omega}\times Y)$. The non degeneracy condition (4.16c) is easily satisfied as in the standard Stokes variational form cf. [13].

We verify the variational form satisfies the inf-sup condition (4.16c). The velocity term is coercive since the tensor $H_0 = J_0F_0^{-1}F_0^{-T}$ is positive definite. Indeed, F_0^{-T} and J_0 satisfy the lower bound conditions (4.44) and (4.45). Furthermore, the Poincar inequality is satisfied since $w = 0$ on Y_Γ. Hence, for a positive constant $C > 0$, the

following estimate holds

$$\int_{Y_{\mathcal{F}}} \nabla_y w H_0 \nabla_y w dy = \int_{Y_{\mathcal{F}}} \nabla_y w J_0 F_0^{-1} F_0^{-T} \nabla_y w dy,$$
$$= \int_{Y_{\mathcal{F}}} |F_0^{-T} \nabla_y w|^2 J_0 dy > C||w||^2_{(H^1(Y_{\mathcal{F}}))^{d\times d}}.$$

The pressure term satisfies the so-called Babuška-Brezzi condition [6]. Indeed, we must show that for all $\pi \in (L^2_{\int=0}(Y_{\mathcal{F}}))^d$

$$\sup_{w\in(H^1_{\#,0}(Y_{\mathcal{F}}))^{d\times d}} \frac{\int_{Y_{\mathcal{F}}} \pi \mathrm{div}_y(G_0^T w) dy}{||w||_{(H^1(Y_{\mathcal{F}}))^{d\times d}}} \geq C||\pi||_{(L^2_{\int=0}(Y_{\mathcal{F}}))^d}.$$

Let $v = G_0^T w$, then, $||G_0^{-T} v||_{(H^1_{\#,0}(Y_{\mathcal{F}}))^{d\times d}} \leq ||G_0^{-T}||_\infty ||v||_{(H^1_{\#,0}(Y_{\mathcal{F}}))^{d\times d}}$. Note that the tensor

$$G_0^{-T}(x,y) = \frac{\nabla_x \widetilde{X}_0(x) + \nabla_y \widetilde{X}_1(x,y)}{J_0(x,y)},$$

is bounded, since $\widetilde{X}_0(x) \in C^2(\bar{\Omega})$, $\widetilde{X}_1(x,y) \in C^2(\bar{\Omega}\times Y)$ and the non degeneracy of $J_0(x,y)$. The standard Stokes operator satisfies the Babuška-Brezzi condition [13]. Indeed, we have

$$\sup_{v\in(H^1_{\#,0}(Y_{\mathcal{F}}))} \frac{\int_{Y_{\mathcal{F}}} \pi \mathrm{div}_y(v) dy}{||G_0^{-T} v||_{(H^1_{\#,0}(Y_{\mathcal{F}}))^{d\times d}}} \geq \sup_{v\in(H^1_{\#,0}(Y_{\mathcal{F}}))} C \frac{\int_{Y_{\mathcal{F}}} \pi \mathrm{div}_y(v) dy}{||v||_{(H^1_{\#,0}(Y_{\mathcal{F}}))^{d\times d}}} \geq C||\pi||_{(L^2_{\int=0}(Y_{\mathcal{F}}))^d}.$$

Therefore, the variational form $\mathcal{A}_y(x)$ satisfies the inf-sup conditions (4.16b) and we obtain the desired *a-priori* bound on the initial data.

The variational form $\mathcal{A}_y(x)$ is Lipschitz, in the sense outlined in Assumption C.2. Note that G_0 and H_0 are of class $C^1(\bar{\Omega}\times Y)$ and hence, are Lipschitz in x. Indeed, we have for $x, x' \in \Omega$

$$|\mathcal{A}_y(x)(w,\pi),(q,\zeta) - \mathcal{A}_y(x')(w,\pi),(q,\zeta)| \leq$$
$$C(||G_0^T(x,\cdot) - G_0^T(x',\cdot)|| + ||H_0(x,\cdot) - H_0(x',\cdot)||) \leq C|x-x'|,$$

where C depends on the norms of (w, π) and (q, ζ) and the Lipschitz constants of G_0^T and H_0.

□

Remark Concerning the regularity space $\mathcal{U}$ of Assumption C.3. We may obtain the desired regularity of the cell problem by assuming appropriate smoothness on the cell geometry, the mapping, and related tensors. We suppose the regularity space $\mathcal{U} = (H^2(Y_\mathcal{F}))^{d\times d} \times (H^1(Y_\mathcal{F}))^d$. For more on regularity issues of Stokes equations we refer the reader to [2, 36].

With Lemma IV.4, and utilizing the proof of Theorem IV.2, we are now in a position to summarize our results in a theorem. We have the following error estimate for our efficient multiscale FEM applied to the modified cell equations (4.31) and (4.32).

Theorem IV.5. Suppose the assumptions in Lemma IV.4 hold.

Suppose that (w, π) as a map from Ω to $\mathcal{U} = (H^2(Y_\mathcal{F}))^{d\times d} \times (H^1(Y_\mathcal{F}))^d$ is $C^1(\Omega)$ to satisfy Assumption C.5. Suppose further that the nested sequence of FE spaces $\{\mathcal{V}_l\}_{l=0}^L$ satisfies the error bounds of Assumption C.4, and inf-sup conditions of Assumption C.4. Let $\{S_l\}_{l=0}^L$ be a dense hierarchy of macro-grids having the properties outlined in the algorithm. Then, the FE approximate solutions $(\bar{w}_j(x,\cdot), \bar{\pi}_j(x,\cdot))$ to (4.31) and (4.32) satisfy the error estimate

$$\|\pi_j(x,\cdot) - \bar{\pi}_j(x,\cdot)\|_{L^2(Y_\mathcal{F})} + \|w_j(x,\cdot) - \bar{w}_j(x,\cdot)\|_{H^1(Y_\mathcal{F})} \le c_*(l+1)h. \tag{4.36}$$

Remark Any pairs of finite element approximating spaces in $\mathcal{V}$, given by (4.34), that satisfy the inf-sup condition for the Stokes equations will satisfy the inf-sup condition for the operator $\mathcal{A}_y(x)$ in (4.35). The proof is identical to that as presented above in

Lemma IV.4. More precisely, elements stable for the standard Stokes equations will be stable for our modified equations. In the numerical examples below, we choose the well known Taylor-Hood type $\mathbb{P}_2/\mathbb{P}_0$ elements.

E. Numerical Example

In this section, we propose an example for the implementation of the efficient multi-scale FEM method. We apply the computational methodology outlined in previous sections to the Stokes cell equations $\mathcal{L}_y(x)$ in the ALE formulation. We begin by constructing an initial periodic reference domain Ω. Then, we propose a mapping $\widetilde{X}_\varepsilon$ that is smooth and depends only on the macroscopic slow variable in one direction. This symmetry makes the macro-grid essentially one-dimensional. We build a nested sequence of four FE spaces by decreasing mesh size and construct a hierarchy of macro-grids. After averaging, we compute a component of the modified permeability. We do this for a small stretch and large stretch mapping. Finally, we compare our fine mesh standard solve to our efficient hierarchical solve for both mappings.

1. Example Problem Formulation

Here, we formulate our example domain, mapping, corresponding equations, and variational form. We begin with the description of the periodic domain. Let $\Omega = [0,1]^2$ be the macroscopic domain and define the unit cell to be $Y = [0,1]^2$. The solid part of the cell is given by the square inclusion $Y_{\mathcal{S}} = [1/4, 3/4]^2$ and hence, the fluid domain is given by $Y_{\mathcal{F}} = Y \backslash Y_{\mathcal{S}}$. The interface of the cell Y_Γ is $\partial Y_{\mathcal{S}}$. Thus, $\mathcal{F}_\varepsilon$ and $\mathcal{S}_\varepsilon$, periodic fluid and solid domains, are given by (4.1). Since the domain is periodic, we will have a single unit cell $Y = Y_{\mathcal{F}} \cup Y_{\mathcal{S}}$.

We suppose the mapping $\widetilde{X}_\varepsilon : \Omega \to \widetilde{\Omega}_\varepsilon$ to be a stretch in the x_1 direction given

by

$$\widetilde{X}_\varepsilon(x) = (x_1, x_2) + \alpha(x_1^2, 0), \tag{4.37}$$

where $x = (x_1, x_2)$ are coordinates in Ω. This map preserves the periodicity in the x_2 direction, but periodicity in the x_1 direction is broken. Fixing x_1 but varying x_2 will yield the same cell solution, making the macro-griding essentially one dimensional. It is important to note that the local cell problems in $y = (y_1, y_2)$ are still two dimensional in Y.

Recall the two-scale representation for $\widetilde{X}_\varepsilon(x) = \widetilde{X}_0(x) + \varepsilon\widetilde{X}_1(x)$ as in (4.41). We see that $\widetilde{X}_1 = 0$, as there is no dependence on ε or the fast variable $y = (y_1, y_2)$. Thus, $\widetilde{X}_\varepsilon(x) = \widetilde{X}_0(x)$. Calculating the gradient of this mapping we see that

$$F_0(x_1) = \begin{pmatrix} 1 + \alpha x_1 & 0 \\ 0 & 1 \end{pmatrix},$$

and from here we may build the Jacobian and related tensors $J_0(x_1) = \det(F_0(x_1))$, $G_0(x_1) = J_0(x_1)F_0^{-T}(x_1)$, and $H_0(x_1) = F_0^{-1}(x_1)G_0(x_1)$.

To simplify the implementation, we assume that we have no external body force, that is, $f = 0$. If the body force in present, we must solve two cell problems (4.31) and (4.32). We wish to find $(w^i, \pi^i) \in \mathcal{V}$, for $i = 1, 2$, such that

$$-G_0(x_1)\nabla_y\pi^i + \mu\mathrm{div}_y\left(\nabla_y w^i H_0(x_1)\right) = G_0(x_1)e_i \text{ in } Y_\mathcal{F}, \tag{4.38a}$$

$$\mathrm{div}_y(G_0^T(x_1)w^i) = 0 \text{ in } Y_\mathcal{F}, \tag{4.38b}$$

with w^i and π^i being y-periodic, $w^i = 0$ on Y_Γ and $\langle\pi^i\rangle_Y = 0$. For simplicity of notation, in the following we adopt a notation similar to that used in the section on abstract formulation. We let $v = (w, \pi)$ be the solution and $\phi = (q, \zeta)$ the test function. Then, (4.38) has the corresponding variational formulation. We wish to

(a) $x_1 = 0$ (b) $x_1 = 1$

Fig. 13. Pressure π^1 (triangle shading) and velocity w^1 (vectors) plots for $\alpha = 1/2$, $h = 1/12$ for (a) $x_1 = 0$, (b) $x_1 = 1$, in the periodic reference configuration.

find $v \in \mathcal{V}$ such that

$$\mathcal{A}_y(x_1)(v, \phi) = \int_{Y_\mathcal{F}} G_0(x_1) : q dy \text{ for all } \phi \in \mathcal{V}, \tag{4.39}$$

where $\mathcal{A}_y(x_1)$ has the same form as (4.35).

It is useful to visualize the solutions. Fixing x_1, we solve the above variational form using $\mathbb{P}_2/\mathbb{P}_0$ Taylor-Hood finite elements over $Y_\mathcal{F}$. These elements satisfy the inf-sup stability conditions in Assumption C.4 cf. [16]. We use quadratic elements for velocity and piecewise constants for pressure. In Figure 13, we plot the pressure π^1 and velocity w^1 cell solutions to (4.38) with, right-hand-side $G_0(x_1)e_1 = (1, 0)$ for $x_1 = 0, 1$, and $\alpha = 1/2$. We see that, as we move from $x_1 = 0$ to $x_1 = 1$, the tensor coefficients change. This, in turn, changes the pressure and velocity fields. As we stretch, the solid inclusion is thinner and has less effect on the flow in the horizontal direction. In the next section, we will compare the standard full solves ($h = 1/24$) to the hierarchical solve using our efficient algorithm.

Remark It is important to note here that our inclusion has sharp corners. Near those regions, we will not be able to guarantee the solutions will be in our regularity

space $\mathcal{U}$. However, since the data and other regions of the domain are smooth enough, this will not affect our results in a significant way.

2. Implementation of the Algorithm

In this section, we implement the efficient hierarchical multiscale algorithm. We apply these methods to equations (4.38). First, we build the nested sequence of FE spaces by coarsening the initial fine mesh in a structured way. From this sequence of meshes, we use, $\mathbb{P}_2/\mathbb{P}_0$ Taylor-Hood elements to build the FE approximation spaces. Recall that the mapping (4.37) depends only on x_1, implying that the macro-grid need only vary in one direction. Hence, we construct a corresponding one dimensional hierarchy of grids. Then, we implement the algorithm by computing the velocity. After averaging, we compute the modified permeability and compare our algorithm to the standard full solve at each point in our hierarchical grid.

With the intent of building our nested FE spaces, we begin with our meshes. We use the four meshes in Figure 14. We can view the generation of these meshes as either a coarsening of the finest mesh or refinement of the coarsest mesh. As a characteristic mesh size h, we mean the length of the base of a triangular element (non-hypotenuse side). We use these meshes to build a nested sequence of FE spaces. Using, $\mathbb{P}_2/\mathbb{P}_0$ Taylor-Hood elements, where quadratics are used for velocity and constant for pressure, we denote the FE spaces as $\{\mathcal{V}_{3-l}\}_{l=0}^{3}$. Each space has the corresponding mesh size $h_l = 2^l(\frac{1}{24})$ for $l = 0, 1, 2, 3$ ($\kappa = 2$, FE coarsening factor). With these approximation spaces we will have the error estimate

$$\inf_{\phi \in \mathcal{V}_{3-l}} \|v - \phi\|_{\mathcal{V}} \leq C \left(\frac{2^l}{24}\right) \|v\|_{\mathcal{U}}.$$

Remark Here the Sobolev space $\mathcal{V}$ is given by (4.34), and the regularity space is given by $\mathcal{U} = (H^2_{\#,0}(Y_{\mathcal{F}}))^{d\times d} \times (H^1_{\int=0}(Y_{\mathcal{F}}))^d$. Note also that, since we are using quadratics

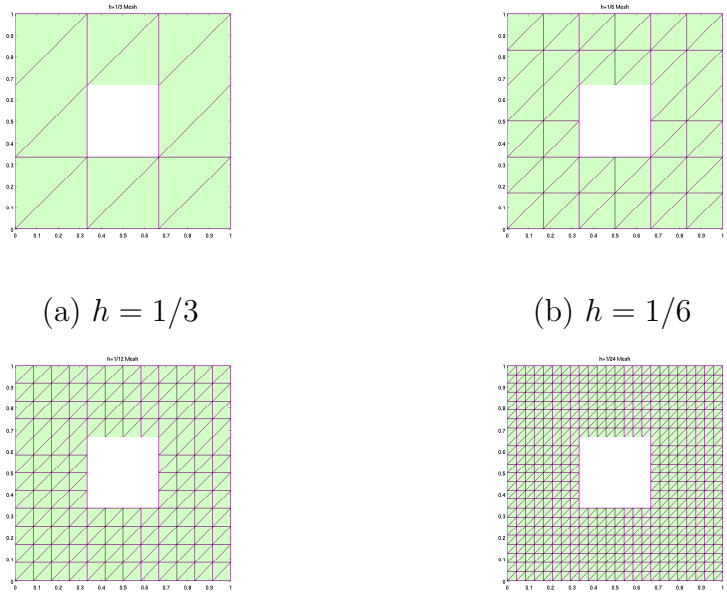

(a) $h = 1/3$ (b) $h = 1/6$

(c) $h = 1/12$ (d) $h = 1/24$

Fig. 14. 4-levels of meshes with coarsening factor $\kappa = 2$.

for velocity, we will have an error estimate of h_l^2. However, due to using constant pressure, the overall estimate will be order h_l.

We now construct the nested macro-grids $\{\mathcal{T}_l\}_{l=0}^3 \subset [0,1]$ and subsequently the hierarchy of macro-grids $\{S_l\}_{l=0}^3$. Recall our coarsening of the FE error is inversely proportional to the macro-grid spacing. With this in mind, we let $\mathcal{T}_0 = \{0, 1/2, 1\}$, then the initial grid spacing is $H2^0$, where is given by $H = 1/2$. The next macro-grids must have grid spacing $H2^{-l}$, for $l = 1, 2, 3,$. Thus, we have $\mathcal{T}_l = \{k/2^{l+1}\}_{k=0}^{2^{l+1}}$. We can now construct our hierarchy of grids S_l for $l = 0, 1, 2, 3$. Let the coarsest grid be $\mathcal{T}_0 = S_0 = \{0, 1/2, 1\}$, then $S_1 = \{1/4, 3/4\}$, $S_2 = \{(2k+1)/8\}_{k=0}^3$, and $S_3 = \{(2k+1)/16\}_{k=0}^7$. A schematic diagram of this hierarchy of grids and their relationship to the correction term procedure can be seen in Figure 15.

We implement the algorithm on the variational form (4.39) as follows. For $x' \in S_0 = \{0, 1/2, 1\}$, the so-called anchor points, we then solve for $v(x', \cdot) \in \mathcal{V}_3$ using

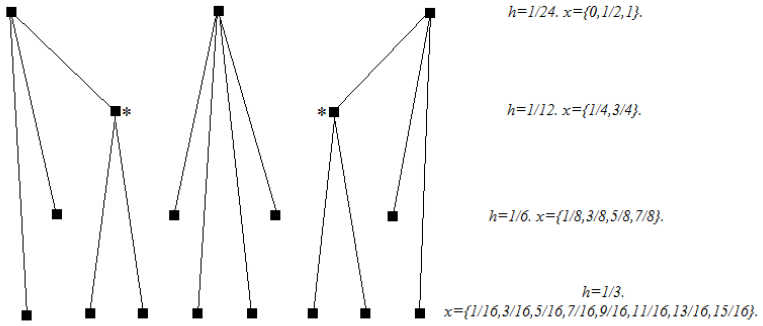

Fig. 15. Schematic diagram of hierarchy of macro-grids and corresponding FE spaces. With stratification of spaces and lines to indicate correction term relationships. The $*$ indicates where corrected solutions are used to correct once more.

the standard Galerkin FEM. We proceed to solve the lower level macro-grids by our inductive procedure. We use a simple 1-point interpolation to compute the correction term. For $x \in S_l$, then for $x' \in (\cup_{k<l} S_k)$ we let

$$I_l^x(v) = v(x_1', \cdot),$$

be the macro-grid interpolation. For example, using $x' = 0 \in S_0$, we have computed $\bar{v}(0,\cdot) \in \mathcal{V}_3$ by standard Galerkin FEM. We want to calculate $\bar{v}(1/4,\cdot)$, where $x = 1/4 \in S_1$. Using $I_1^{1/4}(\bar{v}) = \bar{v}(0,\cdot)$ as known data, we find the correction term $\bar{v}_c(1/4,\cdot) \in \mathcal{V}_2$ such that

$$\mathcal{A}_y(1/4)(\bar{v}_c, \phi) = \int_{Y_{\mathcal{F}}} G_0(1/4) : q dy - \mathcal{A}_y(1/4)(\bar{v}(0,\cdot), \phi),$$

for all $\phi \in \mathcal{V}_2$. We write the solution at $x = 1/4$ as

$$\bar{v}(1/4,\cdot) = \bar{v}_c(1/4,\cdot) + \bar{v}(0,\cdot).$$

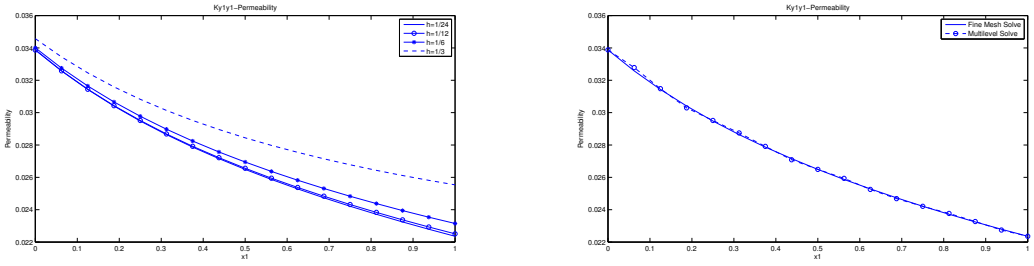

(a) Permeability h-values

(b) Permeability, Fine Mesh vs. Hierarchical

Fig. 16. Interpolated permeability values for $x_1^i = i/16$, $i = 0, \cdots, 16$, with $\alpha = 1/2$. (a) Varying $h = 1/3, 1/6, 1/12, 1/24$, (b) Hierarchical Solve "- o -" vs. Fine Mesh Solve "—".

We continue this procedure. For $x = 3/4$, we use $I_1^{3/4}(\bar{v}) = \bar{v}(1,\cdot)$ as known data as above. Since $x = 3/4 \in S_1$, we solve for $\bar{v}_c \in \mathcal{V}_2$ and write $\bar{v}(3/4,\cdot) = \bar{v}_c(3/4,\cdot)+\bar{v}(1,\cdot)$. Continuing on in this manner, we use the corrected solution $\bar{v}(1/4,\cdot)$ to compute the correction terms at $x = 3/16, 5/16$ in $\mathcal{V}_0$. We also use the corrected solution $\bar{v}(3/4,\cdot)$ to compute the correction terms at $x = 11/16, 13/16$ in $\mathcal{V}_0$. Indeed, using $\bar{v}(0,\cdot)$, we build the correction terms at $x = 1/8$ in $\mathcal{V}_1$ and at $x = 1/16$ in $\mathcal{V}_0$. Using $\bar{v}(1/2,\cdot)$, we build the correction terms at $x = 3/8, 5/8$ in $\mathcal{V}_1$ and at $x = 7/16, 9/16$ in $\mathcal{V}_0$. Finally, using $\bar{v}(1,\cdot)$, we build the correction terms at $x = 7/8$ in $\mathcal{V}_1$ and at $x = 15/16$ in $\mathcal{V}_0$. In this way, we build all solutions in $\mathcal{T}_3 = \{k/16\}_{k=0}^{16}$. We summarize this procedure in Figure 15.

We compute the solutions to cell equations (4.38) for $i = 1$. First, we compare the convergence results for standard solves, for varying h_l values. We then compare the convergence results for the finest mesh standard Galerkin solve to the implementation of our efficient algorithm (hierarchical solve). To this end, we define the modified

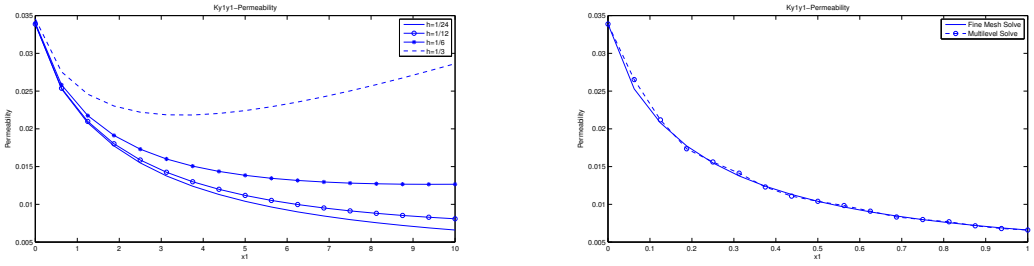

(a) Permeability h-values

(b) Permeability, Fine Mesh vs. Hierarchical

Fig. 17. Interpolated permeability values for $x_1^i = i/16$, $i = 0, \cdots, 16$, with $\alpha = 5$. (a) Varying $h = 1/3, 1/6, 1/12, 1/24$, (b) Hierarchical Solve "- o -" vs. Fine Mesh Solve "—".

permeability in the y_1 direction as

$$K_{y_1 y_1}(x_1) = \int_{Y_{\mathcal{F}}} w^1(x_1, y) dy, \tag{4.40}$$

where $w_1^1(x_1, y)$ is the y_1 component of the velocity in (4.38) for $i = 1$. Ultimately, we want to compute permeability, so this is a reasonable measure of accuracy.

In Figure 16 and Figure 17, we present a summary of our results. In Figure 16, we let $\alpha = 1/2$ where the mapping (4.37) is weak. Using the standard Galerkin FEM for the macro-points $\mathcal{T}_3 = \{k/16\}_{k=0}^{16}$, in 16(a), we compute modified permeabilities in the y_1 direction (4.40) for varying values of h_l. Then, we interpolate the values to make the trends clearer. Since the mapping is weak, the solution changes very slowly and not much is gained from decreasing h_l past a certain value. In 16(b), we compare our efficient algorithm described above with the finest mesh solution $h = 1/24$, used at all points in $\mathcal{T}_3$. We see that we obtain the same order of accuracy using the standard solve as with our efficient hierarchical algorithm.

In Figure 17, we proceed exactly as in Figure 16, but we let $\alpha = 5$. This corresponds to a strong stretch. In this case, the microstructure varies greatly. We

observe that as we move to the right of the domain, the deformation from our mapping is greatest. Using the standard Galerkin FEM, we observe strong errors in Figure 17(a) when larger values of h_l are used. Comparing the standard solve with $h = 1/6$ to the standard solve $h = 1/24$, we observe vary large errors at $x_1 = 1$. In Figure 17(b), we again compare our efficient algorithm to the standard solve with the finest mesh $h = 1/24$. We observe that we obtain the same order of accuracy. Moreover, we observe good convergence in the right side of the domain with our hierarchical solve. The two examples serve as a "proof of concept" and demonstrate that the algorithm can be simply implemented and is the same order of accuracy as the standard full solve.

F. Appendix

In this appendix, we apply the method of two-scale asymptotic expansion as in [33], to the modified Stokes operator $\mathcal{L}_\varepsilon\left(x, \frac{x}{\varepsilon}\right)$ given by (4.30). Recall these equations are presented in the periodic reference domain Ω. This is the so-called ALE formulation of the Stokes equations cf. [15]. From this procedure, we obtain, modified cell and homogenized operators $\mathcal{L}_y(x)$ and $\mathcal{L}(x)$, respectively.

To this end, we let $y = x/\varepsilon$ and thus derivatives transform as $\nabla \to \nabla_x + \frac{1}{\varepsilon}\nabla_y$. In addition, assume the following ansatz for the deformation $\widetilde{X}_\varepsilon(x)$

$$\widetilde{X}_\varepsilon(x) = \widetilde{X}_0(x) + \varepsilon \widetilde{X}_1(x, y). \tag{4.41}$$

We assume the regularity $\widetilde{X}_0 \in C^2(\bar{\Omega})$ and $\widetilde{X}_1(x, y) \in C^2(\bar{\Omega} \times Y)$, thus, $\widetilde{X}_\varepsilon(x) \in C^2(\bar{\Omega})$.

Remark This ansatz is reasonable for many applications cf. [32]. Essentially, the mapping has a large macroscopic part and a small oscillatory correction. In the

context of FSI, we have some macroscopic deformation over the whole domain and some small pore-scale deformation throughout.

We expand the gradient, Jacobian and related tensors as

$$F_\varepsilon(x) = \left(\nabla_x \widetilde{X}_0(x) + \nabla_y \widetilde{X}_1(x,y)\right) + \varepsilon\left(\nabla_x \widetilde{X}_1(x,y)\right) = F_0(x,y) + \varepsilon F_1(x,y), \quad (4.42)$$

and

$$G_\varepsilon(x) = G_0(x,y) + \varepsilon G_1(x,y) + \cdots\ , \ H_\varepsilon(x) = H_0(x,y) + \varepsilon H_1(x,y) + \cdots\ , \quad (4.43a)$$

$$J_\varepsilon(x) = J_0(x,y) + \varepsilon J_1(x,y) + \cdots\ . \quad (4.43b)$$

Here, the functions J_i,F_i,G_i, and H_i are y-periodic for $i = 0, 1, ...,$.

Remark To ensure that we have a meaningful deformation, we assume the non degeneracy condition. There exists a c such that

$$J_\varepsilon(x) > c > 0 \text{ and } J_0(x,y) > c > 0 \text{ for all } x \in \Omega. \quad (4.44)$$

In addition, $F_0(x,y)$ is of class C^1 and therefore bounded. Hence, there exists c such that

$$\left\|F_0^{-T}(x,y)\right\| > c > 0 \text{ for all } x \in \Omega. \quad (4.45)$$

These bounds will ensure a well-posed modified Stokes problem.

We expand velocity and pressure as in the case of slowly varying media (4.3),

$$v_\varepsilon(x) = \varepsilon^2\left(v_0(x,y) + \varepsilon v_1(x,y) + \cdots\right), \quad (4.46a)$$

$$p_\varepsilon(x) = p_0(x) + \varepsilon p_1(x,y) + \cdots\ , \quad (4.46b)$$

Using the above two-scale expansions (4.42-4.46), we can write the momentum equa-

tion (4.30a) as

$$
\begin{aligned}
&-\left(\mathrm{div}_x+\frac{1}{\varepsilon}\mathrm{div}_y\right)\left(\left(p_0(x)+\varepsilon p_1(x,y)\cdots\right)\left(G_0(x,y)+\varepsilon G_1(x,y)+\cdots\right)\right)\\
&+\mu\left(\mathrm{div}_x+\frac{1}{\varepsilon}\mathrm{div}_y\right)\Bigg[\left(\left(\nabla_x+\frac{1}{\varepsilon}\nabla_y\right)\left(\varepsilon^2 v_0(x,y)+\varepsilon^3 v_1(x,y)\cdots\right)\right)\\
&\times\left(H_0(x,y)+\varepsilon H_1(x,y)+\cdots\right)\Bigg]=f(x)\left(J_0(x,y)+\varepsilon J_1(x,y)\cdots\right),
\end{aligned}
$$

and for the conservation of mass equation (4.30b)

$$
\left(\mathrm{div}_x+\frac{1}{\varepsilon}\mathrm{div}_y\right)\left(\left(G_0^T(x,y)+\varepsilon G_1^T(x,y)+\cdots\right)\left(\varepsilon^2 v_0(x,y)+\cdots\right)\right)=0.
$$

Collecting the ε^0 terms from conservation of momentum, we have

$$
\begin{aligned}
-\mathrm{div}_x\left(p_0(x)G_0(x,y)\right)-\mathrm{div}_y(p_0(x)G_1(x,y))-\mathrm{div}_y(p_1(x,y)G_0(x,y))&\\
+\mu\mathrm{div}_y\left(\nabla_y v_0(x,y)H_0(x,y)\right)=f(x)J_0(x,y),&\qquad(4.47)
\end{aligned}
$$

and the ε^1 terms from the conservation of mass equation

$$
\mathrm{div}_y\left(G_0^T(x,y)v_0(x,y)\right)=0.\qquad(4.48)
$$

We may simplify (4.47) by noting that Piola transform $G_\varepsilon(x)$ is divergence free via the identity

$$
\begin{aligned}
\int_{\mathcal{P}_\varepsilon}\mathrm{div}_x(G_\varepsilon(x))dx&=\int_{\partial\mathcal{P}_\varepsilon}G_\varepsilon(x)\cdot n(x)dx\\
&=\int_{\partial\widetilde{\mathcal{P}}_\varepsilon}I\cdot\widetilde{n}(\tilde{x})d\tilde{x}=\int_{\widetilde{\mathcal{P}}_\varepsilon}\mathrm{div}_{\tilde{x}}(I)d\tilde{x}=0.
\end{aligned}
$$

From here, we see that the tensor $G_\varepsilon(x)$ satisfies $\mathrm{div}_x(G_\varepsilon(x))=0$. Using the asymptotic expansions (4.43a), we obtain

$$
\left(\mathrm{div}_x+\frac{1}{\varepsilon}\mathrm{div}_y\right)\left(G_0(x,y)+\varepsilon G_1(x,y)+\cdots\right)=0.
$$

Gathering similar terms in ε, terms we see that for ε^{-1}

$$\mathrm{div}_y(G_0(x,y)) = 0,$$

and for ε^0

$$\mathrm{div}_x(G_0(x,y)) + \mathrm{div}_y(G_1(x,y)) = 0.$$

Using these identities, we deduce

$$\begin{aligned} -\mathrm{div}_x(p_0(x)G_0(x,y)) - \mathrm{div}_y(p_0(x)G_1(x,y)) - \mathrm{div}_y(p_1(x,y)G_0(x,y)) \\ = -G_0(x,y)\nabla_x p_0(x) - G_0(x,y)\nabla_y p_1(x,y). \end{aligned}$$

Using the above identity, we simplify (4.47) along with the incompressibility equation (4.48). We write the cell problem for the modified Stokes equations in the periodic fluid cell $Y_{\mathcal{F}}$

$$-G_0(x,y)\nabla_y p_1(x,y) + \mu\mathrm{div}_y(\nabla_y v_0(x,y)H_0(x,y)) = G_0(x,y)\nabla_x p_0(x) + f(x)J_0(x,y),$$
$$\mathrm{div}_y(G_0^T(x,y)v_0(x,y)) = 0,$$

where v_0 and p_1 are $y-$periodic, also $v_0 = 0$ on Y_Γ and $\langle p_1 \rangle_Y = 0$. Note that the right-hand-side of the above problem contains components that depend on the fast variable y unlike in the slowly varying case. Indeed, letting

$$v_0(x,y) = w_1(x,y)\nabla_x p_0(x) + w_2(x,y)f(x), \tag{4.49a}$$
$$p_1(x,y) = \pi_1(x,y)\nabla_x p_0(x) + \pi_2(x,y)f(x), \tag{4.49b}$$

where $(w_j^i(x,y), \pi_j^i(x,y))$, $i = 1, \ldots, d$, are the solutions to the modified Stokes cell

equations

$$-G_0\nabla_y\pi_1^i + \mu\mathrm{div}_y\left(\nabla_y w_1^i H_0\right) = G_0 e_i \text{ in } Y_{\mathcal{F}},$$
$$\mathrm{div}_y(G_0^T w_1^i) = 0 \text{ in } Y_{\mathcal{F}},$$

and for the second cell

$$-G_0\nabla_y\pi_2^i + \mu\mathrm{div}_y\left(\nabla_y w_2^i H_0\right) = J_0 e_i \text{ in } Y_{\mathcal{F}},$$
$$\mathrm{div}_y(G_0^T w_2^i) = 0 \text{ in } Y_{\mathcal{F}},$$

with w_j^i and π_j^i being $y-$periodic, $w_j^i = 0$ on Y_Γ and $\left\langle \pi_j^i \right\rangle_Y = 0$. The above equations are the modified Stokes cell operator $\mathcal{L}_y(x)$ with differing right-hand-side data. Taking the next term in the two-scale expansion of (4.30b), we have

$$\mathrm{div}_x(G_0^T(x,y)v_0(x,y)) + \mathrm{div}_y(G_1^T(x,y)v_0(x,y)) + \mathrm{div}_y(G_0^T(x,y)v_1(x,y)) = 0.$$

Taking the average over the unit cell, using y-periodicity, $v_\varepsilon(x,y) = 0$ on Γ_ε, and divergence theorem, the div_y terms vanish. We obtain the homogenized operator $\mathcal{L}(x)$ in the periodic reference domain

$$\mathrm{div}_x\left(\left\langle G_0^T(x,y)v_0(x,y)\right\rangle_Y\right) = 0 \text{ in } \Omega.$$

Using the relation (4.49), we see that

$$\mathrm{div}_x\left(\left\langle G_0^T(x,y)w_1(x,y)\right\rangle_Y \nabla_x p_0(x)\right) + \mathrm{div}_x\left(\left\langle G_0^T(x,y)w_2(x,y)\right\rangle_Y f(x)\right) = 0.$$

Letting

$$K(x) = \left\langle G_0^T(x,y)w_1(x,y)\right\rangle_Y \text{ and } \bar{f}(x) = \left\langle G_0^T(x,y)w_2(x,y)\right\rangle_Y f(x),$$

we write this effective homogenized equation as

$$\mathrm{div}_x \left(K(x) \nabla_x p_0(x) + \bar{f}(x) \right) = 0 \text{ in } \Omega.$$

Here, we may make parallel comparisons to the Darcy law (4.9). We have the x-dependent modified permeability $K(x)$ and the modified Darcy velocity $\xi = K(x)\nabla_x p_0(x) + \bar{f}(x)$. We also require the boundary conditions $\xi \cdot \nu = 0$ on $\partial\Omega$, where ν is the unit normal.

Remark Note here that if our mapping is the identity, that is $\widetilde{X}_\varepsilon(x) = x$, all the related tensors are the identity matrix. In this case, we observe that the equations are the same as the purely periodic setting.

CHAPTER V

CONCLUSION

In this dissertation, we developed theory and computational methodologies to deal with multiscale Fluid-Structure Interaction (FSI) problems. Such problems exhibit highly nonlinear behavior and, with the added complexity of complex multiscale geometries, new theoretical and computational tools are necessary. We recall here the methods and state conclusions of the dissertation.

We began by deriving a homogenization result for Stokes flow in slowly varying media. Traditionally, these homogenization techniques have relied on the medium in question having periodic microstructure. Recall, that FSI generates slowly varying geometries and can break the periodicity of the medium. When developing multiscale iterative techniques for FSI, such homogenization results are critical in the analysis of such algorithms. Using our theoretical result, we developed a computational methodology to compute downscaled quantities. We compute cell problems at select RVEs and interpolate the result. We demonstrated this technique on two slowly varying geometries and on these examples obtained better than theoretical convergence rates.

The homogenization result for Stokes flow is essentially a result for iterative multiscale FSI problems. In Chapter III, we developed a fully coupled formal homogenization of the fine-scale FSI model. This is done with the intent of developing a homogenized Biot poroelasticity model that includes pore-scale deformation. The linear Biot equation can be obtained via homogenization techniques, however, these methods assume no pore-scale deformation. Due to large deformations, the fluid and solid equations are presented in differing domains for FSI. Fluid equations are presented the moving Eulerian frame, while solid equations are presented in the fixed Lagrangian frame. To apply two-scale homogenization techniques we reformulate the

FSI equations in the Arbitrary Lagrange-Eulerian frame. This unified framework allowed us obtain homogenized equations whose coefficients depend nonlinearly on pressure and gradient of displacement. We then applied several simplifications to the equations. Using these simplifications, we were able to obtain a numerical result for a three dimensional cell geometry. We obtained a table for permeability and Biot coefficient values. In future work, we will to apply these tables of coefficients to a full three dimensional Biot equations.

Finally, we developed a multiscale hierarchical finite element method for Stokes equations. Computing permeability for complex microstructures can be prohibitively expensive. The reason is two fold: for varying media, the microscale properties must be resolved through the entire domain and each such cell may exhibit complex geometry. We recall the main themes of the algorithm. We built a nested set of finite element approximation spaces. Then, a corresponding hierarchy of macro-grids throughout the entire domain. At certain points in the hierarchy we solved using very high accuracy approximations spaces. Then at other points we solved with lower accuracy spaces and used nearby high accuracy solves to correct. Since the algorithm requires the approximation spaces to be nested, we utilized the Arbitrary Lagrange-Eulerian formulation of the Stokes equations. We then applied the method to a test geometry that was periodic in the vertical direction, making the macro-grid essentially one dimensional, while cell equation is the two dimensional. Applying these methods to the fully coupled nonlinear FSI cell problem is being currently explored.

REFERENCES

[1] A. Allaire, *Homogenization and two-scale convergence*, SIAM J. Math. Anal., 23 (1992), pp. 1482–1518.

[2] C. Amrouche and V. Girault, *On the existence and regularity of the solution of stokes problem in arbitrary dimension*, SIAM J. Math. Anal., 67 (1991), pp. 171–175.

[3] A. Bensoussan, J. Lions, and G. Papanicolaou, *Asymptotic Analysis for Periodic Structures*, vol. 5 of Studies in Mathematics and Its Applications, North-Holland, Amsterdam, 1978.

[4] M. Biot, *General theory of three dimensional consolidation*, J. Appl. Phys., 12 (1941), pp. 155–164.

[5] S. Brenner and R. Scott, *The Mathematical Theory of Finite Element Methods*, vol. 15 of Texts in Applied Mathematics, Springer, New York, NY, 2008.

[6] F. Brezzi and M. Fortin, *Mixed and hybrid finite element methods*, Springer, Berlin, Heidelberg, New York, 1991.

[7] D. Brown, P. Popov, and Y. Efendiev, *On homogenization of stokes flow in slowly varying media with applications to fluid-structure interaction*, Int J. Geomathematics, 2 (2011), pp. 281–305.

[8] R. Burridge and J. Keller, *Poroelasticity equations derived from microstructure*, J. Acoust. Soc. of Amer., 70 (1981), pp. 1140–1146.

[9] G. A. Chechkin, A. L. Piatniski, and A. S. Shamev, *Homogenization: Methods and Applications*, vol. 234 of Translations of Mathematical Monographs, American Mathematical Society, Providence, RI, 2007.

[10] H. Darcy, *Les fontaines publique de la ville de Dijon*, Librairie des Corps Impériaux des Ponts et Chaussées et des Mines, Paris, 1856.

[11] Y. Efendiev and T. Hou, *Multiscale Finite Element Methods: Theory and Applications*, vol. 4 of Surveys and Tutorials in the Applied Mathematical Sciences, Springer, New York, NY, 2009.

[12] Y. Efendiev and A. Pankov, *Numerical homogenization of monotone elliptic operators*, Multiscale Modeling and Simulation, 2 (2003), pp. 62–79.

[13] A. Ern and J. Guermond, *Theory and Practice of Finite Elements*, Applied Mathematical Sciences, Springer, New York, NY, April 29, 2004.

[14] L. Formaggia, A. Quarteroni, and A. Veneziani, *Cardiovascular Mathematics: Modeling and simulation of the circulatory system*, Modeling, Simulation, & Applications, Springer, Milan, Italy, 2009.

[15] G. Galdi and R. Rannacher, *Fundamental Trends in Fluid-structure Interaction*, vol. 1 of Contemporary Challenges in Mathematical Fluid Dynamics and Its Applications, World Scientific Publishing Company, Singapore, 2010.

[16] V. Girault and P. Raviart, *Finite Element Methods for Navier-Stokes Equations*, Springer-Verlag, Berlin, 1986.

[17] M. E. Gurtin, *An Introduction to Continuum Mechanics*, Academics Press, San Diego, CA, 1981.

[18] V. Hoang and C. Schwab, *High-dimensional finite elements for elliptic problems with multiple scales*, Multiscale Model. Simul., 3 (2005), pp. 168–194.

[19] O. Iliev, A. Mikelic, and P. Popov, *On upscaling certain flows in deformable porous media*, SIAM MMS, 7 (2008), pp. 93–123.

[20] W. Jaeger and A. Mikelic, *On the flow conditions at the boundary between a porous media and an impervious solid, in Progress in partial differential equations: the Metz surveys, Volume 3*, Longman Scientific and Technical, London, 1994.

[21] C. K. Lee and C. C. Mei, *Re-examination of the equations of poroelasticity*, Int. J. Eng. Sci., 35 (1997), pp. 329–352.

[22] J. L. Lions, *Some methods in the mathematical analysis of systems and their control*, Gordon and Breach, New York, 1981.

[23] R. Lipton and M. Avellaneda, *Darcy's law for slow viscous flow past a stationary array of bubbles*, Proc. of the Royal Soc. of Edin., A, 114 (1990), pp. 71–79.

[24] E. Marusic-Paloka and A. Mikelic, *An error estimate for correctors in the homogenization of the Stokes and Navier-Stokes equations in a porous medium*, Bollettino U.M.I, 7 (1996), pp. 661–671.

[25] A. Mikelic, *Homogenization theory and applications to filtration through porous media*, in Filtration in porous media and industrial application, A. Fasano, ed., Springer. Lect. Notes Math. 1734, Berlin, 1998, ch. 2, pp. 127–214.

[26] G. Nguetseng, *A general convergence result for a functional related to the theory of homogenization*, SIAM J. Math. Anal., 20 (1989), pp. 608–623.

[27] I. G. A. Oleinik, O. A. and S. A. S., *Mathematical problems in elasticity and homogenization*, Elsevier, Amsterdam, 1992.

[28] M. Peter, *Homogenisation in domains with evolving microstructure*, C. R. Mecanique, 335 (2007), pp. 357–362.

[29] ——, *Homogenisation of a chemical degradation mechanism inducing an evolving microstructure*, C. R. Mecanique, 335 (2007), pp. 679–684.

[30] P. Popov, *Constitutive modelling of Shape Memory Alloys and upscaling of deformable porous media*, PhD thesis, Texas A&M University, 2005.

[31] P. Popov, Y. Efendiev, and G. Y., *Multiscale modeling and simulation of fuid flows in highly deformable porous media*, in Proceedings of the 7-th Conference on Large-Scale Scientific Computing, I. Lirkov, S. Margenov, and J. Wasniewski, eds., Springer LNCS 5910, 2009.

[32] P. Popov, Y. Gorb, and Y. Efendiev, *Iterative upscaling of flows in deformable porous media*, (2012). (submitted).

[33] E. Sanchez-Palencia, *Non-Homogeneous Media and Vibration Theory*, vol. 127 of Lecture Notes in Physics, Springer-Verlag, Berlin, 1980.

[34] E. Sanchez-Palencia and H. Ene, *Equations et phénomènes de surface pour l'écoulement dans un modèle de milieu poreux*, J. Mécanique, 14 (1975), pp. 73–108.

[35] L. Tartar, *Incompressible Fluid Flow in a Porous Medium - Convergence of the Homogenization Process*, vol. 127 of Lecture Notes in Physics, Springer-Verlag, Berlin, 1980, pp. 368–377.

[36] R. Temam, *Navier-Stokes Equations: Theory and Numerical Analysis*, Elsevier North-Holland, New York, 1977.

[37] V. Zhikov, S. Kozlov, and O. Oleinik, *Homogenization of Differential Operators and Integral Functionals*, Springer-Verlag, Berlin, 1994.

VITA

Donald Lee Brown was born in Cincinnati, Ohio, USA. He received his Bachelor of Arts in Mathematical Sciences from the University of Cincinnati in June 2007. He began his studies at Texas A&M University in August 2007. He received his Ph.D. in Mathematics in August 2012. Donald Brown can be contacted by writing to: Mathematical and Computer Science and Engineering Division, Building 1, 4700 King Abdullah University of Science and Technology, Thuwal, 23955-6900, Kingdom of Saudi Arabia, or by the email at donaldbrowdr@gmail.com